Mercury Stable Isotopes as Tracers in the Environment: Applications to Aquatic and Natural Gas Systems

by

Spencer J. Washburn

A dissertation submitted in partial fulfillment
of the requirements for the degree of
Doctor of Philosophy
(Earth and Environmental Sciences)
in the University of Michigan
2018

Doctoral Committee:

Professor Joel D. Blum, Chair
Professor G. Allen Burton
Associate Professor Rose M. Cory
Professor Kyger C. Lohmann

Spencer J. Washburn

sjwash@umich.edu

ORCID iD: 0000-0002-6176-8297

Acknowledgements

First I would like to thank my wife Kalli for her unwavering support, keen assistance, and timely encouragement over the last five years.

I would like to extend my sincere gratitude and many thanks to my advisor, Dr. Joel Blum, for his patience, guidance, and encouragement throughout my entire time at the University of Michigan. His mentorship has been an invaluable part of my PhD experience.

I would like to thank all of my co-authors, who have been the source of excellent scientific discourse and support. I would also like to thank my dissertation committee members, who have provided guidance throughout this process.

I would like to thank Marcus Johnson, who has been a wonderful source of technical advice and laboratory assistance.

I would like to thank the other graduate students who have been members of the BEIGL lab group - Patrick Donovan, Sae Yun Kwon, Laura Motta Medina, and Aaron Kurz - for all of the discussions and friendship over the last 5 years. I would also like to thank the other members of the BEIGL lab group during my tenure, particularly Laura Sherman, Jamie Gleason, and Jason Demers.

Lastly, I would like to acknowledge my cat, Tokki, who has borne witness to more poorly prepared practice presentations than anyone else over the last five years.

Table of Contents

Lists of Tables

Lists of Figures

Abstract

Mercury (Hg) is a neurotoxic trace metal pollutant with a global distribution and a complex biogeochemical cycle. Gaining a better understanding of the behavior of Hg in the environment has implications for both environmental and human health. Anthropogenic activity has directly altered the biogeochemical cycling of Hg, both by the direct release of Hg to the environment related to historic use (i.e. mining, industrial activity) as well as ongoing emissions of Hg as a byproduct of energy production (i.e. coal and natural gas combustion). There are still significant uncertainties in the understanding of how anthropogenic Hg sources, both legacy and modern, affect global Hg cycling and environmental health. The developing study of Hg stable isotope ratios in environmental samples has presented a new tool for understanding the processes that control Hg biogeochemistry. Throughout this dissertation, we have applied measurements of Hg stable isotope ratios in samples from sites affected by anthropogenic Hg contamination to enhance understanding of the biogeochemical behavior of Hg. In Chapter 2 and 3, we focused on understanding the Hg cycling within freshwater aquatic ecosystems by studying the South River, VA, which is the site of historic industrial Hg contamination. To describe the large range of observed Hg isotopic variation within the channel environment, a source end-member mixing model was proposed, identifying a regional background end-member and two end-members deriving from the historic industrial activities. We observed for the first time a discharge-dependent isotopic partitioning of Hg between the dissolved and suspended particulate phase of surface waters and proposed a fractionation mechanism to explain this observation. Examination of sediments of a floodplain profile provided evidence that there was significant temporal

variability of the isotopic composition of past releases of Hg into the South River, with brief excursions in isotopic composition in the past recorded in the floodplain profile. In Chapter 4, we present the first measurements of the isotopic composition of Hg within natural gas. To obtain these measurements, we analyzed catalysts from mercury removal units at gas processing facilities that served to concentrate Hg for isotopic analysis. Significant variation in the isotopic composition of Hg within natural gas on a global scale was observed, as well as the regional scale. With further work these results could be used to investigate the impacts of natural gas processing at a local scale and could be included in Hg emissions models that incorporate Hg isotope mass balances. Altogether, this dissertation has expanded the use of stable Hg isotope ratios as tracers of anthropogenic Hg releases to the environment.

Chapter 1 Introduction

1.1 Mercury as a Global Pollutant

Mercury (Hg) is a neurotoxic trace metal with a global distribution due to natural processes and human activities. A number of natural sources of Hg contribute to the global Hg budget, including volcanic and geothermal emissions, re-emission from soils, and biomass burning. The impact of Hg on environmental and human health depends in large part on geochemical reactions and processes (Selin, 2009). For example, the redox cycling of Hg is an important control on the common Hg species found in the environment in solid, aqueous phase, and gaseous forms. Transformation of inorganic Hg species into the more toxic organometallic species monomethylmercury (MMHg) occurs in the environment via microbial activity, primarily by iron- and sulfate- reducing bacteria in anoxic environments.

Anthropogenic activity has altered how Hg species cycle through the biosphere on a global scale (Driscoll et al., 2013), and many questions remain regarding critical aspects of these cycles. Anthropogenic emissions of Hg to the atmosphere (e.g. as a byproduct of coal combustion) contribute to the global atmospheric pool of Hg that has a relatively long residence time of ~0.5 to 1 years (Gustin et al., 2015). Direct impacts of anthropogenic activity are also observed at a local scale at sites of Hg contamination, which historically have resulted from activities such as artisanal small-scale gold mining, chlor-alkali production, non-ferrous metal smelting, and a number of other industrial processes (Kocman et al., 2013). Of particular concern are Hg contamination sites with aquatic impairment, as inorganic Hg released to aquatic environments is readily transformed into the more toxic MMHg form, and subsequently

bioaccumulated and biomagnified up aquatic food chains. Consumption of high trophic level fish represents a major exposure pathway for humans to MMHg (Mergler et al., 2007). Additionally, discharges of anthropogenic Hg to freshwater ecosystems are understudied relative to other components of the global Hg cycle, and understanding the balance of Hg sources (diffusive inputs from the catchment, current primary anthropogenic releases, re-emission from historic Hg deposits) in these complex aquatic environments represents a substantial challenge (Kocman et al., 2017). The analysis of stable Hg isotope ratios in environmental samples is an emerging tool for answering many of the questions that remain in regards to the biogeochemical cycling of Hg.

1.2 Mercury Stable Isotope Fundamentals

Measurements of Hg isotopic composition are made possible by separation and pre-concentration of Hg from samples followed by introduction as a Hg cold vapor into the plasma source of a multi-collector inductively coupled mass spectrometer (MC-ICP-MS). The methods of Hg pre-concentration from environmental samples presented throughout this dissertation have been well established in the literature (e.g. Biswas et al., 2008; Demers et al., 2013), and the number of studies using high precision measurements of Hg isotopic composition via MC-ICP-MS has expanded in the last decade. Hg has seven stable isotopes (masses 196, 198, 199, 200, 201, 202, and 204) and participates in a variety of redox reactions, which can cause isotope fractionation. Hg can undergo two general types of isotope fractionation: mass-dependent fractionation (MDF) and mass-independent fractionation (MIF). MDF occurs in reactions with nuclear mass selectivity (i.e. classic isotope effect), and is generally reported as the δ^{202}Hg value, where:

$$\delta^{202}\text{Hg}\ (‰) = ([(^{202}\text{Hg}/^{198}\text{Hg})_{\text{Sample}} / (^{202}\text{Hg}/^{198}\text{Hg})_{\text{NIST3133}}] - 1) \times 1000$$

MDF of Hg has been documented for a wide range of processes that influence Hg biogeochemical cycling, such as aqueous sorption (Wiederhold et al., 2010; Jiskra et al., 2012), diffusion (Koster Van Groos et al., 2014), and abiotic reduction (Zheng and Hintelmann, 2010). In addition to abiotic reactions, MDF has been observed in a number of biological reactions, including microbial methylation and demethylation, and microbial reduction (Kritee et al., 2007; Kritee et al., 2008; Rodriguez-Gonzalez et al, 2009; Kritee et al., 2013; Janssen et al., 2016).

MIF of Hg has been documented for a distinct subset of reactions, and is represented with Δ^{199}Hg, Δ^{200}Hg, Δ^{201}Hg, and Δ^{204}Hg, which are calculated as the deviation of the odd-mass isotopes from the predicted kinetic isotope fractionation law in units of permil (‰) (Blum and Bergquist, 2007), where:

$$\Delta^{xxx}\text{Hg}\ (‰) = \delta^{xxx}\text{Hg} - (\delta^{202}\text{Hg} \times \beta)$$

with $\beta = 0.252$, $\beta = 0.502$, $\beta = 0.752$, and $\beta = 1.493$, respectively. In the environment, large magnitude odd MIF anomalies (affecting the Δ^{199}Hg and Δ^{201}Hg values) have been observed in environmental reservoirs that incorporate Hg that has undergone photochemical reactions, such as MeHg in fish (Bergquist and Blum, 2007; Blum et al., 2014). These large magnitude MIF anomalies are thought to be related to fractionation caused by the magnetic isotope effect, and the isotopes of mass 199 and 201 have non-zero nuclear spin and magnetic moments (Bergquist and Blum, 2007; Zheng and Hintelmann, 2009; Chandan et al., 2015). Much smaller magnitude odd MIF anomalies have been observed due to fractionation associated with the nuclear volume, or nuclear field shift, effect during equilibrium reactions (Schauble, 2007; Wiederhold et al.,

2010; Ghosh et al., 2013). Small but significant magnitude even MIF anomalies (affecting the Δ^{200}Hg and Δ^{204}Hg values) have been observed for samples that contain Hg that has undergone atmospheric cycling, namely precipitation and atmospheric gaseous elemental Hg (Blum et al., 2014; Cai and Chen, 2015). The exact mechanism causing even MIF is still unknown, although some authors have suggested UV self-shielding as potential explanation (Mead et al., 2013; Blum and Johnson, 2017). Despite the lack of understanding as to the causal mechanism of even MIF, it is widely accepted that even MIF can be used as a conservative tracer for Hg that has been subject to atmospheric cycling prior to inclusion in the measured sample reservoir.

The measurement of Hg isotope ratios in the environment has been used extensively in previous studies to identify sources of anthropogenic Hg and to trace the movement of Hg between reservoirs (Blum et al., 2014; Yin et al. 2010). This is because in addition to the fact that stable isotope analysis can be used to track the sources of environmental contamination (e.g. source tracing), it can also reveal specific chemical mechanisms can result in both MDF and MIF, resulting in a additional "two-dimensional tracer" of Hg source and transformations (Wiederhold, 2015). This ability to accurately "fingerprint" the complex transformations of Hg in environmental systems makes stable isotope studies an excellent tool for understanding the transport of Hg contamination from anthropogenic origins and the conditions affecting its mobility and bioavailability in the environment.

1.3 Applications of Mercury Stable Isotopes: Dissertation Narrative Structure

Overall, this dissertation used Hg stable isotope analysis to gain insights into the biogeochemical cycling of Hg in environmental systems. In Chapters 2&3, we investigated Hg cycling within the contaminated South River, VA. The South River is a site of extensive anthropogenic Hg contamination originating from a former DuPont textile manufacturing plant

in Waynesboro, VA. Mercuric sulfate was used as a catalyst at the plant between 1929 and 1950 in the production of acetate fibers (Carter, 1977). During this period of mercuric sulfate catalyst use at the former DuPont facility, significant amounts of Hg were lost and entered the South River channel. Hg-contaminated sediments have been identified throughout South River ecosystem, and a substantial body of literature has demonstrated the ongoing impacts of this Hg contamination on downstream ecosystems. Studies have documented elevated Hg levels within the biota of both the aquatic (Murphy et al., 2007; Neufeld 2009; Bergeron et al., 2010; Brent & Kain, 2011) and associated terrestrial environments of the South River (Cristol et al., 2008; Jackson et al., 2011).

In Chapter 2 (published in *Environmental Science & Technology*), we present a survey of the Hg isotopic composition of the main physical reservoirs of Hg within the South River (Washburn et al., 2017). Samples were collected along a longitudinal transect of the South River, starting upstream of the historic Hg contamination point-source and extending downstream to the confluence with the South Fork Shenandoah River. Analysis of the THg concentration and Hg isotopic composition of these reservoirs indicates that the regional background mercury source is isotopically distinct in both Δ^{199}Hg and δ^{202}Hg from Hg derived from the original source of contamination, allowing for the tracing of contamination-sourced Hg throughout the study reach. An end-member mixing model is developed, as three distinct end-members are required to explain the Hg isotopic and concentration variation observed in the South River channel. A consistent negative offset in δ^{202}Hg values (~0.28‰) was observed between Hg in the suspended particulate and dissolved phases of surface, and a mechanism for this fractionation is proposed.

In Chapter 3 (in review at *Chemical Geology*), we expanded upon the work of Chapter 2 to quantify the spatial, temporal, and hydrologic constraints on Hg isotopic composition within

the South River (Washburn et al., 2018, *in review*). Increased spatial resolution sampling in the reach adjacent to the former DuPont industrial facility allowed for the identification of the physical source, upstream streambed sediments, of the previously unknown end-member identified in Chapter 2. This allowed us to update the end-member mixing model for the South River, which is able to explain the full range of Hg isotope variation observed within the South River channel. By sampling surface waters at elevated flow conditions, we demonstrated that hydrologic conditions alter the isotopic partitioning of Hg between dissolved and particulate phases in these surface waters. Brief temporal excursions in δ^{202}Hg values were observed in sediments collected from a dated floodplain profile, indicating that past releases of Hg to the South River did not have a completely homogenous isotopic composition, providing a potential explanation for heterogeneity in isotopic composition observed in the present. Taken together, Chapters 2&3 underscored the utility of Hg stable isotopes to both identify and trace Hg sources in environmental systems, as well as the need for future studies to account for the full range of full range of biogeochemical conditions and potential source variations within these complex environments.

In Chapter 4 (published in *ACS Earth and Space Chemistry*), we shifted focus to study Hg in natural gas (NG) (Washburn et al., 2018). A number of commercially relevant hydrocarbon sources contain trace levels of Hg, although the concentrations of Hg within NG deposits can vary widely at both the basin level and within single gas production field, with Hg concentrations commonly observed to range between 0.01 and 5,000 μg/m^3 (Wilhelm, 2001: Liu, 2013). At sites with particularly elevated Hg concentrations, NG production could be a significant source of Hg emissions to local environments (Spiric and Mashyanov, 2000; Horvat et al., 2000). Some NG production facitilites have identified the need to remove Hg from

production streams prior to processing, installing mercury removal units (MRU) consisting of pelletized inorganic metal sulfide pellets to ensure safe plant operation. In an effort to gain a better understanding of the Hg dynamics associated with NG production, we conducted the first survey of the Hg isotopic composition in NG, as collected on MRU catalysts. Our results indicate that the Hg isotopic composition varies significantly on a global scale (δ^{202}Hg = -3.75 to -0.68‰), as well as at a regional scale [SE Asia] (δ^{202}Hg = -2.57 to -0.68‰). Analysis of samples from within a single MRU reactor suggested that significant fractionation observed within MRU reactors was related to sorption of gas phase Hg to catalyst surfaces, and was proposed to follow a Rayleigh fractionation model. With further efforts, Hg isotope analysis of NG could be used to trace atmoshperic Hg in local and regional environments, and used in atmospheric Hg isotope models.

References

(1) Bergeron, C. M.; Bodinof, C. M.; Unrine, J. M.; Hopkins, W. A. Mercury Accumulation along a Contamination Gradient and Nondestructive Indices of Bioaccumulation in Amphibians. *Environ. Toxicol. Chem.* **2010**, *29* (4), 980–988 DOI: 10.1002/etc.121.

(2) Bergquist, B. a; Blum, J. D. Mass-Dependent and -Independent Fractionation of Hg Isotopes by Photoreduction in Aquatic Systems. *Science*. **2007**, *318* (5849), 417–420 DOI: 10.1126/science.1148050.

(3) Biswas, A.; Blum, J. D.; Bergquist, B. A.; Keeler, G. J.; Xie, Z. Natural Mercury Isotope Variation in Coal Deposits and Organic Soils. *Environ. Sci. Technol.* **2008**, *42* (22), 8303–8309 DOI: 10.1021/es801444b.

(4) Blum, J. D.; Bergquist, B. a. Reporting of Variations in the Natural Isotopic Composition of Mercury. *Anal. Bioanal. Chem.* **2007**, *388* (2), 353–359 DOI: 10.1007/s00216-007-1236-9.

(5) Blum, J. D.; Johnson, M. W. Recent Developments in Mercury Stable Isotope Analysis. *Rev. Mineral. Geochemistry* **2017**, *82* (1), 733–757 DOI: https://doi.org/10.2138/rmg.2017.82.17.

(6) Blum, J. D.; Sherman, L. S.; Johnson, M. W. Mercury Isotopes in Earth and Environmental Sciences. *Annu. Rev. Earth Planet. Sci.* **2014**, *42* (1), 249–269 DOI: 10.1146/annurev-earth-050212-124107.

(7) Brent, R. N.; Kain, D. G. Development of an Empirical Nonlinear Model for Mercury Bioaccumulation in the South and South Fork Shenandoah Rivers of Virginia. *Arch. Environ. Contam. Toxicol.* **2011**, *61* (4), 614–623 DOI: 10.1007/s00244-011-9664-0.

(8) Cai, H.; Chen, J. Mass-Independent Fractionation of Even Mercury Isotopes. *Sci. Bull.* **2015**, *61*, 116–124 DOI: 10.1007/s11434-015-0968-8.

(9) Carter, L. J. Chemical Plants Leave Unexpected Legacy for Two Virginia Rivers. *Science* **1977**, *198* (4321), 1015–1020 DOI: 10.1126/science.198.4321.1015.

(10) Chandan, P.; Ghosh, S.; Bergquist, B. a. Mercury Isotope Fractionation during Aqueous Photoreduction of Monomethylmercury in the Presence of Dissolved Organic Matter. *Environ. Sci. Technol.* **2015**, *49* (1), 259–267 DOI: 10.1021/es5034553.

(11) Cristol, D. a; Brasso, R. L.; Condon, A. M.; Fovargue, R. E.; Friedman, S. L.; Hallinger, K. K.; Monroe, A. P.; White, A. E. The Movement of Aquatic Mercury through Terrestrial Food Webs. *Science (80-.).* **2008**, *320* (5874), 335 DOI: 10.1126/science.1154082.

(12) Demers, J. D.; Blum, J. D.; Zak, D. R. Mercury Isotopes in a Forested Ecosystem: Implications for Air-Surface Exchange Dynamics and the Global Mercury Cycle. *Global Biogeochem. Cycles* **2013**, *27*, n/a-n/a DOI: 10.1002/gbc.20021.

(13) Driscoll, C. T.; Mason, R. P.; Chan, H. M.; Jacob, D. J.; Pirrone, N. Mercury as a Global Pollutant: Sources, Pathways, and Effects. *Environ. Sci. Technol.* **2013**, *47* (10), 4967–4983 DOI: 10.1021/es305071v.

(14) Ghosh, S.; Schauble, E. a.; Lacrampe Couloume, G.; Blum, J. D.; Bergquist, B. a. Estimation of Nuclear Volume Dependent Fractionation of Mercury Isotopes in Equilibrium Liquid–vapor Evaporation Experiments. *Chem. Geol.* **2013**, *336*, 5–12 DOI: 10.1016/j.chemgeo.2012.01.008.

(15) Groos, P. G. K. Van; Esser, B. K.; Williams, R. W.; Hunt, J. R. Isotope Effect of Mercury Diffusion in Air. *Environ. Sci. Technol.* **2014**, *48*, 227–233.

(16) Gustin, M. S.; Amos, H. M.; Huang, J.; Miller, M. B.; Heidecorn, K. Measuring and Modeling Mercury in the Atmosphere: A Critical Review. *Atmos. Chem. Phys.* **2015**, *15* (10), 5697–5713 DOI: 10.5194/acp-15-5697-2015.

(17) Horvat, M.; Jeran, Z.; Špirič, Z.; Jaćimović, R.; Miklavčič, V. Mercury and Other Elements in Lichens near the INA Naftaplin Gas Treatment Plant, Molve, Croatia. *J. Environ. Monit.* **2000**, *2* (2), 139–144 DOI: 10.1039/a906973i.

(18) Jackson, A. K.; Evers, D. C.; Folsom, S. B.; Condon, A. M.; Diener, J.; Goodrick, L. F.; McGann, A. J.; Schmerfeld, J.; Cristol, D. A. Mercury Exposure in Terrestrial Birds Far Downstream of an Historical Point Source. *Environ. Pollut.* **2011**, *159* (12), 3302–3308 DOI: 10.1016/j.envpol.2011.08.046.

(19) Janssen, S. E.; Schaefer, J. K.; Barkay, T.; Reinfelder, J. R. Fractionation of Mercury Stable Isotopes during Microbial Methylmercury Production by Iron- and Sulfate-Reducing Bacteria. *Environ. Sci. Technol.* **2016**, *50* (15), 8077–8083 DOI: 10.1021/acs.est.6b00854.

(20) Jiskra, M.; Wiederhold, J. G.; Bourdon, B.; Kretzschmar, R. Solution Speciation Controls Mercury Isotope Fractionation of Hg(II) Sorption to Goethite. *Environ. Sci. Technol.* **2012**, *46* (12), 6654–6662 DOI: 10.1021/es3008112.

(21) Kocman, D.; Horvat, M.; Pirrone, N.; Cinnirella, S. Contribution of Contaminated Sites to the Global Mercury Budget. *Environ. Res.* **2013**, *125*, 160–170 DOI: 10.1016/j.envres.2012.12.011.

(22) Kocman, D.; Wilson, S. J.; Amos, H. M.; Telmer, K. H.; Steenhuisen, F.; Sunderland, E. M.; Mason, R. P.; Outridge, P.; Horvat, M. Toward an Assessment of the Global Inventory of Present-Day Mercury Releases to Freshwater Environments. *Int. J. Environ. Res. Public Health* **2017**, *14* (2) DOI: 10.3390/ijerph14020138.

(23) Kritee, K.; Barkay, T.; Blum, J. D. Mass Dependent Stable Isotope Fractionation of Mercury during Mer Mediated Microbial Degradation of Monomethylmercury. *Geochim. Cosmochim. Acta* **2009**, *73* (5), 1285–1296 DOI: 10.1016/j.gca.2008.11.038.

(24) Kritee, K.; Blum, J. D.; Johnson, M. W.; Bergquist, B. A.; Barkay, T. Mercury Stable Isotope Fractionation during Microbial Reduction of Hg(II) to Hg(0). *Environ. Sci. Technol.* **2007**, *41* (6), 1889–1895.

(25) Kritee, K.; Blum, J. D.; Reinfelder, J. R.; Barkay, T. Microbial Stable Isotope Fractionation of Mercury: A Synthesis of Present Understanding and Future Directions. *Chem. Geol.* **2013**, *336*, 13–25 DOI: 10.1016/j.chemgeo.2012.08.017.

(26) Liu, Q. Mercury Concentration in Natural Gas and Its Distribution in the Tarim Basin. *Sci. China Earth Sci.* **2013**, *56* (8), 1371–1379 DOI: 10.1007/s11430-013-4609-2.

(27) Mead, C.; Lyons, J. R.; Johnson, T. M.; Anbar, A. D. Unique Hg Stable Isotope Signatures of Compact Fluorescent Lamp- Sourced Hg. *Environ. Sci. Technol.* **2013**, *47*, 2542–2547 DOI: 10.1021/es303940p.

(28) Mergler, D.; Anderson, H. A.; Chan, L. H. M. H.; Mahaffey, K. R.; Murray, M.; Sakamoto, M.; Stern, A. H.; Panel on Health Risks and Toxicological Effects of Methylmercury. Methylmercury Exposure and Health Effects in Humans: A Worldwide Concern. *Ambio* **2007**, *36* (1), 3–11.

(29) Murphy, G. W.; Newcomb, T. J.; Orth, D. J. Sexual and Seasonal Variations of Mercury in Smailmouth Bass. *J. Freshw. Ecol.* **2007**, *22* (1), 135–144 DOI: 10.1080/02705060.2007.9664153.

(30) Neufeld, D. S. G. Mercury Accumulation in Caged Corbicula: Rate of Uptake and Seasonal Variation. *Environ. Monit. Assess.* **2009**, *168* (1–4), 385–396 DOI: 10.1007/s10661-009-1121-4.

(31) Pirrone, N.; Cinnirella, S.; Feng, X.; Finkelman, R. B.; Friedli, H. R.; Leaner, J.; Mason, R.; Mukherjee, A. B.; Stracher, G. B.; Streets, D. G.; Telmer, K. Global Mercury Emissions to the Atmosphere from Anthropogenic and Natural Sources. *Atmos. Chem. Phys.* **2010**, *10* (13), 5951–5964 DOI: 10.5194/acp-10-5951-2010.

(32) Rodŕiguez-Gonźalez, P.; Epov, V. N.; Bridou, R.; Tessier, E.; Guyoneaud, R.; Monperrus, M.; Amouroux, D. Species-Specific Stable Isotope Fractionation of Mercury during Hg(II) Methylation by an Anaerobic Bacteria (Desulfobulbus Propionicus) under Dark Conditions. *Environ. Sci. Technol.* **2009**, *43* (24), 9183–9188 DOI: 10.1021/es902206j.

(33) Schauble, E. a. Role of Nuclear Volume in Driving Equilibrium Stable Isotope Fractionation of Mercury, Thallium, and Other Very Heavy Elements. *Geochim. Cosmochim. Acta* **2007**, *71* (9), 2170–2189 DOI: 10.1016/j.gca.2007.02.004.

(34) Selin, N. E. Global Biogeochemical Cycling of Mercury: A Review. *Annu. Rev. Environ. Resour.* **2009**, *34* (1), 43–63 DOI: 10.1146/annurev.environ.051308.084314.

(35) Spirić, Z.; Mashyanov, N. R. Mercury Measurements in Ambient Air near Natural Gas Processing Facilities. *Fresenius. J. Anal. Chem.* **2000**, *366* (5), 429–432 DOI: 10.1007/s002160050087.

(36) Washburn, S. J.; Blum, J. D.; Demers, J. D.; Kurz, A. Y.; Landis, R. C. Isotopic Characterization of Mercury Downstream of Historic Industrial Contamination in the South River, Virginia. *Environ. Sci. Technol.* **2017**, *51* (19), 10965–10973 DOI: 10.1021/acs.est.7b02577.

(37) Washburn, S. J.; Blum, J. D.; Johnson, M. W.; Tomes, J. M.; Carnell, P. J. Isotopic Characterization of Mercury in Natural Gas via Analysis of Mercury Removal Unit Catalysts. *ACS Earth Sp. Chem.* **2018**, acsearthspacechem.7b00118 DOI: 10.1021/acsearthspacechem.7b00118.

(38) Washburn, S. J.; Blum, J. D.; Kurz, A.Y.; Pizzuto, J.E. Spatial and Temporal Variation in the Isotopic Composition of Mercury in the South River, VA. *Chem. Geol.* **In Review**

(39) Wiederhold, J. G. Metal Stable Isotope Signatures as Tracers in Environmental Geochemistry. *Environ. Sci. Technol.* **2015**, *49* (5), 2606–2624 DOI: 10.1021/es504683e.

(39) Wiederhold, J. G.; Cramer, C. J.; Daniel, K.; Infante, I.; Bourdon, B.; Kretzschmar, R. Equilibrium Mercury Isotope Fractionation between Dissolved Hg (II) Species and Thiol-Bound Hg. *Environ. Sci. Technol.* **2010**, *44* (11), 4191–4197.

(40) Wilhelm, S. M. *Mercury in Petroleum and Natural Gas: Estimation of Emissions from Production, Processing, and Combustion*; EPA-600/R- 01-066; U.S. Environmental Protection Agency, Office of Research and Development: Washington, DC 20460, 2001. (4)

(41) Yin, R.; Feng, X.; Shi, W. Application of the Stable-Isotope System to the Study of Sources and Fate of Hg in the Environment: A Review. *Appl. Geochemistry* **2010**, *25* (10), 1467–1477 DOI: 10.1016/j.apgeochem.2010.07.007.

(42) Zheng, W.; Hintelmann, H. Nuclear Field Shift Effect in Isotope Fractionation of Mercury during Abiotic Reduction in the Absence of Light. *J. Phys. Chem. A* **2010**, No. 1, 4238–4245.

(43) Zheng, W.; Hintelmann, H. Mercury Isotope Fractionation during Photoreduction in Natural Water Is Controlled by Its Hg/DOC Ratio. *Geochim. Cosmochim. Acta* **2009**, *73* (22), 6704–6715 DOI: 10.1016/j.gca.2009.08.016.

Chapter 2 Isotopic Characterization of Mercury Downstream of Historic Industrial Contamination in the South River, Virginia

Authors: Spencer J. Washburn, Joel D. Blum, Jason D. Demers, Aaron Y. Kurz, and Richard C. Landis

Citation: Washburn, S. J.; Blum, J. D.; Demers, J. D.; Kurz, A. Y.; Landis, R. C. Isotopic Characterization of Mercury Downstream of Historic Industrial Contamination in the South River, Virginia. Environ. Sci. Technol. 2017, 51 (19), 10965–10973.

Abstract: Historic point source mercury (Hg) contamination from industrial processes on the South River (Waynesboro, Virginia) ended decades ago, but elevated Hg concentrations persist in the river system. In an effort to better understand Hg sources, mobility, and transport in the South River, we analyzed total Hg (THg) concentrations and Hg stable isotope compositions of streambed sediments, stream bank soils, suspended particles, and filtered surface waters. Samples were collected along a longitudinal transect of the South River, starting upstream of the historic Hg contamination point-source and extending downstream to the confluence with the South Fork Shenandoah River. Analysis of the THg concentration and Hg isotopic composition of these environmental samples indicates that the regional background Hg source is isotopically distinct in both Δ^{199}Hg and δ^{202}Hg from Hg derived from the original source of contamination, allowing the tracing of contamination-sourced Hg throughout the study reach. Three distinct end-members are required to explain the Hg isotopic and concentration variation observed in the South River. A consistent negative offset in δ^{202}Hg values (~ 0.28‰) was observed between Hg

in the suspended particulate and dissolved phases, and this fractionation provides insight into the processes governing partitioning and transport of Hg in this contaminated river system.

2.1. Introduction

Mercury (Hg) is a toxic trace metal and its global distribution and active geochemical cycle have important environmental and human health implications. Anthropogenic activity has altered how Hg cycles through the environment and there are still many uncertainties regarding critical steps in the Hg biogeochemical cycle.[1] The measurement of Hg isotope ratios in environmental reservoirs has been used to identify sources of anthropogenic Hg and trace the movement of Hg between reservoirs. This has been demonstrated in a number of recent studies in contaminated freshwater river systems,[2-9] as well as in a relatively uncontaminated river system.[10,11] Thus, there is the potential to trace the transport of Hg contamination from industrial sites and to gain insight into chemical and biological transformations of Hg that effect its mobility and bioavailability using Hg stable isotopes.

Mercuric sulfate was used as a catalyst in the production of acetate fibers at the former DuPont textile manufacturing plant in Waynesboro, VA between 1929 and 1950.[12] The production of acetic anhydride produced a sludge that contained mercury, which was transported from one building to another building that housed a retort furnace that was used to recover elemental mercury.[13] During this period, significant amounts of Hg entered the South River, and Hg-contaminated sediments have been identified throughout the channel, river banks, and over-bank deposits of the South River and the South Fork Shenandoah River.[14] A series of studies have demonstrated the ongoing impacts that this Hg contamination has had on the aquatic, riparian, and terrestrial ecosystems of the South River and South Fork Shenandoah River. Ongoing field monitoring data indicate that total Hg and methyl mercury (MeHg) concentrations

in small mouth bass (*Micropterus dolomieu*) remain elevated and have not decreased over the past several decades.[15,16] The migration of legacy aquatic Hg into terrestrial ecosystems has been demonstrated by elevated blood Hg concentrations found in a variety of terrestrial feeding birds,[17,18] as well as models of MeHg biomagnification from contaminated floodplain soils into trophic food webs which include avian predators.[19] MeHg concentrations in sediments during seasonal sampling is not well correlated with total Hg in sediments, suggesting that a complex set of processes are likely controlling mercury methylation and demethylation rates.[16] Thus, significant knowledge gaps exist with regard to spatial and temporal variations in Hg transport, MeHg production, and biotic uptake within the South River. The aim of this study is to provide enhanced insight into the processes controlling the transport and aquatic biogeochemical cycling of Hg in the South River through analysis of the stable Hg isotopic composition of a variety of inorganic mercury (IHg) reservoirs along a longitudinal transect of the South River, Virginia.

2.2 Materials and Methods

2.2.1 Regional Setting

The South River is a fourth order, single-thread, gravel-bed river located in the Valley and Ridge Province of Virginia, USA (Figure S1).[20,21] This study focuses on a 48 km reach of the river, from 4 km upstream of the former DuPont plant in Waynesboro, VA to the confluence of the South River with North River where they become the South Fork of the Shenandoah River in Port Republic, VA. Thirteen mill dams existed between Waynesboro and Port Republic before 1957, but all were breached by 1974.[22] Previous studies have indicated that on the upstream side of these mill dams there were areas of deposition for Hg-laden sediments and today these are areas with elevated rates of bank erosion.[20] Overall, sample sites were chosen to provide a broad understanding of the sources of Hg to the various physical reservoirs in which Hg is stored in the

South River, and of the transport of Hg between these reservoirs and the channel environment. Streambed sediments and bank soils were collected to characterize the Hg isotopic composition at a reach scale between these significant Hg storage reservoirs. Groundwater influxes, release from floodplains, and modern releases from the former DuPont facility could all potentially be additional Hg inputs to the channel, so representative sampling locations for each potential Hg source were chosen. Finally, surface water samples were collected to evaluate the Hg dynamics within the channel. A site on the Middle River about 12 km west of the South River (Figure S1) was chosen as an appropriate reference site due to its lack of known Hg point-source contamination, location in the adjacent valley, and its similar river characteristics.

2.2.2 Sample Collection and Processing

Streambed sediment and bank soil samples were collected from eight locations along the South River channel and from one floodplain pond (Figure S1) in April 2014. Following the convention of previous work on the South River system,[21] sampling locations are labeled according to their distance, in relative river kilometers (RRKm) along the channel from a known historic point source of Hg at the former DuPont plant (e.g., RRKm 0.0). Bulk bank soil samples were collected as composite grab samples from exposed banks. Streambed sediments were collected using a hand-operated PVC bilge pump to effectively sample interstitial fine-grained sediment from between cobbles on the coarse streambed.[21] Sediments and bank soils were collected into acid washed containers in the field. Sample containers were placed on ice in the field, frozen within 8 hours of collection, shipped on ice back to the University of Michigan where they were stored at -18 ºC. Sediment and bank soil samples were subsampled, freeze-dried, and dry sieved through acid-cleaned nylon mesh to remove detritus > 2mm. The < 2mm size fraction was then homogenized in an alumina ball mill that was cleaned between samples.

To evaluate the contributions to the channel from groundwater influxes, bank porewater samples were collected from two permanent piezometer wells installed at the RRKm 5.6 sampling site. Samples were also collected at Wertman pond, a small pond (surface area of 450 m^2) located in the 2-year floodplain, 195m from the main channel of the South River at approximately RRKm 14.5 to better characterize the dynamics of Hg storage within the floodplain environments. To assess the impact of current minor releases of Hg from the former DuPont facility, water was collected from Outfall 001, an outfall pipe with an average output of 0.14 m^3/s that delivers water from an onsite wastewater treatment plant and stormwater system to the South River channel at ~RRKm -0.8.

Filtered stream water and suspended sediment samples were collected under baseflow conditions during June 2014. Samples were collected at each of the locations where sediment and bank soil had been collected, as well as at reference sites on the Middle River (MR-01) and the South Fork Shenandoah (SFR-01) (Figure S1) and the two permanent stream bank piezometers at RRKm 5.6. Water samples were collected, filtered, and preserved in the field, using trace-metal clean sampling methods following a modified EPA Method 1669.[23] Filters were frozen and water samples were placed in refrigerated storage at the end of each sampling day and transported in coolers back to the University of Michigan. Filters were freeze-dried and stored in desiccating chambers. Water samples were oxidized with 1% BrCl (w/v), which was allowed to react with the water sample in dark, refrigerated storage for a minimum of one month.[24] Field blanks were collected periodically during the sampling campaign using 1L of de-ionized water, processed in parallel with samples, and were determined to not contain significantly more Hg than procedural blanks. At each site, 1L of water was collected into a HDPE bottle and used to determine the total suspended solids (TSS) of surface water.[25] TSS

values were used in the calculation of distribution coefficients ($\log(K_d)$) using THg values of the associated filtered surface water and suspended material following the method of Hurley et al. (1998).[26]

2.2.3 Sample Preparation for Isotope Analysis and THg Concentrations

Hg in streambed sediments, bank soils, and suspended materials (filters) was separated for THg concentration and Hg stable isotope measurement by offline combustion, as described in detail elsewhere.[27,28] Filtered surface water was purged and trapped into 1% $KMnO_4$ in 10% H_2SO_4 (w/w) [1% $KMnO_4$] solution for isotope analysis following the procedure outlined in Demers et al. (2013)[28] with slight modifications. Prior to purging and trapping, THg concentrations of each sample bottle were determined by running small aliquots via cold vapor atomic fluorescence spectroscopy [CV-AFS] (Nippon Instruments RA-3000FG+). For each sampling site, the THg concentration for the filtered surface water sample is reported as the average of measured THg concentrations (ng/L) in each bottle collected at that site.

Trapping solutions of both combustion and purge and trap samples were partially reduced with 2% (w/w) of a 30% solution of $NH_2OH{\cdot}HCl$, then a small aliquot was taken and measured for THg by CV-AAS (Nippon Instruments MA-2000). Combustion trap contents were then purged into a secondary 1% $KMnO_4$ trapping solution to remove potential matrix components from combustion residues and to adjust Hg concentrations prior to isotopic analysis.[29,30]

2.2.4 Hg Isotope Analysis

The Hg isotopic composition of the secondary trapping solution was measured by cold vapor multi-collector inductively coupled plasma mass spectrometry (CV-MC-ICP-MS, Nu Instruments). Trapping solutions were partially reduced with a 30% solution of $NH_2OH{\cdot}HCl$ at 2% of the total sample by weight and diluted with a similarly reduced 1%$KMnO_4$ solution to

between 0.95 and 5.7 ng/g. Hg was reduced online to Hg(0) by the addition of 2% (w/w) $SnCl_2$ and separated from solution using a frosted tip gas-liquid separator designed and built at the University of Michigan.[31] Hg(0) was then carried into the MC-ICP-MS inlet by an Ar gas stream. An internal Tl standard (NIST 997) was introduced as a dry aerosol into the carrier Ar gas stream and used to correct for instrumental mass bias. Strict sample-standard bracketing with a solution of NIST 3133 that was matched for both concentration and solution matrix was further used for mass bias correction.[32]

Mercury stable isotope compositions are reported throughout this paper in permil (‰) using delta notation (δ^{xxx}Hg) relative to NIST Standard Reference Material (SRM) 3133 (Eq. 1), with mass dependent fractionation (MDF) based on the $^{202}Hg/^{198}Hg$ ratio (δ^{202}Hg).[32] Mass independent fractionation (MIF) is reported as the deviation from the theoretically predicted δ^{xxx}Hg values based on the kinetic mass fractionation law and is reported with capital delta notation (Δ^{xxx}Hg) according to Eq. 2. In this study MIF is represented with Δ^{199}Hg, Δ^{200}Hg, Δ^{201}Hg, and Δ^{204}Hg, using $\beta = 0.252$, $\beta = 0.502$, $\beta = 0.752$, and $\beta = 1.493$,respectively.[32]

Equation 1: $\delta^{xxx}Hg\ (‰) = ([(^{xxx}Hg/^{198}Hg)_{Sample} / (^{xxx}Hg/^{198}Hg)_{NIST3133}] - 1) \times 1000$

Equation 2: $\Delta^{xxx}Hg\ (‰) = \delta^{xxx}Hg - (\delta^{202}Hg \times \beta)$

Procedural blanks and SRMs (NIST 3133 and NIST SRM 2711 “Montana Soil”) were processed in parallel with samples for THg concentration and Hg isotopic composition. The THg of NIST 2711 measured by offline combustion agreed within 5% of certified values (6.24±0.14µg/g, n=7; Table S2), and recoveries during secondary trapping were 98.8±3.4% (1SD, n=7, min= 91.8%). The Hg isotopic composition of NIST 2711 was consistent with previously reported values (Table S2).[33,34,35] External reproducibility of Hg isotope measurements was estimated from measurements of the standard error (2SE) of the mean

isotopic composition of NIST 2711 replicates and NIST 3133 procedural standard replicates. The analytical uncertainty associated with NIST 2711 was lower than the uncertainty associated with the UM-Almadén standard (Table S2) and we therefore represent the uncertainty of Hg isotope measurements of combustion samples (e.g. bank soils, streambed sediments, and suspended particulates) in this study as the 2SD of mean Hg isotope values of replicate UM-Almadén measurements in this study: ±0.04‰ for δ^{202}Hg and ±0.03‰ for Δ^{199}Hg and Δ^{201}Hg. However, the analytical uncertainty associated with NIST 3133 procedural standards was greater than that associated with UM-Almadén (Table S2). We therefore represent the uncertainty of Hg isotope measurements of filtered surface water samples in this study as the 2SE of mean Hg isotope values of replicate NIST 3133 procedural standards: ±0.13‰ for δ^{202}Hg, ±0.11‰ for Δ^{199}Hg, and ±0.02‰ for Δ^{201}Hg.

2.3. Results and Discussion

2.3.1 Mercury Concentration and Isotopic Variation in Streambed Sediments and Bank Soils

Streambed sediment and bank soil THg concentrations at the site upstream of the historic industrial source (RRKm -4.0) are low (0.08 and 0.04 μg/g, respectively) and similar to other non-impacted sites in fluvial systems in the region.[36] The Hg isotopic composition for streambed sediment at the upstream site is δ^{202}Hg = -1.27 ± 0.04‰, and Δ^{199}Hg = -0.21 ± 0.03‰ and bank soil values are δ^{202}Hg = -1.01 ± 0.04‰ and Δ^{199}Hg = -0.18 ± 0.03‰ (Table S1). The Hg isotopic composition of sediments and soils in this upstream reach of the South River are similar to those previously reported for sediments from non-point-source-impacted streams in the region (δ^{202}Hg of −1.40 ± 0.06‰),[2] which were presumed to be representative of both geogenic Hg inputs and atmospherically deposited Hg to the watershed. In comparison to the regional

background, the concentrations of sediment and bank soil (2.81 and 53.3 μg/g, respectively) found at the first site impacted by industrial contamination (RRKm 0.0) are orders of magnitude higher, representing the substantial amounts of Hg that were added to these reservoirs during the period of Hg use at the historic plant site. Reflecting the industrial source of this Hg, the Hg isotopic composition at this first contamination impacted site, RRKm 0.0, for both sediment (δ^{202}Hg = -0.60 ± 0.04‰, Δ^{199}Hg = 0.04 ± 0.03‰) and bank soils (δ^{202}Hg = -0.65 ± 0.04‰, Δ^{199}Hg = 0.03 ± 0.03‰), is significantly different from background values. These contaminated sediment Hg isotope values are comparable to what has been observed in bulk Hg ores (δ^{202}Hg = -0.56 ± 0.63‰, Δ^{199}Hg = 0.01 ± 0.02‰),[37,38] as well as sediments that have been heavily contaminated by industrial Hg inputs (δ^{202}Hg = -0.42 ± 0.67‰, Δ^{199}Hg = -0.06 ± 0.06‰).[2,39]

The δ^{202}Hg and Δ^{199}Hg values of samples collected along the longitudinal transect of the South River are presented in Figure 1. The THg concentration profiles are in general agreement with previous studies, with concentrations elevated directly downstream of the historic plant site (Table S1).[16,21] Within the initial reach downstream of RRKm 0.0 to RRKm 2.2, the sediment and bank soil have very similar δ^{202}Hg and Δ^{199}Hg values at each sampling site, suggesting that the Hg came from the same industrial source and has not been subjected to processes that cause significant isotope fractionation.

Downstream of RRKm 2.2, both streambed sediments and bank soils display variation in δ^{202}Hg values, while maintaining largely invariant Δ^{199}Hg values (Figure 1). Impacted bank soils have a range of δ^{202}Hg values from -0.18 to -1.05‰, while impacted stream sediments have a range of δ^{202}Hg values from -0.42 to -0.69‰. The much smaller range of δ^{202}Hg values in streambed sediments likely represents the homogenization of Hg inputs from bank soils with variable isotopic compositions, given that bank erosion is the major process thought to be

introducing Hg to the South River channel.[16] The bank soils at two sampling sites, RRKm 13.9 and RRKm 35.4, had the most variable isotopic compositions. At RRKm 13.9, the bank soil has the highest δ^{202}Hg value of any sample in this study (δ^{202}Hg of -0.18 ± 0.04‰, Δ^{199}Hg of 0.01± 0.03‰). In contrast, the bank soil at RRKm 35.4 has the lowest contamination-impacted solid-phase δ^{202}Hg value (δ^{202}Hg of -1.05 ± 0.04‰, Δ^{199}Hg of 0.10± 0.03‰). This is a significant amount of variation in δ^{202}Hg values for bank soils that are still impacted by contamination (THg conc. of 18.2 and 1.11 μg/g, respectively).

We consider two potential explanations for the significant variation in δ^{202}Hg values of impacted bank soils. The first is that Hg in the banks and streambed channel at these particular sampling sites have undergone significant amounts of post depositional fractionation and loss of Hg, and the second is that these sites experienced deposition of industrially sourced Hg with a significantly different isotopic composition. Although we are unable to rule out either of these explanations with the current data, the elevated THg concentrations and significantly different isotopic composition in reaches known to have contained historic mill dams associated with sediment deposits is suggestive of deposition of industrial sources with periodically varying Hg isotopic composition. For post-depositional, within-bank processes (e.g. microbial activity, hydrologic loss of Hg associated with porewater transport, etc.) to impart the variation in isotopic composition observed in these bulk bank soils, there would have to be large-scale reduction and loss of Hg(0) from the sediments. Based on fractionation factors for microbial reduction of Hg(II) to Hg(0),[40] a loss of ~30% of the total Hg pool present in the soils is needed to explain the maximum positive isotopic shift observed in the bank soils relative to the assumed industrial source. However, variations in the isotopic composition of the bulk bank soils are not consistently positive or negative relative to the assumed industrial source, which suggests that a

single fractionation process (e.g., microbial reduction) cannot explain the observed pattern. Given the similarity of the sampling sites, we conclude that it is unlikely that large differences in the relative magnitude of fractionation processes occurs spatially along the study reach and suggest instead that there was variability in the isotopic composition of Hg released from the industrial facility during its operation.

2.3.2 Mercury Concentration and Isotopic Variation in Suspended Particulates and Filtered Surface Water

In the following sections, the THg concentration and isotopic compositions of suspended particulates and filtered surface water are presented. Observation of a novel isotopic partitioning between Hg in the dissolved phase in filtered surface water and particulate-bound Hg in the suspended particulates is discussed, and a fractionation mechanism is proposed to explain the isotopic partitioning.

2.3.2.1 Patterns of Isotopic Variation and Mercury Concentration in Suspended Particulates and Filtered Surface Water in the Study Reach

THg concentrations for the dissolved and suspended particulate loads collected as part of this study are similar to values for previously published longitudinal profiles.[16,21] Reference sites (RRKm -4.0 and Middle River) have low THg concentrations in the dissolved and suspended particulate loads. THg concentrations are significantly elevated in the contamination-impacted portions of the study reach, and decline further downstream while remaining elevated significantly above background levels (Table S1).

Calculation of the distribution coefficient (K_d) between dissolved and suspended Hg is a useful method for describing the partitioning of Hg in fluvial systems. Following the method described by Hurley et al. (1998)[26] we calculated the distribution coefficient between the

suspended particulate and dissolved Hg phases in the South River, which are presented as $\log(K_d)$ values in Table S1. In general, the relatively high $\log(K_d)$ values (6.04 to 6.47) calculated for the South River indicate that Hg is overwhelmingly associated with the suspended particulate phase.[26,41,42] The $\log(K_d)$ values observed in the South River are on the high end of the range of values (2.8 – 6.6) observed in a study of a freshwater rivers in the United States.[42] The $\log(K_d)$ data suggests a slightly greater relative predominance of particle bound Hg in the reach between RRKm 2.2 – 13.9, followed by a decreased predominance of particle bound Hg in the downstream reach, RRKm 13.9-35.4. Although slight changes in the $\log(K_d)$ data are observed longitudinally in the study region, there is no associated change in the isotopic composition of Hg in the dissolved and suspended fractions or in the negative δ^{202}Hg offset between the fractions. The much lower $\log(K_d)$ values observed at the sample sites on the Middle River ($\log(K_d) = 5.58$) and the South Fork Shenandoah River ($\log(K_d) = 5.65$) indicate a lower predominance of particle bound Hg at these sites, which may be related to the much lower THg concentration in sediments at these sites as well as differing Hg speciation and particle composition in point-source contaminated watersheds versus watersheds where Hg is largely of atmospheric origin.

Due to very low THg concentrations, we were unable to obtain Hg isotope values for either suspended particulates or filtered surface water at the RRKm -4.0 reference site. The isotopic composition of Hg in the dissolved loads at both the RRKm 0.0 sampling site (δ^{202}Hg = -1.45 ± 0.13‰, Δ^{199}Hg = 0.06 ± 0.11‰) and RRKm 0.4 sampling site (δ^{202}Hg = -1.45 ± 0.13‰, Δ^{199}Hg = -0.04 ± 0.11‰) vary significantly from that observed at sampling sites in the rest of the impacted reach covered in this study (δ^{202}Hg range -0.95 to -0.79‰, Δ^{199}Hg range 0.02 to 0.32‰) (Figure 1). A similar pattern is observed for the suspended load. For the suspended load,

mixing to the industrial source Hg isotopic value occurs at RRKm 2.2, after which point the δ^{202}Hg values of the suspended load remain relatively constant. Even after such mixing has occurred, the dissolved Hg load maintains significantly lower negative δ^{202}Hg values relative to the suspended load (between -0.30‰ and -0.09‰) (Table S1).In the initial reach below the former DuPont facility (downstream of RRKm 0.0 extending to RRKm 0.4) the suspended load shows a slightly positive Δ^{199}Hg value (~0.10‰), but downstream of this reach there is limited variation in isotopic composition between the suspended load and streambed sediments. Potential hypotheses explaining these longitudinal patterns in isotopic composition of the dissolved and suspended phases are discussed in the following sections.

2.3.2.2 Partitioning Between Dissolved and Suspended Hg

Hg in the dissolved load is isotopically distinct from Hg in the suspended load, with a consistent negative δ^{202}Hg offset (between -0.30‰ and -0.09‰). Despite the fact that some of the filtered surface water samples have δ^{202}Hg values that are within analytical uncertainty (2σ) of the associated suspended sediment samples, the consistent δ^{202}Hg offset observed between filtered surface water and suspended sediment samples is statistically significant throughout the South River study reach [paired t-Test, n=9, T=5.94, p=0.01]. This consistent pattern of negative δ^{202}Hg offset in Hg isotope ratios between suspended particles and dissolved phase Hg contrasts with the pattern observed in the Murray Brook mine watershed by Foucher et al. (2013).[5] Those authors observed no significant relationship between the δ^{202}Hg values of suspended particulates and filtered surface water, but did observe a significant positive δ^{202}Hg offset between filtered surface water and streambed sediments. The authors attributed this apparent fractionation to removal of Hg species from the water column, possibly due to degradation of Hg-cyanide

complexes associated with mine waste leachates, a type of Hg complex we would not expect to be present in the South River.

We hypothesize that the consistent negative δ^{202}Hg offset pattern we observe in the South River is caused by sorption of a relatively small proportion of Hg to high affinity thiol-bearing ligand sites associated with colloidal dissolved organic matter (DOM). Furthermore, we suggest that sorption to these functional groups is inducing an isotopic equilibrium fractionation between the bulk Hg source to the South River and colloid bound Hg, which appears as a fractionation between dissolved and suspended Hg fractions. Hg in the smallest size fraction (referred to throughout as dissolved, but functionally the Hg that passed through a 0.45μm filter) is likely to be associated with colloidal DOM rather that in a truly dissolved form, as colloidal DOM can contain numerous types of ligands with high affinity for Hg.[43]

2.3.2.3 Proposed Mechanism for Observed Fractionation between Suspended and Dissolved Hg

Our explanation for the offset between dissolved and suspended δ^{202}Hg values may at first seem counterintuitive because it does not agree with the expected sign of MDF for the "dissolved" phase observed in experimental studies documented in the literature,[44,45] which suggest that the dissolved phase retains a positive MDF signature during sorption reactions. However, we suggest that a small fraction of the total Hg input into the system undergoes rapid sorption to a limited number of thiol-like moieties with a high affinity for Hg in colloidal DOM, which experience equilibrium fractionation that imparts a more negative δ^{202}Hg value in accordance with sorption experiments. The high-affinity sites associated with the colloidal DOM may quickly become saturated after initial exposure to the bulk Hg source, and the remaining Hg may become associated with larger particulates. Via this mechanism, the larger particulate

fractions would retain a Hg isotopic composition similar to the bulk isotopic composition of the South River system, while the "dissolved" size fraction would obtain a Hg isotopic composition (more negative δ^{202}Hg value) similar to what would be expected experimentally for the sorbed Hg fractions.

Lending support to the hypothesis that colloidal DOM is driving the observed fractionation between "particulate" and "dissolved" phases is the observation that for the sample site (RRKm 5.6) at which surface water was filtered with both 0.45μm and 0.20μm pore sizes, we did not observe a significant difference in isotopic composition or Hg concentration between particulates in these two size fractions (Table S1). A number of studies have shown that Hg(II) binds preferentially to high-affinity reduced organic S sites in organic matter fractions, and that these strong adsorption sites can become saturated, allowing binding sites with lower affinity (containing O- and N- ligands) to dominate Hg(II) binding.[46,47,48] It has also been suggested that Hg in heavily polluted areas is mainly adsorbed onto mineral fractions of bottom sediments, because organic matter sorption sites are rapidly saturated by Hg.[49] Once the high affinity thiol-like sites have all bound Hg, sorption and complexation with lower-affinity DOM ligands and mineral particulates becomes more favorable.

The majority of the Hg in the South River downstream of the industrial site is bound to suspended particulates (62-91%), rather than present in the <0.45μm size fraction. Bonds between Hg and reduced organic S likely exist in the >0.45μm size fraction as well as the <0.45 μm size fraction, but the isotopic composition of the >0.45μm size fraction is dominated by the large pool of Hg associated with particulates in the South River system. The similar isotopic compositions of suspended particulates and streambed sediment at most sampling locations, as well as the relatively high log(K_d) values observed throughout the study reach, support the

hypothesis that the isotopic composition of the suspended particulates is close to the bulk isotopic composition of the contaminated Hg source to the South River.

Previous experimental studies have suggested that binding of Hg with the DOM complex is initially dominated by a kinetic process and that equilibrium conditions are not reached for significant timescales on the order of hours.[50] Although we have hypothesized a fractionation mechanism that occurs under equilibrium conditions in accordance with available experimental data, a prevalence of kinetic processes may explain why the observed isotopic fractionation between dissolved and suspended particles (δ^{202}Hg≈0.20‰) is not as large as that observed during equilibrium sorption experiments (δ^{202}Hg≈0.40‰). Additionally, the processes of re-suspension of particulates from the streambed into the water column and aggregation of colloids to larger particulates may diminish the total observed fractionation by the mixing of fractionated Hg bound to colloids with Hg that retains the bulk isotopic composition of the contaminated source.

Since the offset between dissolved and suspended δ^{202}Hg values is observed throughout the study reach, it would be necessary for Hg to be released into the river channel and exposed to colloidal DOM at numerous points through the study reach to maintain this consistent offset. This scenario is supported by previous work, which suggest that the second largest source of Hg to the South River channel is the diffusive flux of Hg from Hg-laden sediments stored within gravel beds.[16] This flux of Hg from sediments within gravel beds, along with the significant amounts of Hg released due to bank erosion, would provide significant amounts of Hg that could undergo our proposed fractionation mechanism once entrained in the surface water of the channel. Given the significant amount of Hg stored within the sediment gravel beds in the South River, common sources of Hg to the dissolved loads of other fluvial systems, such as

precipitation-derived Hg, are thought to be relatively minor contributors to the total Hg load.[51] Neither the dissolved nor suspended particulate Hg collected from the South River exhibit significant even MIF (Δ^{204}Hg and Δ^{200}Hg) anomalies or patterns that would be indicative of Hg derived from precipitation or other atmospheric sources (Table S1). Alternative explanations for the isotopic pattern observed between suspended particulate Hg and dissolved Hg in the South River is are discussed in detail in Section 2.4.3.

2.3.3 Connections to the Floodplain

The isotopic composition of the porewater sampled from the piezometers at site RRKm 5.6 and the Wertman Pond samples are shown in Figure S2. The Wertman Pond (floodplain pond) bank soil (δ^{202}Hg = -0.68 ± 0.04‰ and Δ^{199}Hg = 0.04 ± 0.03‰), and sediment (δ^{202}Hg = -0.58 ± 0.04‰ and Δ^{199}Hg = 0.04 ± 0.03‰) samples are isotopically very similar to mercury in suspended particulates in the water column directly upstream at RRKm 12.2 (δ^{202}Hg = -0.60 ± 0.04‰ and Δ^{199}Hg = 0.03 ± 0.03‰), consistent with the hypothesis that movement of sediment loads during flood events is a source of mercury to floodplains along the South River.[16] The filtered surface water within the pond (δ^{202}Hg = -0.12 ± 0.13‰ and Δ^{199}Hg = 0.57 ± 0.11‰) has a distinctly more elevated Δ^{199}Hg value compared to the sediment within the pond, and Δ^{204}Hg and Δ^{200}Hg values (-0.01 ± 0.17‰ and 0.10 ± 0.10‰, respectively) that are not significantly different from 0.00‰. The lack of an even MIF anomaly in the filtered surface water suggests that the Hg in the dissolved phase is unlikely to have been derived from atmospheric sources, instead suggesting that significant photochemical reduction of Hg has occurred within this environment. Using the fractionation factors for photochemical reduction of Hg(II), the δ^{202}Hg value prior to photochemical reduction of the Hg in the dissolved phase can be calculated, giving a value of δ^{202}Hg = -0.56‰ for the dissolved phase without the influence of photoreduction.[32]

The similarity of this to the δ^{202}Hg value of the sediment in the pond (δ^{202}Hg = -0.58‰) suggests that the Hg in the dissolved phase was likely sourced from the pond sediments.

At RRKm 5.6, we observe that the dissolved Hg load in bank porewater is isotopically distinct in δ^{202}Hg values (P1-B δ^{202}Hg = -0.61 ± 0.13‰ and P3-B δ^{202}Hg = -0.40 ± 0.13‰) from the suspended load (P1-B δ^{202}Hg = -0.83 ± 0.04‰ and P3-B δ^{202}Hg = -0.66 ± 0.04‰) for both of the sampled wells (Table S1). Porewater from the P-3B well has a Δ^{199}Hg value that is distinct from that of the surrounding bank soil. We suggest that this is the result of two fractionation processes occurring simultaneously. The first process is the sorption of Hg in the dissolved phase to particulates, including Fe-oxides and thiol functional groups.[44,45] , which is in agreement with the positive δ^{202}Hg shift between suspended and dissolved bank porewater Hg. This interpretation is supported by the high distribution coefficients in these piezometer waters. The second process that we suggest is occurring within the river banks is that Hg, which has been photochemically reduced in surface water within the stream channel, is flowing through the hyporheic zone and mixing with Hg in porewater within the banks. This flow path is in agreement with the general discharge flow patterns observed for this section of the river bank, as flow can be parallel to channel flow for this particular bank section.[52] The Hg that has undergone partial photochemical reduction and evasion in the surface water in the river channel will have positive Δ^{199}Hg values such as those seen at the most immediate upstream site of the piezometers (RRKm 2.2, Δ^{199}Hg = 0.32 ± 0.11‰),[53] and mixing would result in elevated Δ^{199}Hg values of the Hg within the porewater relative to the Hg in the associated bank soils. To date, the reactions that have been demonstrated to cause significant amounts of positive MIF under dark conditions such as those within the stream banks (e.g. equilibrium evaporation and dark abiotic reduction) produce Hg(0) vapor with a more negative δ^{202}Hg value than the starting reactant pool of Hg

stored within the banks.[54,55] If these reactions were occurring at a significant level within the banks then we would expect the produced Hg(0) to either evade, or be re-oxidized and reincorporated into the dissolved/suspended phases. However, the δ^{202}Hg values of the porewater and suspended particulates in both sampled wells are more positive than the associated bank soil, allowing us to rule out contributions to a MIF signature from dark reactions. Since these processes can be ruled out, the observation of positive MIF signatures within the bank porewater suggests that Hg derived from surface water, that has been photochemically processed is infiltrating the hyporheic zone and isotopic mixing is occurring with bank porewater Hg at this sampling site.

The observation of positive MIF in the piezometer waters suggests that surface water containing photochemically reduced Hg is exchanging and mixing with the bank porewater Hg at this location. This result implies that with further sampling and analysis, the influence of bank porewater on dissolved Hg in river water may be traceable and it may be possible to detect Hg originating from surface water. Yin et al. (2013)[38] conducted experiments to determine the water soluble fraction of Hg stored within soils contaminated due to Hg mine waste, and observed a positive isotopic fractionation in the water soluble Hg fraction of δ^{202}Hg ≈ 0.7‰ compared to the isotopic composition of the Hg entrained within the soils. This observation does not match well with our observation of more positive δ^{202}Hg values in the bank porewater as compared to the bulk bank soil. This difference may reflect contrasts in the Hg speciation within the soil matrix between the two study sites, as Hg is predominantly found in the bank soils of the South River as metacinnabar,[16] and Hg found in the mine waste contaminated soils by Yin et al. (2013)[38] was mainly in the form of mine waste calcine, which contains within it a mixture of cinnabar, metacinnabar and mercuric chloride.

2.3.4 Identification of Unknown Hg Source Via Hg Endmember Mixing Model

In order to better understand the contributions that present-day release of legacy Hg from the former DuPont site is having on the isotopic composition of Hg in the South River channel system, water samples were collected from a plant outfall (Outfall 001) that drains the onsite wastewater treatment facility (see Section 2.4.2.2 for sampling details). It was suspected that Hg found in the outflow of this plant outfall might be representative of the small amounts of legacy Hg that have been documented to be flushed from the stormwater system at the plant,[13,16] and that the released legacy Hg may have had a distinct isotopic composition that could potentially explain some of the variation observed in the surface water and suspended particulate isotopic composition profiles in the channel near the plant site. However, the Hg isotopic composition of both the filtered surface water (δ^{202}Hg =-0.73 ‰ and Δ^{199}Hg = 0.12‰) and suspended particulates (δ^{202}Hg =-0.34 ‰ and Δ^{199}Hg = 0.15‰) of Outfall 001 are similar to what is observed in contamination impacted bank soils and streambed sediments downstream of the former plant site, not what is observed in the channel where Outfall 001 discharges into the river. Additionally, the contribution of Outfall 001 to the total Hg concentration observed in the channel is relatively small. Outfall 001 contributes ~10% of the total Hg flux in the channel of South River at RRKm 00.0 as calculated from discharge at the Waynesboro USGS gauge due to relatively low discharge and moderate THg concentrations. Thus, the Hg input from Outfall 001 is not able to explain the low δ^{202}Hg values observed in the filtered surface water and suspended particulates at RRKm 0.0 and RRKm 0.4 (Figure 1).

In order to better understand the changing Hg isotopic values between RRKm 0.0 and RRKm 2.2, we first considered the simple situation of a 2 end-member model of Hg in suspended particulates involving a regional background isotopic composition and an end-member reflecting

the Hg isotope composition of contaminated Hg. Although we chose to focus on Hg in suspended particulates because we had been able to measure a reference site value (Middle River), the following arguments also hold true for Hg in the dissolved load. A number of previous studies have shown the utility of Hg isotope analysis as a tool for determining Hg sources and mixing in contaminated aquatic environments.[2,8,56] The Middle River reference site was used to represent the regional background Hg isotopic end-member (δ^{202}Hg =-1.22‰ and THg = 2.03 ng/L), and we used the average of contamination impacted sediment δ^{202}Hg values to represent the industrially contaminated isotopic end-member (δ^{202}Hg =-0.59±0.11‰ [±1SD] and THg = 7465 µg/L). This two end-member mixing model fails to account for the observed variation in δ^{202}Hg values for suspended particulates, particularly for the RRKm 0.0 site, which has a deviation of nearly -0.60‰ from the expected value based on a 2 end-member mixing line. Although some deviation from a mixing line would be expected due to possible in situ fractionation processes occurring at each sampling site, for this degree of isotopic shift to occur due to localized fractionation processes at sampling sites RRKm 0.0 and RRKm 0.4, large amounts of Hg (> 65%) would have to be lost from the system and this interpretation is not supported by the THg data from these sites (Table S1). We therefore suggest that a 3 end-member mixing model is necessary to explain the observed variation in isotopic composition and THg concentration observed in this reach of the South River, with the third end-member being of an unknown origin with a high THg concentration (~10 ng/L) and relatively negative δ^{202}Hg value (~ -1.10‰) (Figure 2). It is important to note that the identification of this end-member is not necessarily indicative of greater Hg inputs to the South River channel, as the two sites with high THg concentrations and relatively negative δ^{202}Hg compositions (RRKm 0.0 & 0.4) do not

have THg concentrations above what has previously been attributed to contamination related to processes at the DuPont plant.[16,21]

The unknown end-member may be representative of legacy Hg with a different isotopic composition (δ^{202}Hg ~ -1.10‰) than the majority of the legacy Hg in the South River system ((δ^{202}Hg ~ -0.65‰), which is currently being released from the area of the plant site. The different isotopic composition of the Hg that makes up this unknown end-member could be related to use of varying Hg ore or liquid Hg^0 sources during the period of industrial Hg use at the DuPont plant, as different Hg ores and liquid Hg^0 sources have been shown to have varying isotopic compositions (δ^{202}Hg range of -3.88 to 2.10‰ for Hg ores and -1.05 to 0.05‰ for liquid Hg^0).[37,38,39,57,58] Alternatively, current release of Hg to the channel in this reach may be associated with a Hg reservoir with a different isotopic composition resulting from a different part of the acetic anhydride production process or it could be due to fractionation caused by the onsite Hg retort process. A previous study has demonstrated that the same industrial process (chlor-alkali process) can produce contamination with a range of Hg isotopic values that vary in δ^{202}Hg by up to 0.80‰ at a given site, and up to 2.60‰ between sites using the same source of Hg ore.[56] Even if the Hg ore or liquid Hg^0 source did not change during the period of Hg use at the former DuPont facility, changes in the catalytic process or of the retorting to recover Hg could likely produce Hg waste with an isotopic composition that varied by the amount observed between end-members (δ^{202}Hg = 0.45‰). Previous work on fractionation associated with Hg ore retorting demonstrated that Hg^0_{liq} and co-produced Hg^0_{gas} can differ in δ^{202}Hg values by 1.31‰ on average, a range more than double that observed between South River end-members.[59]

Acknowledgements

We thank Marcus Johnson for his generous assistance and guidance in operating the CV-MC-ICP-MS. The authors acknowledge partial funding from E.I. du Pont de Nemours and Company. We would also like to thank the members of the South River Science Team for their beneficial discussions and assistance.

Figure 2.1 Longitudinal profiles along the South River of Hg isotopic composition.

Longitudinal profiles along the South River of Hg isotopic composition. Sampling locations are presented in relative river kilometers [see Section 2.2.2]. The analytical uncertainty of Hg isotopic measurements (2σ) is presented based on the sample preparation method used, with bank soils, sediments, and suspended particulates represented as combusted samples, and dissolved phase Hg associated with the uncertainty of filtered water samples.

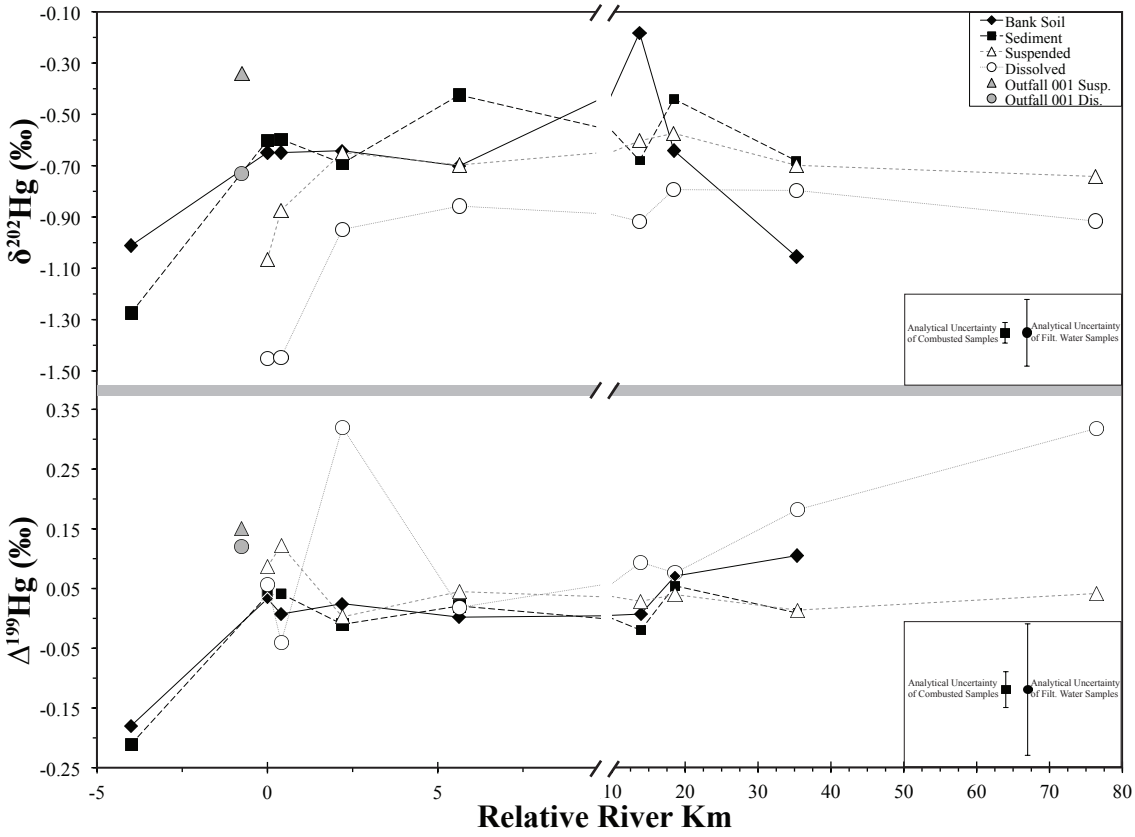

Figure 2.2 Three end-member isotopic mixing model for suspended particulates in the South River

Three end-member isotopic mixing model for suspended particulates in the South River, presented as 1/THg conc. (L/ng of Hg) vs. δ^{202}Hg values. Analytical uncertainty of Hg isotopic measurements (2σ) is displayed for suspended particulates. The mean (±1σ) of δ^{202}Hg values for streambed sediments is shown as a black square for reference. Grey areas represent suggested end-member ranges, and black lines (solid and dashed) are lines of isotopic mixing.

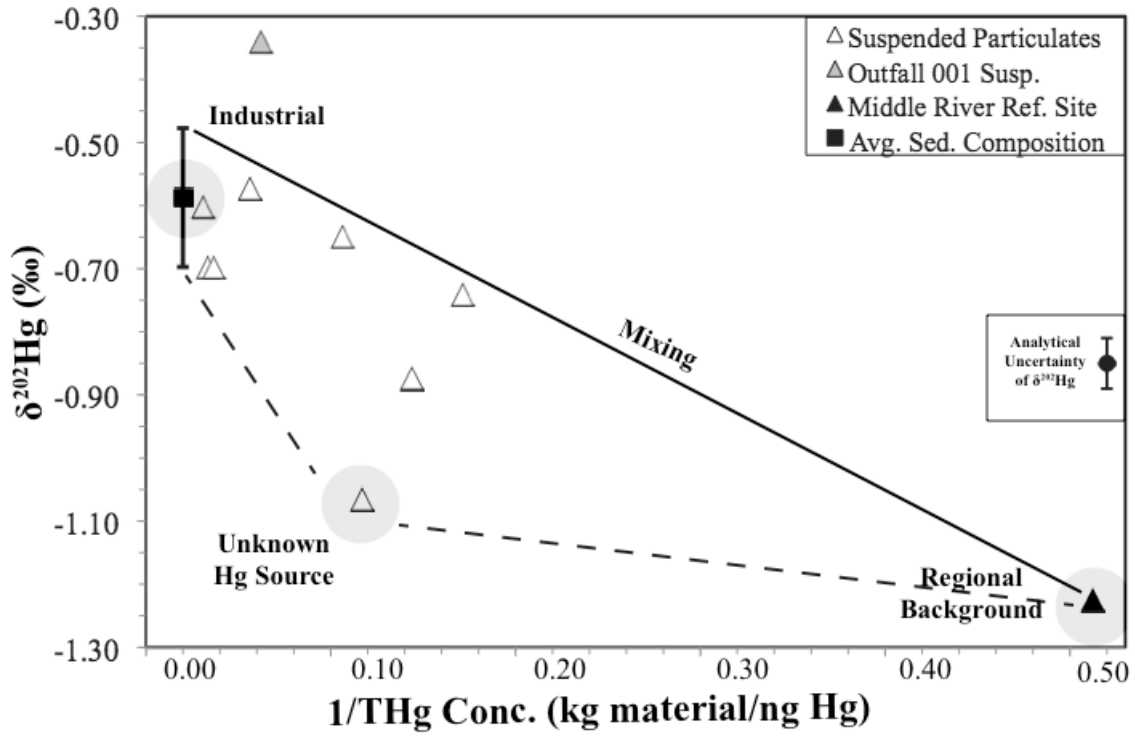

References

(1) Selin, N. E. Global Biogeochemical Cycling of Mercury: A Review. *Annu. Rev. Environ. Resour.* **2009**, 34 (1), 43–63 DOI: 10.1146/annurev.environ.051308.084314.

(2) Donovan, P. M.; Blum, J. D.; Demers, J. D.; Gu, B.; Brooks, S. C.; Peryam, J. Identification of Multiple Mercury Sources to Stream Sediments near Oak Ridge, TN, USA. *Environ. Sci. Technol.* **2014**, *48* (7), 3666–3674.

(3) Donovan, P. M.; Blum, J. D.; Singer, M. B.; Marvin-DiPasquale, M.; Tsui, M. T. K. Isotopic Composition of Inorganic Mercury and Methylmercury Downstream of a Historical Gold Mining Region. *Environ. Sci. Technol.* **2016**, *50* (4), 1691–1702 DOI: 10.1021/acs.est.5b04413.

(4) Donovan, P. M.; Blum, J. D.; Singer, M. B.; Marvin-DiPasquale, M.; Tsui, M. T. K. Methylmercury Degradation and Exposure Pathways in Streams and Wetlands Impacted by Historical Mining. *Sci. Total Environ.* **2016,** *568*, 1192-1203 DOI: 10.1016/j.scitotenv.2016.04.139.

(5) Foucher, D.; Hintelmann, H.; Al, T. A.; MacQuarrie, K. T. Mercury Isotope Fractionation in Waters and Sediments of the Murray Brook Mine Watershed (New Brunswick, Canada): Tracing Mercury Contamination and Transformation. *Chem. Geol.* **2013**, *336*, 87–95 DOI: 10.1016/j.chemgeo.2012.04.014.

(6) Smith, R. S.; Wiederhold, J. G.; Jew, A. D.; Brown, G. E.; Bourdon, B.; Kretzschmar, R. Stable Hg Isotope Signatures in Creek Sediments Impacted by a Former Hg Mine. *Environ. Sci. Technol.* **2015**, *49* (2), 767–776 DOI: 10.1021/es503442p.

(7) Yin, R.; Feng, X.; Wang, J.; Li, P.; Liu, J.; Zhang, Y.; Chen, J.; Zheng, L.; Hu, T. Mercury Speciation and Mercury Isotope Fractionation during Ore Roasting Process and Their Implication to Source Identification of Downstream Sediment in the Wanshan Mercury Mining Area, SW China. *Chem. Geol.* **2013**, *336*, 72–79 DOI: 10.1016/j.chemgeo.2012.04.030.

(8) Liu, J.; Feng, X.; Yin, R.; Zhu, W.; Li, Z. Mercury Distributions and Mercury Isotope Signatures in Sediments of Dongjiang, the Pearl River Delta, China. *Chem. Geol.* **2011**, *287* (1–2), 81–89 DOI: 10.1016/j.chemgeo.2011.06.001.

(9) Sonke, J. E.; Schäfer, J.; Chmeleff, J.; Audry, S.; Blanc, G.; Dupré, B. Sedimentary Mercury Stable Isotope Records of Atmospheric and Riverine Pollution from Two Major European Heavy Metal Refineries. *Chem. Geol.* **2010**, *279* (3–4), 90–100 DOI: 10.1016/j.chemgeo.2010.09.017.

(10) Tsui, M. T. K.; Blum, J. D.; Kwon, S. Y.; Finlay, J. C.; Balogh, S. J.; Nollet, Y. H. Sources and Transfers of Methylmercury in Adjacent River and Forest Food Webs. *Environ. Sci. Technol.* **2012**, *46* (20), 10957–10964 DOI: 10.1021/es3019836.

(11) Tsui, M. T. K.; Blum, J. D.; Finlay, J. C.; Balogh, S. J.; Kwon, S. Y. Photodegradation of Methylmercury in Stream Ecosystems. *Limnol. Oceanogr.* **2013**, *58* (1), 13–22 DOI: 10.4319/lo.2013.58.1.0013.

(12) Carter, L. J. Chemical Plants Leave Unexpected Legacy for Two Virginia Rivers. *Science* **1977**, *198* (4321), 1015–1020 DOI: 10.1126/science.198.4321.1015.

(13) URS Corporation. *Comprehensive RFI Report. Former DuPont Waynesboro Plant, Waynesboro, Virginia*. Revised 2015(a). southriverscienceteam.org/news

(14) Turner, R. R.; Southworth, G. R. Mercury-Contaminated Industrial and Mining Sites in North America: An Overview with Selected Case Studies. In *Mercury Contaminated Sites: Characterization, Risk Assessment*

and Remediation; Ebinghaus, R., Turner, R. R., de Lacerda, L. D., Vasiliev, O., Salomons, W., Eds.; Springer Berlin Heidelberg: Berlin, Heidelberg, 1999; pp 89–112.

(15) Murphy, G. W.; Newcomb, T. J.; Orth, D. J. Sexual and Seasonal Variations of Mercury in Smailmouth Bass. *J. Freshw. Ecol.* **2007**, *22* (1), 135–144 DOI: 10.1080/02705060.2007.9664153.

(16) URS Corporation. *Final Report: Ecological Study of the South River and a Segment of the South Fork Shenandoah River, Virginia*. Revised 2012. southriverscienceteam.org/news

(17) Cristol, D. A; Brasso, R. L.; Condon, A. M.; Fovargue, R. E.; Friedman, S. L.; Hallinger, K. K.; Monroe, A. P.; White, A. E. The Movement of Aquatic Mercury through Terrestrial Food Webs. *Science* **2008**, *320* (5874), 335 DOI: 10.1126/science.1154082.

(18) Jackson, A. K.; Evers, D. C.; Folsom, S. B.; Condon, A. M.; Diener, J.; Goodrick, L. F.; McGann, A. J.; Schmerfeld, J.; Cristol, D. A. Mercury Exposure in Terrestrial Birds Far Downstream of an Historical Point Source. *Environ. Pollut.* **2011**, *159* (12), 3302–3308 DOI: 10.1016/j.envpol.2011.08.046.

(19) Newman, M. C.; Xu, X.; Condon, A.; Liang, L. Floodplain Methylmercury Biomagnification Factor Higher than that of the Contiguous River (South River, Virginia USA). *Environ. Pollut.* **2011**, *159* (10), 2840–2844 DOI: 10.1016/j.envpol.2011.04.045.

(20) Rhoades, E. L.; O'Neal, M. A.; Pizzuto, J. E. Quantifying Bank Erosion on the South River from 1937 to 2005, and Its Importance in Assessing Hg Contamination. *Appl. Geogr.* **2009**, *29* (1), 125–134 DOI: 10.1016/j.apgeog.2008.08.005.

(21) Flanders, J. R.; Turner, R. R.; Morrison, T.; Jensen, R.; Pizzuto, J.; Skalak, K.; Stahl, R. Distribution, Behavior, and Transport of Inorganic and Methylmercury in a High Gradient Stream. *Appl. Geochemistry* **2010**, *25* (11), 1756–1769 DOI: 10.1016/j.apgeochem.2010.09.004.

(22) Pizzuto, J.; O'Neal, M. A. Increased Mid-Twentieth Century Riverbank Erosion Rates Related to the Demise of Mill Dams, South River, Virginia. *Geology* **2009**, *37* (1), 19–22 DOI: 10.1130/G25207A.1.

(23) USEPA. 1996. Method 1669: Sampling Ambient Water for Trace metals at EPA Water Quality Criteria Levles. U.S. Environmental Protection Agency, Office of Water, Engineering and Analysis Division (4303), Washington, D.C. USA.

(24) Hammerschmidt, C. R.; Bowman, K. L.; Tabatchnick, M. D.; Lamborg, C. H. Storage Bottle Material and Cleaning for Determination of Total Mercury in Seawater. *Limnol. Oceanogr. Methods*. **2011**, 9 (10), 426–431 DOI: 10.4319/lom.2011.9.426.

(25) USEPA. 1999. Method 160.2: Total Suspended Solids (TSS). U.S. Environmental Protection Agency, Office of Water, Engineering and Analysis Division (4303), Washington, D.C. USA.

(26) Hurley, J. P.; Cowell, S. E.; Shafer, M. M.; Hughes, P. E. Partitioning and Transport of Total and Methyl Mercury in the Lower Fox River, Wisconsin. *Environ. Sci. Technol.* **1998**, *32* (10), 1424-1432 DOI: http://pubs.acs.org/doi/pdf/10.1021/es970685b.

(27) Biswas, A.; Blum, J. D.; Bergquist, B. A.; Keeler, G. J.; Xie, Z. Natural Mercury Isotope Variation in Coal Deposits and Organic Soils. *Environ. Sci. Technol.* **2008**, *42* (22), 8303–8309 DOI: 10.1021/es801444b.

(28) Demers, J. D.; Blum, J. D.; Zak, D. R. Mercury Isotopes in a Forested Ecosystem: Implications for Air-Surface Exchange Dynamics and the Global Mercury Cycle. *Global Biogeochem. Cycles* **2013**, *27* (1) 222-238 DOI: 10.1002/gbc.20021.

(29) Sherman, L. S.; Blum, J. D. Mercury Stable Isotopes in Sediments and Largemouth Bass from Florida Lakes, USA. *Sci. Total Environ.* **2013**, *448*, 163–175 DOI: 10.1016/j.scitotenv.2012.09.038.

(30) Blum, J. D.; Johnson, M. W. Recent Developments in Mercury Stable Isotope Analysis. *Rev. Mineral. Geochemistry* **2017**, *82* (1), 733–757 DOI: 10.2138/rmg.2017.82.17.

(31) Lauretta, D. S.; Klaue, B.; Blum, J. D.; Buseck, P. R. Mercury Abundances and Isotopic Compositions in the Murchison (CM) and Allende (CV) Carbonaceous Chondrites. *Geochim. Cosmochim. Acta* **2001**, *65* (16), 2807–2818 DOI: 10.1016/S0016-7037(01)00630-5.

(32) Blum, J. D.; Bergquist, B. A. Reporting of Variations in the Natural Isotopic Composition of Mercury. *Anal. Bioanal. Chem.* **2007**, *388* (2), 353–359 DOI: 10.1007/s00216-007-1236-9.

(33) Estrade, N.; Carignan, J.; Donard, O. F. X. Tracing and Quantifying Anthropogenic Mercury Sources in Soils of Northern France Using Isotopic Signatures. *Environ. Sci. Technol.* **2011**, *45* (4), 1235–1242 DOI: 10.1021/es1026823.

(34) Jiskra, M.; Wiederhold, J. G.; Skyllberg, U.; Kronberg, R. M.; Hajdas, I.; Kretzschmar, R. Mercury Deposition and Re-Emission Pathways in Boreal Forest Soils Investigated with Hg Isotope Signatures. *Environ. Sci. Technol.* **2015**, *49* (12), 7188–7196 DOI: 10.1021/acs.est.5b00742.

(35) Yin, R.; Feng, X.; Hurley, J. P.; Krabbenhoft, D. P.; Lepak, R. F. Mercury Isotopes as Proxies to Identify Sources and Environmental Impacts of Mercury in Sphalerites. *Sci. Rep.* **2016**, November 2015, 1–8 DOI: 10.1038/srep18686.

(36) Bauch, N. J.; Chasar, L. C.; Scudder, B. C.; Moran, P. W.; Hitt, K. J.; Brigham, M. E.; Lutz, M. A.; Wentz, D. A. Data on Mercury in Water , Bed Sediment , and Fish from Streams Across the United States , 1998 – 2005. *U.S. Geol. Surv. Data Ser. 307* **2009**, 33.

(37) Smith, C. N.; Kesler, S. E.; Blum, J. D.; Rytuba, J. J. Isotope Geochemistry of Mercury in Source Rocks, Mineral Deposits and Spring Deposits of the California Coast Ranges, USA. *Earth Planet. Sci. Lett.* **2008**, *269* (3–4), 398–406 DOI: 10.1016/j.epsl.2008.02.029.

(38) Yin, R.; Feng, X.; Wang, J.; Bao, Z.; Yu, B.; Chen, J. Mercury Isotope Variations between Bioavailable Mercury Fractions and Total Mercury in Mercury Contaminated Soil in Wanshan Mercury Mine, SW China. *Chem. Geol.* **2013**, *336*, 80–86 DOI: 10.1016/j.chemgeo.2012.04.017.

(39) Wiederhold, J. G.; Smith, R. S.; Siebner, H.; Jew, A. D.; Brown, G. E.; Bourdon, B.; Kretzschmar, R. Mercury Isotope Signatures as Tracers for Hg Cycling at the New Idria Hg Mine. *Environ. Sci. Technol.* **2013**, *47* (12), 6137–6145 DOI: 10.1021/es305245z.

(40) Kritee, K.; Blum, J. D.; Johnson, M. W.; Bergquist, B. A.; Barkay, T. Mercury Stable Isotope Fractionation during Microbial Reduction of Hg(II) to Hg(0). *Environ. Sci. Technol.* **2007**, *41* (6), 1889–1895.

(41) Lindström, M. Distribution of Particulate and Reactive Mercury in Surface Waters of Swedish Forest Lakes - An Empirically Based Predictive Model. *Ecol. Modell.* **2001**, *136* (1), 81–93 DOI: 10.1016/S0304-3800(00)00382-3.

(42) Brigham, M. E.; Wentz, D. A; Aiken, G. R.; Krabbenhoft, D. P. Mercury Cycling in Stream Ecosystems . 1 . Water Column Chemistry and Transport. *Environ. Sci. Technol.* **2009**, *43* (8), 2720–2725 DOI: 10.1021/es802694n.

(43) Liu, G.; Li, Y.; Cai, Y. Adsorption of Mercury on Solids in the Aquatic Environment. In *Environmental Chemistry and Toxicology of Mercury*; Liu, G., Cai, Y., O'Driscoll, N., Eds.; John Wiley & Sons, Inc., 2012; pp 367–387.

(44) Jiskra, M.; Wiederhold, J. G.; Bourdon, B.; Kretzschmar, R. Solution Speciation Controls Mercury Isotope Fractionation of Hg(II) Sorption to Goethite. *Environ. Sci. Technol.* **2012**, *46* (12), 6654–6662 DOI:

10.1021/es3008112.

(45) Wiederhold, J. G.; Cramer, C. J.; Daniel, K.; Infante, I.; Bourdon, B.; Kretzschmar, R. Equilibrium Mercury Isotope Fractionation between Dissolved Hg(II) Species and Thiol-Bound Hg. *Environ. Sci. Technol.* **2010**, *44* (11), 4191–4197.

(46) Hesterberg, D.; Chou, J. W.; Hutchison, K. J.; Sayers, D. E. Bonding of Hg(II) to Reduced Organic Sulfur in Humic Acid as Affected by S/Hg Ratio. *Environ. Sci. Technol.* **2001**, *35* (13), 2741–2745 DOI: 10.1021/es001960o.

(47) Hintelmann, H.; Harris, R. Application of Multiple Stable Mercury Isotopes to Determine the Adsorption and Desorption Dynamics of Hg(II) and MeHg to Sediments. *Mar. Chem.* **2004**, *90* (1–4 SPEC. ISS.), 165–173 DOI: 10.1016/j.marchem.2004.03.015.

(48) Skyllberg, U.; Bloom, P. R.; Qian, J.; Lin, C. M.; Bleam, W. F. Complexation of mercury(II) in Soil Organic Matter: EXAFS Evidence for Linear Two-Coordination with Reduced Sulfur Groups. *Environ. Sci. Technol.* **2006**, *40* (13), 4174–4180 DOI: 10.1021/es0600577.

(49) Hissler, C.; Probst, J. L. Chlor-Alkali Industrial Contamination and Riverine Transport of Mercury: Distribution and Partitioning of Mercury between Water, Suspended Matter, and Bottom Sediment of the Thur River, France. *Appl. Geochemistry* **2006**, *21* (11), 1837–1854 DOI: 10.1016/j.apgeochem.2006.08.002.

(50) Miller, C. L.; Southworth, G.; Brooks, S.; Liang, L.; Gu, B. Kinetic Controls on the Complexation between Mercury and Dissolved Organic Matter in a Contaminated Environment. *Environ. Sci. Technol.* **2009**, *43* (22), 8548–8553 DOI: 10.1021/es901891t.

(51) Eggleston, J. Mercury Loads in the South River and Simulation of Mercury Total Maximum Daily Loads (TMDLs) for the South River, South Fork Shenandoah River, and Shenandoah River—Shenandoah Valley, Virginia. *US Geol. Surv. Scientific Investigations Report* **2009**-5076

(52) URS Corporation. *Memorandum: RRM 3.5 Study Area Hydrological Evaluation and Groundwater Flux Estimates (May – October 2013)*. Revised 2015(b).

(53) Bergquist, B. A; Blum, J. D. Mass-Dependent and -Independent Fractionation of Hg Isotopes by Photoreduction in Aquatic Systems. *Science* **2007**, *318* (5849), 417–420 DOI: 10.1126/science.1148050.

(54) Ghosh, S.; Schauble, E. A.; Lacrampe Couloume, G.; Blum, J. D.; Bergquist, B. A. Estimation of Nuclear Volume Dependent Fractionation of Mercury Isotopes in Equilibrium Liquid–vapor Evaporation Experiments. *Chem. Geol.* **2013**, *336*, 5–12 DOI: 10.1016/j.chemgeo.2012.01.008.

(55) Zheng, W.; Hintelmann, H. Nuclear Field Shift Effect in Isotope Fractionation of Mercury during Abiotic Reduction in the Absence of Light. *J. Phys. Chem. A* **2010**, No. 1, 4238–4245.

(56) Wiederhold, J. G.; Skyllberg, U.; Drott, A.; Jiskra, M.; Jonsson, S.; Björn, E.; Bourdon, B.; Kretzschmar, R. Mercury Isotope Signatures in Contaminated Sediments as a Tracer for Local Industrial Pollution Sources. *Environ. Sci. Technol.* **2015**, *49* (1), 177–185.

(57) Smith, C. N.; Kesler, S. E.; Klaue, B.; Blum, J. D. Mercury Isotope Fractionation in Fossil Hydrothermal Systems. *Geology* **2005**, *33* (10), 825 DOI: 10.1130/G21863.1.

(58) Laffont, L.; Sonke, J. E.; Maurice, L.; Monrroy, S. L.; Chincheros, J.; Amouroux, D.; Behra, P. Hg Speciation and Stable Isotope Signatures in Human Hair as a Tracer for Dietary and Occupational Exposure to Mercury. *Environ. Sci. Technol.* **2011**, 45 (23), 9910–9916 DOI: 10.1021/es202353m.

(59) Gray, J. E.; Pribil, M. J.; Higueras, P. L. Mercury Isotope Fractionation during Ore Retorting in the Almaden Mining District, Spain. *Chem. Geol*. **2013**, 357, 150–157 DOI: 10.1016/j.chemgeo.2013.08.036.

2.4 Supporting Information

2.4.1. Unabridged Materials and Methods

2.4.1.1 Regional Setting

The South River is a fourth order, single-thread, gravel-bed river located in the Valley and Ridge Province of Virginia, USA (Figure S1).[1,2] This study focuses on a 48 km reach of the river, from 4 km upstream of the former DuPont plant in Waynesboro, VA to the confluence of the South River with North River where they become the South Fork of the Shenandoah River in Port Republic, VA. The South River has a drainage basin of approximately 606 km^2 at the confluence with the North River. The riverbed is primarily composed of cobble and boulder substrates with fine-grained sediments making up less than 15% of the bed sediment.[2,3] The South River flows through a sequence of unconsolidated Quaternary deposits that overlie the bedrock in this region.[3] Thirteen mill dams existed between Waynesboro and Port Republic before 1957, but all were breached by 1974. Previous studies have indicated that areas on the upstream side of these mill dams may have been areas of deposition for Hg-laden sediments and today are areas with elevated rates of bank erosion.[1] Overall, sample sites were chosen to provide a broad understanding of the sources of Hg to the various physical reservoirs in which Hg is stored in the South River, and of the transport of Hg between these reservoirs and the channel environment. Streambed sediments and bank soils were collected to characterize the Hg isotopic composition at a reach scale between these significant Hg storage reservoirs. Groundwater influxes, release from floodplains, and modern releases from the former DuPont facility could all potentially be additional Hg inputs to the channel, so representative sampling locations for each potential Hg source were chosen. Finally, surface water samples were collected to evaluate the Hg dynamics within the channel. A site on the Middle River about 12 km west of the South

River (Figure S1) was chosen as an appropriate reference site due to its lack of known Hg point-source contamination, location in the adjacent valley, and its similar river characteristics.

2.4.1.2 Sample Collection and Processing

Streambed sediment and bank soil samples were collected from eight locations along the South River channel, and from one floodplain pond (Figure S1) in April 2014. Following the convention of previous work on the South River system,[2] sampling locations are labeled according to their distance, in relative river kilometers (RRKm) along the channel from a known historic point source of Hg at the former DuPont plant (e.g., RRKm 0.0). Bulk bank soil samples were collected as composite grab samples from exposed banks. Streambed sediments were collected using a hand-operated PVC bilge pump to effectively sample interstitial fine-grained sediment from between cobbles on the coarse streambed.[2] Sediments and bank soils were collected into acid washed containers in the field. Sample containers were placed on ice in the field, frozen within 8 hours of collection, shipped on ice back to the University of Michigan, where they were stored at -18 ºC. Sediment and bank soil samples were subsampled, freeze-dried, and dry sieved through acid-cleaned nylon mesh to remove detritus > 2mm. The < 2mm size fraction was then homogenized in an alumina ball mill that was cleaned between samples.

To evaluate the contributions to the channel from groundwater influxes, bank porewater samples were collected from two permanent piezometer wells installed at the RRKm 5.6 sampling site. These piezometers were located 2.4m (P1-B) and 6.9m (P3-B) from the edge of the river channel. Both wells were set into river gravel deposits, at depths of 1.8m (P1-B) and 2.1m (P3-B). Groundwater discharge rates for this section of bank were found to vary between 8 to 50 L/day/m of bank length, with discharge flow direction typically oriented towards the southeast, parallel to the flow of the river channel.[4] Samples were also collected at Wertman

pond, a small pond (surface area of 450 m^2) located in the 2-year floodplain, 195m from the main channel of the South River at approximately RRKm 14.5 to better characterize the dynamics of Hg storage within the floodplain environments. To assess the impact of current minor releases of Hg from the former DuPont facility, water was collected from Outfall 001, an outfall pipe with an average output of 0.14 m^3/s that delivers water from an onsite wastewater treatment plant and stormwater system to the South River channel at ~RRKm -0.8. Outfall water was collected via an exposed access point with a portable peristaltic pump configured with pre-cleaned Teflon tubing, and filtered using the same method described below for in-channel stream waters.

Filtered stream water and suspended sediment samples were collected under baseflow conditions during June 2014. Samples were collected at each of the locations where sediment and bank soil had been collected, as well as at reference sites on the Middle River (MR-01) and the South Fork Shenandoah (SFR-01) (Figure S1) and the two permanent stream bank piezometers at RRKm 5.6. Water samples were collected, filtered, and preserved in the field, using trace-metal clean sampling methods following a modified EPA Method 1669.[5] Water samples were collected from the middle of the channel using an acid-cleaned HDPE bottle, in which samples remained for no more than 15 minutes, then filtered into acid-cleaned 1 L borosilicate glass media bottles containing 5mL of concentrated HCl (trace metal grade). Water samples were filtered using a hand operated vacuum-pump and disposable, pre-cleaned 0.45µm pore-size cellulose nitrate vacuum filter housings (Thermo Scientific). At one site, RRKm 5.6, surface water was filtered through vacuum filter housings with 0.20µm pore-size cellulose nitrate filters in addition to the 0.45µm pore-size filters. Filters were removed from the vacuum housing with acid cleaned forceps, placed in individual acid-cleaned petri dishes, and sealed with Teflon

tape. Filters were frozen and water samples were placed in refrigerated storage at the end of each sampling day and transported in coolers back to the University of Michigan. Filters were freeze-dried and stored in desiccating chambers. Water samples were oxidized with 1% BrCl (w/v), which was allowed to react with the water sample in dark, refrigerated storage for a minimum of one month.[22] Procedural field blanks were collected periodically during the sampling campaign using 1L of de-ionized water. Filters and de-ionized water were processed in parallel with the samples, then checked for THg concentration to assess potential contamination. Filtered water field blanks were subsampled and THg concentrations were analyzed by cold-vapor atomic fluorescence spectroscopy [CV-AFS] (following a modified EPA Method 1631)[19]. All filtered water field blanks (n=5) had THg concentrations that were below method detection limits of 0.2 ng/L. At each site, 1L of water was collected into a HDPE bottle and used to determine the total suspended solids (TSS) of surface water.[6] TSS values were used in the calculation of distribution coefficients ($\log(K_d)$) using THg values of the associated filtered surface water and suspended material following the method of Hurley et al. (1998).[7] For bank porewater samples collected from capped piezometer wells, 1L of porewater was removed from each piezometer with a portable peristaltic pump and acid-cleaned tubing and discarded. Subsequently, an additional 1L of porewater was collected and filtered according to the procedure outlined above for surface water.

2.4.1.3 Sample Preparation for Isotope Analysis and THg Concentrations

Hg in streambed sediments, bank soils, and suspended materials (filters) was separated for THg concentration and Hg stable isotope measurement by offline combustion, as described in detail elsewhere.[8,9] Briefly, 0.01 to 1.00 g of sample was packed into a ceramic boat and placed into the first stage of a two-furnace combustion system. Freeze dried filters were cut with a clean

stainless steel razor blade and packed into ceramic boats in a similar manner to ground samples. The first-stage furnace was slowly ramped to 750 ºC over a six hour period while the second-stage furnace was held at 1000 ºC. Hg released from the sample matrix was carried through the combustion tube in a flow of Hg-free O_2 and into a 1% $KMnO_4$ in 10% H_2SO_4 (w/w) [1% $KMnO_4$] trapping solution.

Filtered surface water was purged and trapped into 1% $KMnO_4$ solution for isotope analysis, following the procedure outlined in Demers et al. (2013)[9] with slight modifications. Approximately 1L of previously acidified and oxidized surface water was weighed into a clean 2L borosilicate glass media bottle. Samples were treated with 10 ml of concentrated hydroxylamine hydrochloride to destroy free halogens, capped tightly, and allowed to react for a minimum of 30 minutes. Through one port of a three-port Teflon transfer cap, 100mL of 10% $SnCl_2$ was delivered to the reaction bottle via a peristaltic pump, at a rate of ~3.3 ml/min. Another port delivered Hg-free air (Au-filtered) to sparge the ~1L sample volume into the reactor headspace, while the final port removed gas from the reactor headspace into a borosilicate glass trap containing between 5.5 and 7.0 g of 1% $KMnO_4$ trapping solution. Samples were purged for 3 hours while being vigorously stirred with a clean Teflon stir bar. Prior to purging and trapping, THg concentrations of each sample bottle were determined by running small aliquots via CV-AFS (Nippon Instruments RA-3000FG+). For each sampling site, the THg concentration for the filtered surface water sample is reported as the average of measured THg concentrations (ng/L) in each bottle collected at that site. To determine Hg recovery, the THg concentration of small aliquots of each 1%$KMnO_4$ trapping solution were determined prior to transfer into a secondary trapping solution. Purge and trap recoveries of filtered surface water samples ranged between 90.3% and 109.4%, with an average of 98.7±5.4%

(1SD, n=19).

Trapping solutions of both combustion and purge and trap samples were partially reduced with 2% (w/w) of a 30% solution of $NH_2OH{\cdot}HCl$, then a small aliquot was taken and measured for THg by CV-AAS (Nippon Instruments MA-2000). Combustion trap contents were then purged into a secondary 1% $KMnO_4$ trapping solution to remove potential matrix components from combustion residues and to adjust Hg concentrations prior to isotopic analysis.[10,11] Hg recovery during this transfer into secondary 1% $KMnO_4$ trapping solution was evaluated by taking small aliquots of the secondary trapping solution and analyzing the THg concentration by CV-AAS. Hg recoveries for this process ranged from 83.2% to 106.3% with an average of 97.8±4.2 (1SD, n=43).

Procedural blanks were processed in parallel with samples for THg concentration and Hg isotopic composition. The trap contents of combusted field filter blanks contained 153±30 pg of Hg (n=5, ± 1SD), which is not significantly different from procedural combustion blanks (159±87 pg of Hg, n=6, ± 1SD). Offline combustion procedural blanks (including field blank filters) yielded between 81.4 and 264 pg of Hg (n=11, mean±1SD = 156±64pg), representing at most no more than 7.8% of Hg in sample combustion trap solutions. Purge and trap procedural blanks yielded between 46.3 and 252 pg of Hg (n=10, mean±1SD = 102±79pg), representing at most no more than 5.9% of Hg in sample trap solutions.

2.4.1.4 Hg Isotope Analysis

The Hg isotopic composition of the secondary trapping solution was measured by cold vapor multi-collector inductively coupled plasma mass spectrometry (CV-MC-ICP-MS, Nu Instruments). Trapping solutions were partially reduced with a 30% solution of $NH_2OH{\cdot}HCl$ at 2% of the total sample by weight and diluted with a similarly reduced 1%$KMnO_4$ solution to

between 0.95 and 5.7 ng/g. Hg was reduced online to Hg(0) by the addition of 2% (w/w) $SnCl_2$ and separated from solution using a frosted tip gas-liquid separator designed and built at the University of Michigan.[12] Hg(0) was then carried into the MC-ICP-MS inlet by an Ar gas stream. An internal Tl standard (NIST 997) was introduced as a dry aerosol into the Ar gas stream and used to correct for instrumental mass bias. Strict sample-standard bracketing with a solution of NIST 3133 that was matched for both concentration and solution matrix was further used for mass bias correction.[13]

Mercury stable isotope compositions are reported throughout this paper in permil (‰) using delta notation (δ^{xxx}Hg) relative to NIST Standard Reference Material (SRM) 3133 (Eq. 1), with mass dependent fractionation (MDF) based on the $^{202}Hg/^{198}Hg$ ratio (δ^{202}Hg).[13] Mass independent fractionation (MIF) is reported as the deviation from the theoretically predicted δ^{xxx}Hg values based on the kinetic mass fractionation law and is reported with capital delta notation (Δ^{xxx}Hg) according to Eq. 2. In this study MIF is represented with Δ^{199}Hg, Δ^{200}Hg, Δ^{201}Hg, and Δ^{204}Hg, using $\beta = 0.252$, $\beta = 0.502$, $\beta = 0.752$, and $\beta = 1.493$,respectively.[13]

Equation 1: $\delta^{xxx}Hg\ (‰) = ([(^{xxx}Hg/^{198}Hg)_{Sample} / (^{xxx}Hg/^{198}Hg)_{NIST3133}] - 1) \times 1000$

Equation 2: $\Delta^{xxx}Hg\ (‰) = \delta^{xxx}Hg - (\delta^{202}Hg \times \beta)$

Standard reference materials (NIST 3133 and NIST SRM 2711"Montana Soil") were processed in parallel with samples for THg concentration and Hg isotopic composition. The THg of NIST 2711 measured by offline combustion agreed within 5% of certified values (6.24±0.14µg/g, n=7; Table 2), and recoveries during secondary trapping were 98.8±3.4% (1SD, n=7, min= 91.8%). The Hg isotopic composition of NIST 2711 was consistent with previously reported values (Table S2).[14,15,16] External reproducibility of Hg isotope measurements was estimated from measurements of the standard error (2SE) of the mean isotopic composition of

NIST 2711 replicates and NIST 3133 procedural standard replicates. The analytical uncertainty associated with NIST 2711 was lower than the uncertainty associated with the UM-Almadén standard (Table S2) and we therefore represent the uncertainty of Hg isotope measurements of combustion samples (e.g. bank soils, streambed sediments, and suspended particulates) in this study as the 2SD of mean Hg isotope values of replicate UM-Almadén measurements in this study: ±0.04‰ for δ^{202}Hg and ±0.03‰ for Δ^{199}Hg and Δ^{201}Hg. However, the analytical uncertainty associated with NIST 3133 procedural standards was greater than that associated with UM-Almadén (Table S2). We therefore represent the uncertainty of Hg isotope measurements of filtered surface water samples in this study as the 2SE of mean Hg isotope values of replicate NIST 3133 procedural standards: ±0.13‰ for δ^{202}Hg, ±0.11‰ for Δ^{199}Hg, and ±0.02‰ for Δ^{201}Hg.

2.4.2. Discussion of Δ^{199}Hg values of Hg in the dissolved load in South River surface water

Hg in the dissolved fraction of surface water has Δ^{199}Hg values within analytical uncertainty (Δ^{199}Hg ± 0.11‰)) of 0.0‰ for most of the study area, similar to the suspended load. However, the dissolved fraction shows significantly elevated Δ^{199}Hg values in two locations, RRKm 2.2 and RRKm 76.4, suggesting photochemical reduction and loss of Hg is occurring in the reaches upstream of these sites (RRKm 0.4 – 2.2 and downstream of RRKm 35.4). Assuming that the major fractionation process inducing MIF in the dissolved phase in these two reaches is photochemical reduction of inorganic Hg, the amount of Hg that has evaded from surface waters can be estimated following the method outlined in Bergquist and Blum (2007)[17] based on their data from Hg photochemical reduction experiments. Calculations were made under the following assumptions: first, that contributions of MeHg photoreduction to the isotopic composition of the dissolved Hg were small; and second, that the starting Δ^{199}Hg value

at each site was 0.0‰ for the dissolved Hg. These are reasonable assumptions given that previous work has shown that filter-passing MeHg concentrations typically represent less than 10% of filtered THg in South River surface water,[2] and this study has demonstrated that contamination impacted Hg in bank soils, sediments and suspended particulates have Δ^{199}Hg values that are near 0.0‰ and largely invariant. Hg loss was calculated using an experimentally determined slope value for a linearized Rayleigh distillation model:

$$\ln(f) = [10^3 \times \ln(10^{-3} \times \Delta^{199}Hg_{Sample} + 1)] / S$$

where S = -1.0054, slope for Hg^{2+} photoreduction based on experimental data and f = fraction of Hg remaining in the dissolved phase.[17]

This calculation indicates that ~27% of the Hg that was originally in the dissolved load at RRKm 2.2 and RRKm 76.4 has been photochemically reduced and evaded from the surface waters. Increased amounts of photochemistry may be occurring within these reaches due to relatively less extensive tree canopy cover and a relatively wider and shallower river channel. Inputs of additional Hg from the bank soils and streambed sediments with Δ^{199}Hg values near 0.0‰ to the water column in the channel may explain the impermanence of the photochemical signal in the dissolved Hg load. We also considered the possibility of bank-erosion derived release of Hg that had been exposed to high levels of photochemical reduction during sediment storage behind historic mill dams, but neither of the reaches which exhibit elevated MIF signatures contained mill dams, and no elevated MIF signatures were observed within the reach that contained the majority of the historic mill dams (~RRKm 5 to RRKm 30).[18]

2.4.3. Alternative Explanations for the Isotopic Pattern Observed in Suspended and Dissolved Hg

The explanation presented in the main text (Sections 2.3.2.1-2.3.2.3) is not the only possible scenario for the observed Hg isotopic difference between the different particle size fractions in the South River. An alternate explanation is that rather than fractionation between the dissolved phase and other phases, the observed isotopic variation is instead the result of end-member mixing between isotopically distinct Hg associated with different size fractions. However, we currently have no evidence for two different Hg isotope sources that would partition to different size fractions of particulates. A third possibility is that metallic Hg (Hg^0_{liq}) stored in the banks is releasing Hg^0_{diss} into solution. Metallic Hg was found at the former plant site,[20] and although the contaminated soil bearing liquid Hg was subsequently remediated, there remains the possibility that small amounts of liquid Hg were mobilized prior to remediation and are still present in the river system. Previous experimental work has shown that equilibrium evaporation of Hg^0_{liq} to Hg^0_{vap} can induce significant $\delta^{202}Hg_{liquid\text{-}vapor}$ fractionation of -1.0 to -1.3‰ for the vapor phase relative to the isotopic composition of the liquid Hg.[21] Although the relevant experiments have not been performed, it is possible that release of Hg from the liquid phase into a dissolved phase could induce a similar fractionation. Thus the $\delta^{202}Hg$ offset observed between the particulate and dissolved phases in the South River channel may represent the influence of Hg^0_{diss} originating from Hg^0_{liq}, but without additional evidence for the occurrence of liquid Hg, this explanation seems less likely than the explanation outlined in Section 2.3.2.2.

Table 2.1 Summary of THg concentration, log(K_d) values, and Hg stable isotope data of collected samples.

River	Location	Sampling Effort	Sample Type	THg	THg	log(K_d)	δ^{204}Hg	δ^{202}Hg	δ^{201}Hg	δ^{200}Hg	δ^{199}Hg	Δ^{204}Hg	Δ^{201}Hg	Δ^{200}Hg	Δ^{199}Hg
				ng/L	µg/g (d.w.)		‰	‰	‰	‰	‰	‰	‰	‰	‰
South River	Upstream Reference Site RRKm - 4.0	Jun-14	Filtered Surface Water	0.21		6.19	NA	NA	NA	NA	NA	NA	NA	NA	NA
		Jun-14	Suspended Material	0.35			NA	NA	NA	NA	NA	NA	NA	NA	NA
		Apr-14	Streambed Sediment		0.08		-1.92	-1.27	-1.16	-0.62	-0.53	-0.02	-0.20	0.02	-0.21
		Apr-14	Bulk Bank Soil		0.04		-1.58	-1.01	-0.98	-0.53	-0.43	-0.07	-0.22	-0.02	-0.18
	Outfall 001 (~RRKm - 0.8)	Jul-15	Filtered Surface Water	13.20		NA	-1.10	-0.73	-0.52	-0.30	-0.07	-0.01	0.03	0.06	0.12
		Jul-15	Suspended Material	23.80			-0.49	-0.34	-0.15	-0.14	0.07	0.03	0.11	0.03	0.15
	RRKm 0.0	Jun-14	Filtered Surface Water	4.64		6.04	-2.15	-1.45	-1.04	-0.82	-0.31	0.02	0.05	-0.09	0.06
		Jun-14	Suspended Material	10.31			-1.50	-1.06	-0.77	-0.54	-0.18	0.09	0.03	-0.01	0.09
		Apr-14	Streambed Sediment		2.81		-0.88	-0.60	-0.46	-0.30	-0.11	0.01	-0.01	0.00	0.04
		Apr-14	Bulk Bank Soil		53.27		-0.97	-0.65	-0.47	-0.35	-0.13	0.00	0.02	-0.02	0.03
	RRKm 0.4	Jun-14	Filtered Surface Water	4.88		6.11	-2.24	-1.45	-1.05	-0.84	-0.40	-0.08	0.04	-0.11	-0.04
		Jun-14	Suspended Material	8.07			-1.26	-0.87	-0.59	-0.47	-0.10	0.04	0.06	-0.03	0.12
		Apr-14	Streambed Sediment		11.08		-0.94	-0.60	-0.43	-0.32	-0.11	-0.05	0.02	-0.02	0.04
		Apr-14	Bulk Bank Soil		65.42		-0.99	-0.65	-0.48	-0.33	-0.16	-0.02	0.01	0.00	0.01
	RRKm 2.2	Jun-14	Filtered Surface Water	3.12		6.35	-1.62	-0.95	-0.58	-0.40	0.08	-0.20	0.13	0.07	0.32
		Jun-14	Suspended Material	11.60			-1.00	-0.65	-0.52	-0.30	-0.16	-0.03	-0.03	0.03	0.00
		Apr-14	Streambed Sediment		7.73		-1.04	-0.69	-0.54	-0.37	-0.18	-0.01	-0.02	-0.02	-0.01
		Apr-14	Bulk Bank Soil		11.57		-0.93	-0.64	-0.47	-0.31	-0.14	0.03	0.02	0.01	0.02
	RRKm 5.6	Jun-14	Filtered Surface Water	7.04		6.47	-1.26	-0.86	-0.58	-0.44	-0.20	0.02	0.06	-0.01	0.02
		Jun-14	Suspended Material	75.09			-1.13	-0.70	-0.45	-0.34	-0.13	-0.09	0.07	0.01	0.04
		Jun-14	Suspended Material (0.20µm)	61.18			-1.00	-0.69	-0.48	-0.30	-0.15	0.03	0.03	0.04	0.02
		Apr-14	Streambed Sediment		45.56		-0.62	-0.42	-0.32	-0.22	-0.09	0.01	0.00	0.00	0.02
		Apr-14	Bulk Bank Soil		29.37		-1.05	-0.70	-0.51	-0.37	-0.17	-0.01	0.01	-0.02	0.00
	RRKm 13.9	Jun-14	Filtered Surface Water	9.69		6.33	-1.48	-0.92	-0.60	-0.46	-0.14	-0.11	0.09	0.00	0.09
		Jun-14	Suspended Material	92.99			-0.90	-0.60	-0.44	-0.28	-0.12	0.00	0.01	0.02	0.03
		Apr-14	Streambed Sediment		13.65		-0.93	-0.68	-0.49	-0.31	-0.19	0.08	0.02	0.03	-0.02
		Apr-14	Bulk Bank Soil		18.19		-0.24	-0.18	-0.16	-0.06	-0.04	0.03	-0.02	0.03	0.01
	RRKm 18.6	Jun-14	Filtered Surface Water	9.40		6.14	-1.22	-0.79	-0.55	-0.37	-0.12	-0.03	0.04	0.03	0.08
		Jun-14	Suspended Material	27.69			-0.89	-0.57	-0.41	-0.25	-0.11	-0.04	0.02	0.03	0.04
		Apr-14	Streambed Sediment		13.78		-0.70	-0.44	-0.32	-0.21	-0.06	-0.04	0.01	0.01	0.05
		Apr-14	Bulk Bank Soil		14.33		-1.01	-0.64	-0.44	-0.30	-0.09	-0.06	0.04	0.02	0.07
	RRKm 35.4	Jun-14	Filtered Surface Water	9.17		6.19	-1.17	-0.79	-0.55	-0.35	-0.02	0.01	0.05	0.05	0.18
		Jun-14	Suspended Material	59.90			-1.01	-0.70	-0.48	-0.37	-0.16	0.03	0.04	-0.02	0.01
		Apr-14	Streambed Sediment		5.13		-1.02	-0.68	-0.51	-0.37	-0.16	-0.01	0.00	-0.03	0.01
		Apr-14	Bulk Bank Soil		1.11		-1.60	-1.05	-0.85	-0.53	-0.16	-0.03	-0.05	0.00	0.10

	Wertman Pond (~RRKm 14.5)	Jun-14	Filtered Surface Water	8.01		6.11	-0.20	-0.12	0.18	0.03	0.54	-0.01	0.27	0.10	0.57
		Jun-14	Suspended Material	103.42			-1.14	-0.77	-0.54	-0.40	-0.11	0.02	0.04	-0.01	0.09
		Apr-14	Sediment		10.74		-0.85	-0.58	-0.41	-0.28	-0.10	0.02	0.03	0.01	0.04
		Apr-14	Bulk Bank Soil		15.42		-1.01	-0.68	-0.49	-0.32	-0.13	0.00	0.02	0.02	0.04
	P-1-B RRKm 5.6 Piezometer	Jun-14	Filtered Porewater	31.85		6.20	-0.90	-0.61	-0.35	-0.29	-0.10	0.01	0.11	0.02	0.06
		Jun-14	Suspended Material	1149.37			-1.23	-0.83	-0.63	-0.43	-0.19	0.00	-0.01	-0.02	0.02
	P-3-B RRKm 5.6 Piezometer	Jun-14	Filtered Porewater	12.29		6.73	-0.82	-0.40	-0.19	-0.23	0.02	-0.23	0.11	-0.03	0.12
		Jun-14	Suspended Material	2565.50			-0.96	-0.66	-0.48	-0.34	-0.13	0.03	0.02	-0.01	0.04
Middle River	Reference Site	Jun-14	Filtered Surface Water	0.42		5.58	NA	NA	NA	NA	NA	NA	NA	NA	NA
		Jun-14	Suspended Material	2.03			-1.86	-1.22	-0.99	-0.59	-0.32	-0.03	-0.07	0.02	-0.01
South Fork Shenandoah River	Reference Site (~RRKm 76.4)	Apr-14	Filtered Surface Water	2.14		5.65	-1.42	-0.91	-0.54	-0.29	0.09	-0.05	0.15	0.17	0.32
		Apr-14	Suspended Material	6.61			-1.12	-0.74	-0.54	-0.34	-0.15	-0.02	0.02	0.03	0.04

Table 2.2 Summary of THg concentration and Hg stable isotope values of Standards and Reference Materials

For SRMS's, N1 denotes the total number of process replicates and N2 denotes the total number of isotope measurements during all analytical sessions. Theta (σ) denotes the standard error of the mean values for process replicates. For UM-Almaden, N1 denotes the number of isotope measurements, N2 denotes the number of analytical sessions that UM Almaden was measured and theta represents the standard deviation of Hg isotope values for individual UM-Almaden measurements between July 2014 and October 2015 during which the run solution concentrations were either between 3 and 5 ng/g, or less than 3 ng/g.

Reference Material	N1	N2	THg	2σ	δ^{204}Hg	2σ	δ^{202}Hg	2σ	δ^{201}Hg	2σ	δ^{200}Hg	2σ	δ^{199}Hg	2σ	Δ^{204}Hg	2σ	Δ^{201}Hg	2σ	Δ^{200}Hg	2σ	Δ^{199}Hg	2σ
			µg/g	µg/g	‰	‰	‰	‰	‰	‰	‰	‰	‰	‰	‰	‰	‰	‰	‰	‰	‰	‰
NIST 3133 P&T Proc. Ref	5	6			-0.03	0.13	0.01	0.13	-0.04	0.13	0.01	0.15	-0.05	0.14	-0.12	0.17	-0.10	0.02	-0.05	0.10	-0.07	0.11
NIST 2711 Proc. Ref.	7	12	6.24	0.28	-0.32	0.07	-0.20	0.04	-0.33	0.04	-0.11	0.03	-0.28	0.02	-0.03	0.04	-0.18	0.02	-0.01	0.01	-0.23	0.01
UM-Almaden (This study)	30	6			-0.87	0.05	-0.59	0.04	-0.48	0.02	-0.30	0.04	-0.17	0.04	0.01	0.09	-0.04	0.03	0.00	0.03	-0.02	0.03
UM-Almaden (3-5 ppb)	214	39			-0.85	0.18	-0.57	0.13	-0.46	0.12	-0.28	0.11	-0.17	0.11	0.00	0.14	-0.03	0.08	0.01	0.09	-0.02	0.10
UM-Almaden (<3 ppb)	46	9			-0.83	0.35	-0.56	0.21	-0.46	0.20	-0.28	0.19	-0.19	0.20	0.01	0.33	-0.04	0.19	0.00	0.17	-0.05	0.19

Figure 2.3 **Location of sampling locations along the South River**

Sampling locations are labeled according to their distance downstream (relative river kilometer, RRKm) of the historic point source at the former DuPont plant site in Waynesboro. Map modified from Ref (3).

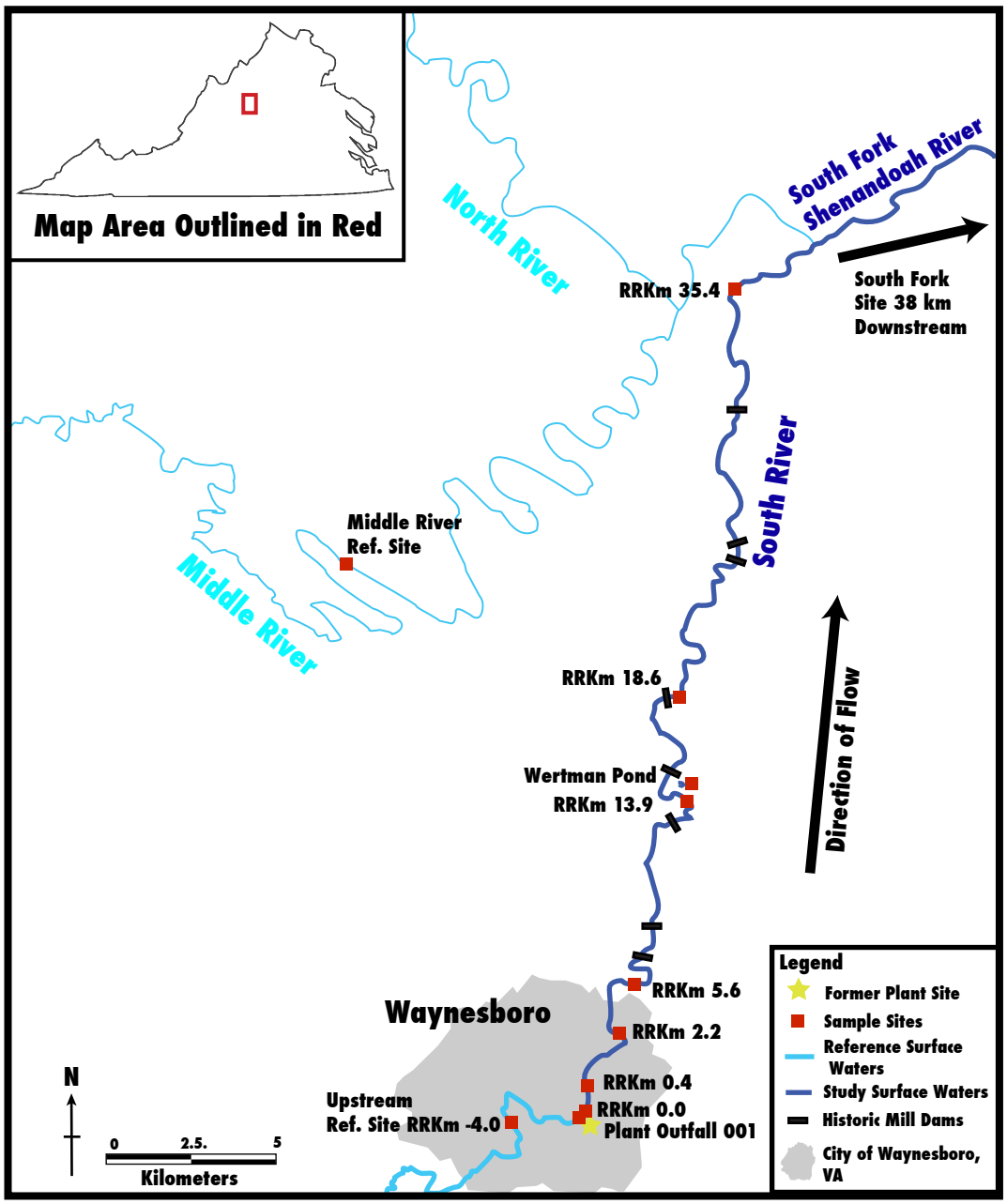

Figure 2.4 Plot of δ^{202}Hg values vs. Δ^{199}Hg values of South River samples

The analytical uncertainty of Hg isotopic measurements (2σ) is presented based on the sample preparation method used, with bank soils, sediments, and suspended particulates represented as combusted samples, and dissolved phase Hg associated with the uncertainty of filtered water samples.

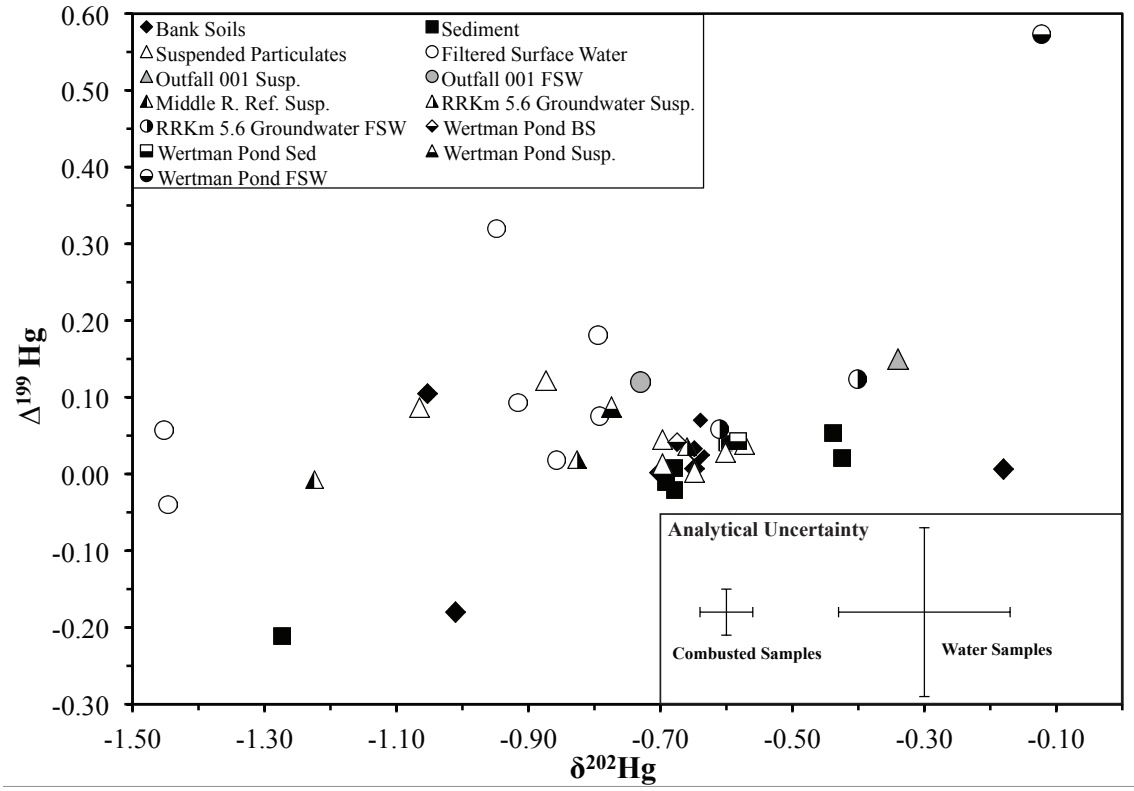

Figure 2.5 Plot of Δ^{201}Hg values vs. Δ^{199}Hg values of South River samples

The black line represents a linear regression line of all collected samples. The analytical uncertainty of Hg isotopic measurements (2σ) is presented based on the sample preparation method used, with bank soils, sediments, and suspended particulates represented as combusted samples, and dissolved phase Hg associated with the uncertainty of filtered water samples.

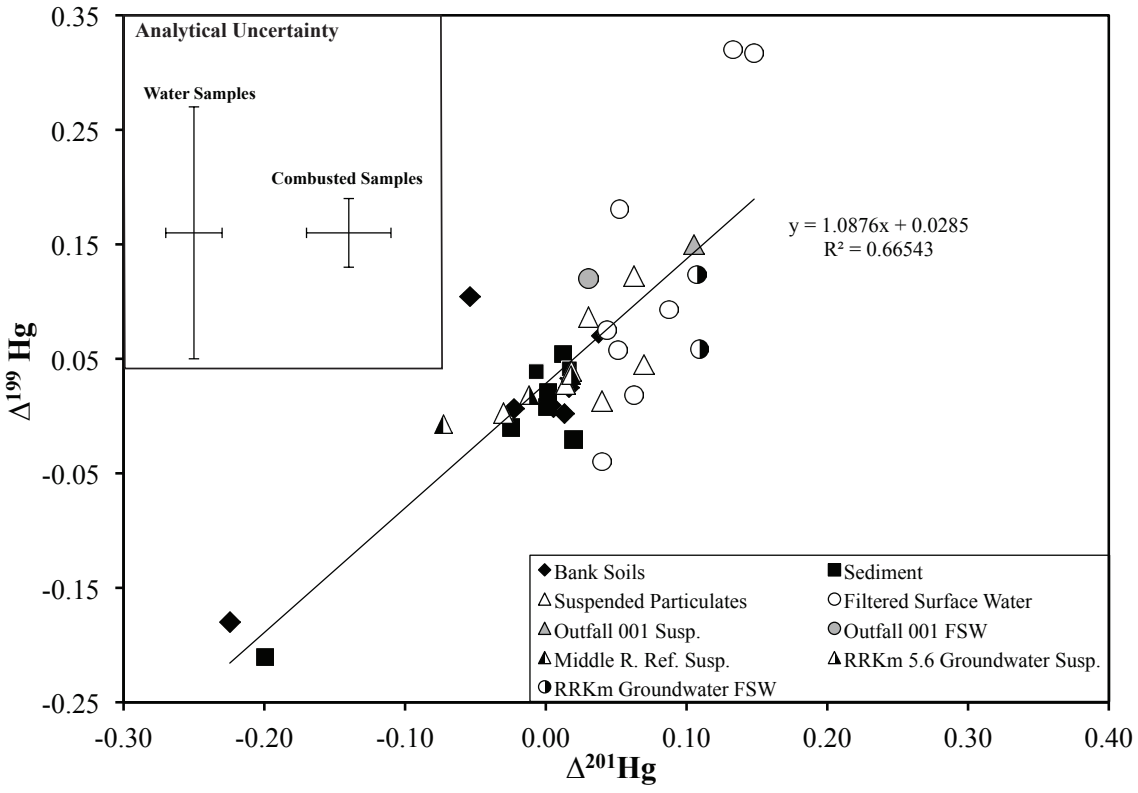

References

(1) Rhoades, E. L.; O'Neal, M. A.; Pizzuto, J. E. Quantifying Bank Erosion on the South River from 1937 to 2005, and Its Importance in Assessing Hg Contamination. *Appl. Geogr.* **2009**, *29* (1), 125–134 DOI: 10.1016/j.apgeog.2008.08.005.

(2) Flanders, J. R.; Turner, R. R.; Morrison, T.; Jensen, R.; Pizzuto, J.; Skalak, K.; Stahl, R. Distribution, Behavior, and Transport of Inorganic and Methylmercury in a High Gradient Stream. *Appl. Geochemistry* **2010**, *25* (11), 1756–1769 DOI: 10.1016/j.apgeochem.2010.09.004.

(3) URS Corporation. *Final Report: Ecological Study of the South River and a Segment of the South Fork Shenandoah River, Virginia*. Revised 2012. southriverscienceteam.org/news

(4) URS Corporation. *Memorandum: RRM 3.5 Study Area Hydrological Evaluation and Groundwater Flux Estimates (May – October 2013)*. Revised 2015(b).

(5) USEPA. 1996. Method 1669: Sampling Ambient Water for Trace metals at EPA Water Quality Criteria Levles. U.S. Environmental Protection Agency, Office of Water, Engineering and Analysis Division (4303), Washington, D.C. USA.

(6) USEPA. 1999. Method 160.2: Total Suspended Solids (TSS). U.S. Environmental Protection Agency, Office of Water, Engineering and Analysis Division (4303), Washington, D.C. USA.

(7) Hurley, J. P.; Cowell, S. E.; Shafer, M. M.; Hughes, P. E. Partitioning and Transport of Total and Methyl Mercury in the Lower Fox River, Wisconsin. *Environ. Sci. Technol.* **1998**, *32* (10), 1424-1432 DOI: http://pubs.acs.org/doi/pdf/10.1021/es970685b.

(8) Biswas, A.; Blum, J. D.; Bergquist, B. A.; Keeler, G. J.; Xie, Z. Natural Mercury Isotope Variation in Coal Deposits and Organic Soils. *Environ. Sci. Technol.* **2008**, *42* (22), 8303–8309 DOI: 10.1021/es801444b.

(9) Demers, J. D.; Blum, J. D.; Zak, D. R. Mercury Isotopes in a Forested Ecosystem: Implications for Air-Surface Exchange Dynamics and the Global Mercury Cycle. *Global Biogeochem. Cycles* **2013**, *27*, 222-238 DOI: 10.1002/gbc.20021.

(10) Sherman, L. S.; Blum, J. D. Mercury Stable Isotopes in Sediments and Largemouth Bass from Florida Lakes, USA. *Sci. Total Environ.* **2013**, *448*, 163–175 DOI: 10.1016/j.scitotenv.2012.09.038.

(11) Blum, J. D.; Johnson, M. W. Recent Developments in Mercury Stable Isotope Analysis. *Rev. Mineral. Geochemistry* **2017**, *82* (1), 733–757 DOI: 10.2138/rmg.2017.82.17.

(12 Lauretta, D. S.; Klaue, B.; Blum, J. D.; Buseck, P. R. Mercury Abundances and Isotopic Compositions in the Murchison (CM) and Allende (CV) Carbonaceous Chondrites. *Geochim. Cosmochim. Acta* **2001**, *65* (16), 2807–2818 DOI: 10.1016/S0016-7037(01)00630-5.

(13) Blum, J. D.; Bergquist, B. A. Reporting of Variations in the Natural Isotopic Composition of Mercury. *Anal. Bioanal. Chem.* **2007**, *388* (2), 353–359 DOI: 10.1007/s00216-007-1236-9.

(14) Estrade, N.; Carignan, J.; Donard, O. F. X. Tracing and Quantifying Anthropogenic Mercury Sources in Soils of Northern France Using Isotopic Signatures. *Environ. Sci. Technol.* **2011**, *45* (4), 1235–1242 DOI: 10.1021/es1026823.

(15) Jiskra, M.; Wiederhold, J. G.; Skyllberg, U.; Kronberg, R. M.; Hajdas, I.; Kretzschmar, R. Mercury Deposition and Re-Emission Pathways in Boreal Forest Soils Investigated with Hg Isotope Signatures. *Environ. Sci. Technol.* **2015**, *49* (12), 7188–7196 DOI: 10.1021/acs.est.5b00742.

(16) Yin, R.; Feng, X.; Hurley, J. P.; Krabbenhoft, D. P.; Lepak, R. F. Mercury Isotopes as Proxies to Identify Sources and Environmental Impacts of Mercury in Sphalerites. *Sci. Rep.* **2016**, November 2015, 1–8 DOI: 10.1038/srep18686.

(17) Bergquist, B. A; Blum, J. D. Mass-Dependent and -Independent Fractionation of Hg Isotopes by Photoreduction in Aquatic Systems. *Science* **2007**, *318* (5849), 417–420 DOI: 10.1126/science.1148050.

(18) Pizzuto, J.; O'Neal, M. A. Increased Mid-Twentieth Century Riverbank Erosion Rates Related to the Demise of Mill Dams, South River, Virginia. *Geology* **2009**, *37* (1), 19–22 DOI: 10.1130/G25207A.1.

(19) USEPA. 2002. Method 1631, Revision E: Mercury in Water by Oxidation, Purge and Trap, and Cold Vapor Atomic Fluorescence U.S. Environmental Protection Agency, Office of Water, Engineering and Analysis Division (4303), Washington, D.C. USA.

(20) Carter, L. J. Chemical Plants Leave Unexpected Legacy for Two Virginia Rivers. *Science* **1977**, *198* (4321), 1015–1020 DOI: 10.1126/science.198.4321.1015.

(21) Ghosh, S.; Schauble, E. A.; Lacrampe Couloume, G.; Blum, J. D.; Bergquist, B. A. Estimation of Nuclear Volume Dependent Fractionation of Mercury Isotopes in Equilibrium Liquid–vapor Evaporation Experiments. *Chem. Geol.* **2013**, *336*, 5–12 DOI: 10.1016/j.chemgeo.2012.01.008.

(22) Hammerschmidt, C. R.; Bowman, K. L.; Tabatchnick, M. D.; Lamborg, C. H. Storage Bottle Material and Cleaning for Determination of Total Mercury in Seawater. *Limnol. Oceanogr. Methods*. **2011**, 9 (10), 426–431 DOI: 10.4319/lom.2011.9.426

Chapter 3 Spatial and Temporal Variation in the Isotopic Composition of Mercury in the South River, VA

Authors: Spencer J. Washburn, Joel D. Blum, Aaron Y. Kurz, and James E. Pizzuto

Citation: Washburn, S. J.; Blum, J. D.; Kurz, A.Y.; Pizzuto, J.E. Spatial and Temporal Variation in the Isotopic Composition of Mercury in the South River, VA. *Chem. Geol.* **In Review**

Abstract: Historic point source mercury (Hg) inputs from industrial processes on the South River (Waynesboro, Virginia) ended many decades ago, but sediment and surface water Hg concentrations remain elevated relative to the regional background. To understand Hg sources, mobility, and fate in the South River, we analyzed THg concentrations and Hg stable isotope compositions of streambed sediments, bank soils, suspended particles, filtered surface waters, and channel margin hyporheic zone pore waters. Hg isotopes allow for the identification of three distinct Hg end-member inputs to the South River, two of which are contaminant sources. Hydrologic conditions are demonstrated to have an influence on within-channel Hg isotope fractionation and Hg partitioning, with no observed isotopic discrimination between suspended particulate Hg and filtered surface water Hg during elevated flow conditions. Channel margin hyporheic zone porewaters had significantly more positive δ^{202}Hg values than surface waters (δ^{202}Hg = -0.52 ± 0.44‰ and δ^{202}Hg = -0.86 ± 0.17‰ respectively [mean ± 1SD]). A subset of porewaters exhibited mass independent fractionation signatures (Δ^{199}Hg = 0.33± 0.06‰; Δ^{200}Hg = 0.19 ± 0.03‰ [mean ± 1SD]) that are suggestive of a precipitation-derived origin for the dissolved Hg pool. Sediments from a floodplain profile were analyzed to explore the temporal

variation in Hg isotopic composition within the South River, indicating brief excursions (up to δ^{202}Hg = +0.40‰) from the average composition observed in the modern (δ^{202}Hg = -0.51 ± 0.07‰). By improving understanding of the spatial, temporal, and hydrologic conditions that contribute to variations in Hg isotopic composition, this study provides insights into the processes that control Hg isotopic end-member sources, Hg-loading to the channel during elevated flows, and Hg fate in the South River.

3.1 Introduction

As a toxic trace metal with an active biogeochemical cycle, mercury (Hg) has been the subject of extensive study (e.g., Selin, 2009). Anthropogenic activity has altered the cycling of Hg in the biosphere on a global scale (Driscoll et al., 2013), and locally at industrial sites where Hg discharges to surface waters often leads to biomagnification in aquatic food webs (Kocman et al., 2013). Discharges of anthropogenic Hg to freshwater ecosystems are understudied compared to other components of the global Hg cycle (Kocman et al., 2017). The South River, VA is the site of extensive anthropogenic Hg contamination originating from a former DuPont textile manufacturing plant in Waynesboro, VA. Mercuric sulfate was used as a catalyst at the plant between 1929 and 1950 in the production of acetate fibers (Carter, 1977). The production of acetic anhydride produced a sludge that contained mercury, and this waste sludge was transported to a building that housed a retort furnace that was used to recover elemental mercury (URS, 2015). During this period of mercuric sulfate catalyst use at the former DuPont facility, a significant amount of Hg was lost and entered the South River channel. Hg-contaminated sediments have been identified throughout the channel, river banks, and over-bank deposits of the South River and the South Fork Shenandoah River (Turner and Southworth, 1999). Prior work has demonstrated the ongoing impacts that this Hg contamination has had on the

downstream ecosystems, documenting elevated Hg levels within the biota of both the aquatic (Murphy et al., 2007; Neufeld 2009; Bergeron et al., 2010; Brent & Kain, 2011) and associated terrestrial environments (Cristol et al., 2008; Jackson et al., 2011).

The current conceptual model for Hg cycling within the South River postulates that erosion of Hg-laden bank soils is the dominant input of Hg into the South River channel environment (Flanders et al., 2010; URS, 2012). Thus, understanding the processes that control Hg mobility within the South River is critical to understanding the Hg-related ecosystem risks. Adaptive management models have demonstrated that uncertainties in Hg loading to the South River contribute to the uncertainty in assessing the most effective remediation efforts (Foran et al., 2015). To this end, studies that add to the understanding of Hg loading dynamics within the South River are important for guiding informed remediation implementation.

Measurement of Hg stable isotope ratios in environmental samples is an excellent tool to probe biogeochemical cycling of Hg in fluvial systems (Blum et al., 2014; Yin et al., 2010). A number of recent studies have explicitly demonstrated the application of Hg isotopes in aquatic freshwater systems, including contaminated rivers (Sonke et al., 2010; Perrot et al., 2010; Liu et al., 2011; Foucher et al., 2013; Bartov et al., 2013; Yin et al., 2013; Donovan et al., 2014; Smith et al., 2015; Donovan et al., 2016a; Donovan et al., 2016b; Demers et al., 2018; Marshall et al., 2018; Baptista-Salazar et al., 2018), relatively pristine rivers (Tsui et al., 2012; Tsui et al., 2013; Tsui et al., 2014; Jiskra et al., 2017; Woerndle et al., 2018), and lakes (Ma et al., 2013; Lepak et al., 2015; Gray et al., 2015; Wiederhold et al., 2016; Guedron et al., 2016; Chen et al., 2016, Xu et al., 2016; Yin et al., 2016a; Yin et al., 2016b). However, environmental systems are complex, and due to the time-intensive sampling and laboratory work necessary for high precision Hg isotope ratio measurements, many of these studies have been limited in either spatial or temporal

scope. Most studies that have explored temporal changes in Hg isotope signatures of sediments have focused their investigations on lake ecosystems (Ma et al., 2013; Guedron et al., 2016; Yin et al., 2016), with no long-term Hg isotope records from fluvial ecosystems, with the exception of an altered oxbow lake sediment core reported in Gray et al. (2015). In addition to temporal variability, environments like the South River exhibit dynamic conditions (e.g. wide ranges in discharge, watershed land use, water column chemistry) that can affect Hg cycling over spatial regions and across hydrologic gradients (e.g. Shanley et al., 2004). For example, a previous study demonstrated that monomethyl-mercury (MMHg) concentrations were the highest in contaminated South River sediments in late May, while the potential methylation rates were highest in August (Yu et al., 2011). The study authors postulated that Hg methylation by sulfate- and iron- reducing bacteria in South River sediments fluctuates due to processes that vary in space and time. Recent mesocosm experiments with periphyton in the South River demonstrated that Hg in the water column had a greater contribution to biological uptake of MeHg in periphyton than Hg associated with sediments (Brent & Berberich, 2013). Taken together, the results of these studies suggest that observations during only one time interval would likely fail to capture important aspects of the Hg dynamics of the ecosystem.

A study by Washburn et al. (2017), established the baseline Hg isotopic composition of the main physical reservoirs of Hg within the South River, although this study was conducted with limited spatial resolution and over a more limited range of hydrologic conditions than is observed in the South River. To address knowledge gaps identified by Washburn et al, we conducted sampling and analysis of additional physical reservoirs of Hg within the South River targeting increased spatial coverage and a wider range of hydrologic conditions. This study expands both spatial resolution in the reach adjacent to the former DuPont facility and

downstream in impacted reaches, needed to provide constraints on the Hg dynamics within the South River channel. In particular, we sampled the South River under an elevated hydrologic flow regime to assess the influence on the observed Hg isotopic compositions of the dissolved and particulate phase Hg within the channel system, and to explore the Hg isotopic composition of the hyporheic zone and its connection to Hg dynamics within the channel. In addition, sediments from a floodplain core were analyzed to understand longer term temporal variations in the isotopic composition of Hg released to South River sediments and stored during sediment deposition. By improving understanding of the spatial and temporal variations in Hg isotopic composition, this study provides insights into the processes that control Hg sources, mobility, and fate in the South River.

3.2 Materials and Methods

3.2.1 Sample Collection and Processing

The South River is a fourth order, single-thread, gravel-bed river located in the Shenandoah Valley of Virginia, USA (Rhoades et al., 2009). The details of sample collection and processing for samples collected during 2014 are presented in Washburn et al. (2017). Additional samples presented in this study were collected during late May of 2016, and were focused on a 7 km reach of the river, from 4km upstream of the former DuPont plant in Waynesboro, VA to 3 km downstream of the former industrial site. During this effort 6 different sample types were acquired: streambed sediments, bulk bank soils, filtered surface water (and associated suspended particulates), and filtered channel-margin hyporheic porewater (and associated suspended particulates). Following the convention of previous work on the South River system (Washburn et al., 2017; Flanders et al., 2010), sampling locations are labeled according to their distance, in relative river kilometers (RRKm), along the channel from a known historic point source of Hg at

the former DuPont plant (e.g., RRKm 0.0). Bank soil and streambed sediment samples were also collected at downstream locations (RRKm 3.9, 7.8, 15.9, 26.4) to improve the spatial resolution of the longitudinal profile presented in Washburn et al. (2017).

Streambed sediment and bank soil samples were collected from fourteen locations along the South River channel in May 2016 (5/24/16 to 5/31/16). Bulk bank soil samples were collected as composite grab samples from exposed banks. Streambed sediments were collected using a hand-operated plastic bilge pump to effectively sample fine-grained sediment distributed within the coarse streambed. Sediments and bank soils were collected into acid washed containers in the field. Sample containers were placed on ice in the field, frozen within 8 hours of collection, shipped on ice to the University of Michigan, and then stored at -18 ºC. Sediment and bank soil samples were subsampled, freeze-dried, and dry sieved through acid-cleaned nylon mesh to remove detritus >2mm. The <2mm size fraction was then homogenized in an alumina ball mill. The mixing mill was cleaned between each sample by washing with water and ethanol and then grinding Hg-free quartz.

Filtered stream water and suspended sediment samples were collected at ten locations during May 2016 (5/25/16 to 5/31/16). Discharge at the USGS Waynesboro gage ranged between 7.08 and 3.26 m^3s^{-1} during the sampling period, with consistently decreasing total discharge rates (USGS, 2017). These discharge conditions represent flow elevated above baseflow for May, with return periods ranging from 7.69 to 2.63. Water samples were collected, filtered, and preserved in the field, using trace-metal clean sampling methods following a modification of EPA Method 1669. Water samples were collected from the middle of the channel using acid-cleaned HDPE bottles, in which samples remained for no more than 15 minutes before being filtered into acid-cleaned 1 L borosilicate glass media bottles containing

5mL of concentrated HCl (trace metal grade). Water samples were filtered using a hand operated vacuum-pump and disposable, pre-cleaned 0.45μm pore-size cellulose nitrate vacuum filter housings (Thermo Scientific). Filters were removed from the vacuum housing with acid cleaned forceps, placed in individual acid-cleaned petri dishes, and sealed with Teflon tape. Filters were frozen and water samples were placed in refrigerated storage at the end of each sampling day, and then transported in coolers to the University of Michigan. Filters were freeze-dried and stored in desiccation chambers. Water samples were oxidized with 1% BrCl (w/v), which was allowed to react with the water sample in dark refrigerated storage for a minimum of one month. Procedural field blanks were collected periodically during the sampling campaign using 1L of de-ionized water. Filters and de-ionized water were processed in parallel with the samples and then analyzed for THg concentration to assess potential contamination. Filtered water field blanks were subsampled and THg concentrations were analyzed by cold-vapor atomic fluorescence spectroscopy [CV-AFS; RA-3000FG+, Nippon Instruments] (following a modified EPA Method 1631). All filtered water field blanks (n=10) had THg concentrations that were below method detection limits of 0.2 ng/L. At each site, 1L of water was collected into a HDPE bottle and used to determine the total suspended solids (TSS) of surface water. TSS values were used in the calculation of distribution coefficients ($\log(K_d)$) using THg values of the associated filtered surface water and suspended material following the method of Hurley et al. (1998).

Filtered channel margin hyporheic zone pore waters and suspended sediment samples were collected at ten locations during May, 2016 (5/25/16-5/31/16). Porewaters were sampled using a piezometer sampler probe (PPX36; M.H.E. Products; Henry Probe), augmented with acid-cleaned 50mL syringes attached to acid-cleaned PTFE tubing (5mm ID) assemblies for collecting water with minimal exposure to metal components. Samples were collected by

inserting the Henry probe to a depth of at least 20cm into the streambed at locations within 1 meter of the channel edge. After Henry probe insertion the syringe-tubing assembly was inserted into the Henry probe and 50mL of porewater was removed and discarded. Porewater was then collected and emptied into an acid-cleaned HDPE bottle, in which samples remained for less than 15 minutes. From each insertion less than 300mL of porewater was removed to prevent sampling of surface waters, and porewater samples represent the aggregation of between 3-5 Henry probe insertions made ~1 meter apart along the same channel margin. Porewater samples were then filtered following the procedure described above for surface water. Porewater samples were labeled according to the RRKm at which they were collected, then given a designation as to which bank they were collected from with a downstream orientation (e.g. right bank samples came from the former DuPont facility side of the channel).

Collection of a floodplain sediment profile (collected at RRKm 4.75) analyzed in this work for THg concentration and Hg isotopic composition is described in detail in Pizzuto et al., 2016. Briefly, sediment samples were collected from the outside bank of a river meander by digging a vertical trench, and collecting sub samples at 3cm intervals to a depth of 20cm, then at 5 cm intervals to a depth of 80cm. Samples were air-dried at the University of Delaware, and then processed as described below at the University of Michigan. Sample ages were estimated using the median sedimentation rate (0.575 ± 0.075 cm/year) given in Pizzuto et al. (2016), which was calculated using the activity of the ^{137}Cs and ^{210}Pb radionuclides measured in each sediment interval. Extending the uncertainty associated with the modeled sedimentation rate to the estimated sample age yields age uncertainties of up to 20.2 years at the bottom profile depth (80cm).

3.2.2 Sample Preparation for Isotope Analysis and THg Concentrations

Hg in streambed sediments, bank soils, floodplain profile sediments, and suspended materials (filters from both surface waters and porewaters) was separated for THg concentration and Hg stable isotope measurement by offline combustion, as described in detail elsewhere (Biswas et al., 2008; Demers et al., 2013). Briefly, 0.01 to 1.00 g of sample was packed into a ceramic boat and placed into the first stage of a two-furnace combustion system. Freeze dried filters were cut with a clean stainless steel razor blade and packed into ceramic boats in a similar manner to ground samples. The first-stage furnace was slowly ramped to 750 ºC over a six hour period while the second-stage furnace was held at 1000 ºC. Hg released from the sample matrix was carried through the combustion tube in a flow of Hg-free O_2 and into a 1% $KMnO_4$ in 10% H_2SO_4 (w/w) [1% $KMnO_4$] trapping solution.

Filtered surface water and filtered porewater was purged and trapped into 1% $KMnO_4$ solution for isotope analysis, following the procedure outlined in Washburn et al. (2017). Briefly, approximately 1L of previously acidified and oxidized surface water was weighed into a clean 2L borosilicate glass media bottle. Samples were treated with 1.0 ml of concentrated hydroxylamine hydrochloride to destroy free halogens, capped tightly, and allowed to react for a minimum of 30 minutes. Through one port of a three-port Teflon transfer cap, 100mL of 10% $SnCl_2$ was delivered to the reaction bottle via a peristaltic pump, at a rate of ~3.3 ml/min. Another port delivered Hg-free air (Au-filtered) to sparge the ~1L sample volume into the reactor headspace, while the final port removed gas from the reactor headspace into a borosilicate glass trap containing between 5.5 and 7.0 g of 1% $KMnO_4$ trapping solution. Samples were purged for 3 hours while being vigorously stirred with a clean Teflon stir bar. Prior to purging and trapping, THg concentrations of each sample bottle were determined by

running small aliquots via CV-AFS. For each sampling site, the THg concentration for the filtered surface water sample is reported as the average of measured THg concentrations (ng/L) in each bottle collected at that site. The THg concentration of filtered porewater samples are reported as the measured THg concentration (ng/L) of each sample according to the sampling location. Due to the low THg concentration of some filtered surface water and filtered porewater samples, it was necessary to aggregate samples from different sampling locations to obtain enough Hg for an accurate Hg isotope analysis. For filtered surface waters, only the samples collected from RRKm -1.1 and -0.75 were combined into composite samples for Hg isotope analysis. For filtered porewaters, all samples collected upstream of RRKm -0.6 were composited (RRKm -4.0 left bank, RRKm -1.1 center channel and right bank, RRKm -0.75 left and right bank, RRKm -0.6 left bank), RRKm 0.0 left bank and RRKm 0.25 left bank were composited, and RRKm 0.7 left bank and RRKm 1.3 right bank were composited for Hg isotope analysis. The Hg isotope data for these composited samples are labeled as the most downstream sample of the aggregated samples in both Tables and Figures, while THg concentration are presented in Figures as average values (separate THg values for composited samples are presented in Table 3.6). To determine Hg recovery, the THg concentration of small aliquots of each 1%$KMnO_4$ trapping solution was determined prior to transfer into a secondary trapping solution. Purge and trap recoveries of filtered surface water and filtered porewater samples averaged 103.0% ± 9.0% (range: 84.9% to 118.2%, n=35).

Trapping solutions of both combustion and purge and trap samples were partially reduced with a 30% solution of $NH_2OH{\cdot}HCl$ using an amount equal to 2% of the total sample by weight (w/w); then a small aliquot was taken and measured for THg by CV-AFS or cold vapor atomic absorption spectroscopy [CV-AAS; MA-2000 Nippon Instruments]. Combustion trap contents

were then purged into a secondary 1% $KMnO_4$ trapping solution to remove potential matrix components from combustion residues and to adjust Hg concentrations prior to isotopic analysis (Sherman and Blum, 2013; Blum and Johnson, 2017). Hg recovery during this transfer into secondary 1% $KMnO_4$ trapping solution was evaluated by taking small aliquots of the secondary trapping solution and analyzing the THg concentration by CV-AFS. Transfers into secondary traps for concentration and matrix- matching for all sample types averaged 98.4% ± 4.8% (range: 84.4% to 110.4%, n=82). None of these transfers were likely to have significantly fractionated the processed samples.

Procedural blanks were processed in parallel with samples for THg concentration and Hg isotopic composition. The trap contents of combusted field filter blanks contained 165±88 pg of Hg (n=16, ± 1SD), which is not significantly different from procedural combustion blanks (150±85 pg of Hg, n=5, ± 1SD). Purge and trap procedural blanks yielded between 28.7 and 67.6 pg of Hg (n=6, mean±1SD = 46.2±15.9pg), representing at most no more than 10.4% of Hg in sample trap solutions.

3.2.3 Hg Isotope Analysis

The Hg isotopic composition of the secondary trapping solution was measured by cold vapor multi-collector inductively coupled plasma mass spectrometry (CV-MC-ICP-MS, Nu Instruments). Trapping solutions were partially reduced with a 30% solution of $NH_2OH{\cdot}HCl$ at 2% of the total sample by weight (w/w) and diluted with a similarly reduced 1%$KMnO_4$ solution to between 0.8 and 5.5 ng/g. Hg was reduced online to Hg(0) by the addition of 2% (w/w) $SnCl_2$ and separated from solution using a frosted tip gas-liquid separator (Lauretta et al., 2001). Hg(0) was then carried into the MC-ICP-MS inlet by an Ar gas stream. An internal Tl standard (NIST 997) was introduced as a dry aerosol into the Ar gas stream and used to correct for instrumental

mass bias. Strict sample-standard bracketing using NIST 3133 that was matched for both concentration and solution matrix was further used for mass bias correction (Blum and Bergquist, 2007).

Mercury stable isotope compositions are reported throughout this paper in permil (‰) using delta notation ($\delta^{xxx}Hg$) relative to NIST SRM 3133 (Eq. 1), with mass dependent fractionation based on the $^{202}Hg/^{198}Hg$ ratio ($\delta^{202}Hg$) (Blum and Bergquist, 2007). Mass independent fractionation is reported as the deviation from the theoretically predicted $\delta^{xxx}Hg$ values based on the kinetic mass fractionation law and is reported with capital delta notation ($\Delta^{xxx}Hg$) according to Eq. 2. In this study MIF is represented with $\Delta^{199}Hg$, $\Delta^{200}Hg$, $\Delta^{201}Hg$, and $\Delta^{204}Hg$, using $\beta = 0.252$, $\beta = 0.502$, $\beta = 0.752$, and $\beta = 1.493$, respectively (Blum and Bergquist, 2007).

Equation 1: $\delta^{xxx}Hg\ (‰) = ([(^{xxx}Hg/^{198}Hg)_{Sample} / (^{xxx}Hg/^{198}Hg)_{NIST3133}] - 1) \times 1000$

Equation 2: $\Delta^{xxx}Hg\ (‰) = \delta^{xxx}Hg - (\delta^{202}Hg \times \beta)$

Certified reference materials and standards were processed and analyzed along with the South River samples. UM-Almáden was used as the process reference material for the purge and trap procedure. Purge and trap recoveries for UM-Almáden averaged 95.3% ± 4.4% (range: 86.9% to 99.7%, n=7). NIST 2711 "Montana Soil," was chosen as a suitable process reference material for offline combustions due to its high THg conc. (6.25µg/g) and similar matrix. Combustion recoveries of NIST 2711 averaged 102.9% ± 6.1% (range: 94.1% to 113.0%, average THg conc = 6.43± 0.38 µg/g, n=12) agreeing with the certified THg values. The average isotopic composition of NIST 2711 ($\delta^{202}Hg$= -0.20 ± 0.02‰, $\Delta^{199}Hg$= -0.21 ± 0.02‰) was consistent with previously reported values (Estrade et al., 2011; Jiskra et al., 2015; Yin et al., 2016; Blum and Johnson, 2017; Washburn et al., 2017; Washburn et al., 2018). UM-Almáden

was measured during each analytical session on the CV-MC-ICP-MS to quantify within-session performance. The isotopic data from these process reference materials and process standards is summarized in Table S2. The analytical uncertainty of Hg isotopic measurements (2σ) is presented based on the sample preparation method used, either offline combustion (for bank soils, streambed sediments, surface water suspended particulates, and porewater suspended particulates) or purge and trap (for filtered surface waters and filtered porewaters). For combusted samples, error is presented as 2SD of UM-Almáden (In-Run) as this value was greater for all measured Hg isotope values than that associated with the NIST 2711 process reference material: δ^{202}Hg ± 0.05‰, Δ^{199}Hg ± 0.06‰, Δ^{200}Hg ± 0.05‰, Δ^{204}Hg ± 0.16‰. For purged and trapped samples, error is presented as 2SE of UM-Almáden process reference material: δ^{202}Hg ± 0.10‰, Δ^{199}Hg ± 0.10‰, Δ^{200}Hg ± 0.07‰, Δ^{204}Hg ± 0.15‰ [Table 3.2].

3.3 Results and Discussion

3.3.1 Hg in Bank Soils and Streambed Sediments

Within the South River ecosystem, river bank soils and streambed sediments are the largest reservoirs of Hg associated with the historic industrial contamination (URS, 2012). Given the large amount of Hg stored within these reservoirs, the Hg isotopic composition of these reservoirs has a strong influence on the Hg isotopic composition of the other Hg reservoirs sampled for this study (Figure 3.1, as well as in Table 3.1). In general, bank soils have THg and Hg isotopic compositions that are similar to what was observed in 2014, and THg values similar to what has been observed by others (Flanders et al., 2010). THg values are relatively low (32.4 ng/g) at the upstream reference site (RRKm -4.0), and the isotopic composition (δ^{202}Hg = -0.99 ± 0.05‰, Δ^{199}Hg = -0.16 ± 0.05‰) is within analytical uncertainty of that measured at this site in 2014 (δ^{202}Hg = -1.01 ± 0.04‰, Δ^{199}Hg = -0.18 ± 0.03‰). At RRKm -0.75, the THg of the bank

soil yielded the lowest value measured over the two sampling efforts (13.3 ng/g). This very low THg value likely indicates an environment unaffected by historic industrial or direct atmospheric contamination, consistent with the isotopic composition of the bank soil at this site (δ^{202}Hg = -1.44 ± 0.05‰, Δ^{199}Hg = -0.25 ± 0.05‰), which is likely representative of the regional background composition. The differences in Hg isotopic composition between RRKm -4.0 and RRKm -0.75 bank soils may reflect the potential heterogeneity of proportional mixing of atmospheric deposition, geogenic materials, and vegetative Hg sources in uncontaminated portions of the South River. From RRKm -0.75 to RRKm 0.0, the THg values of bank soils increased 3 orders of magnitude (from 13.3 ng/g to 62.9 µg/g). The increase in THg was accompanied by a shift in the isotopic composition of the bank soils, from δ^{202}Hg = -1.44 ± 0.05‰ and Δ^{199}Hg = -0.25 ± 0.06‰ at RRKm -0.75 to δ^{202}Hg = -0.63 ± 0.05‰ and Δ^{199}Hg = -0.01 ± 0.05‰ at RRKm 0.0 (Figure 3.10). This pattern is consistent with observations in this river reach in 2014 that indicated a shift from regional background Hg to Hg from industrial contamination from the former DuPont plant. From RRKm 0.7 to RRKm 2.2, bank soil THg values remain elevated (6.30 to 22.6 µg/g), but δ^{202}Hg values increase from -0.93‰ to -0.47‰. This less negative δ^{202}Hg value in the bank soil at RRKm 2.2 is similar to the bank soil isotopic composition at RRKm 13.9 in 2014 (δ^{202}Hg = -0.18 ± 0.04‰) and perhaps represents past deposition of Hg with a relatively more positive δ^{202}Hg value (discussed in Section 3.3.4). The bank soil collected at RRKm 2.2 in 2014 had a more negative δ^{202}Hg value (-0.64 ± 0.04‰), despite a similarly elevated THg (11.6 µg/g) compared to the 2016 bank soil sample, suggesting that depositional patterns of Hg contamination within the impacted downstream reaches of the South River may exhibit significant isotopic heterogeneity.

Streambed sediments collected during 2016 exhibit patterns that were not

observed in 2014. The THg values of 2016 streambed sediments in our detailed longitudinal profile (RRKm -4.0 to 2.2) were lower than those observed in 2014, never exceeding 0.64 μg/g (at RRKm 2.2). By comparison, in 2014 we observed a THg value of 7.73 μg/g at RRKm 2.2, and THg concentrations were elevated significantly above background at RRKm 0.0 (2.81 μg/g). The Hg isotopic composition of the streambed sediments at the upstream reference site (RRKm -4.0) were significantly different between the two sampling years (2016: δ^{202}Hg = -0.69 ± 0.05‰ and Δ^{199}Hg = -0.13 ± 0.05‰; 2014: δ^{202}Hg = -1.27 ± 0.04‰, Δ^{199}Hg = -0.21 ± 0.03‰), although the THg values were of a similar magnitude (2016: 12.9 ng/g; 2014: 76.1 ng/g). The lower THg and more positive δ^{202}Hg value in the 2016 RRKm -4.0 streambed sediment could represent a relatively smaller influence of Hg associated with allocthonous organic matter, which would be expected to have more negative δ^{202}Hg values reflecting inputs of Hg associated with riparian vegetation (Demers et al 2013; Jiskra et al., 2015; Zheng et al., 2016; Enrico et al., 2016).

The Hg isotopic composition of streambed sediments in the reach adjacent to the industrial facility also varied between the two sampling years. In 2016, the sediments from RRKm -1.1 to 2.2 had an average isotopic composition of δ^{202}Hg = -1.11 ± 0.17‰ and Δ^{199}Hg = 0.05 ± 0.09‰ (±1SD, n=9), with a decreasing trend in δ^{202}Hg values relative to stream position (Figure 3.10), whereas sediments collected in the same reach from 2014 had an average isotopic composition of δ^{202}Hg = -0.63± 0.05 ‰ and Δ^{199}Hg = 0.02 ± 0.03‰ (±1SD, n=3) with no discernible trend in δ^{202}Hg values. This difference in average Hg isotopic composition may reflect the movement of relatively less contaminated sediments into this reach due to streambed scouring and sediment transport during high flow events.

Streambed sediments collected in 2016 at sites farther downstream (RRKm 3.9 to 26.4)

also have similar THg (3.68 to 17.8 μg/g) and Hg isotopic compositions (δ^{202}Hg = -0.57 to -0.44‰ and Δ^{199}Hg = 0.01 to 0.06‰) as observed in 2014 sampling, with the exception of sediment from RRKm 7.8 (Table 3.1). Bank soils collected in 2016 at sites farther downstream (RRKm 3.9 to 26.4) also have similar THg (6.33 to 45.2 μg/g) and Hg isotopic compositions (δ^{202}Hg = -0.72 to -0.47 and Δ^{199}Hg = 0.05 to 0.08) as observed in 2014 sampling (Table 3.1). The streambed sediment at RRKm 7.8 has a relatively lower THg (1.54 μg/g) and an unusual Hg isotopic composition (δ^{202}Hg = -1.93 ± 0.05‰ and Δ^{199}Hg = 0.14 ± 0.05‰). Streambed sediment at RRKm 7.8 has the lowest δ^{202}Hg value we have observed for any sample from the South River, and seems to be an outlier when compared to the relatively small range of δ^{202}Hg values observed for all other samples collected from downstream reaches (RRKm 3.9 to 35.4) [Table 3.1]. RRKm 7.8 is just upstream of the historic Dooms mill dam, which is still partially intact, and creates depositional areas within the river channel (Pizzuto and O'Neal, 2009). The low δ^{202}Hg value in the sediment may be related to varying patterns of deposition of sediment size fractions with distinct Hg isotope compositions or hydrologic processes within depositional zones that are not seen in other portions of the South River channel (Donovan et al., 2014). However, without additional information about the biogeochemical and hydrologic characteristics of this site and additional sampling, it is difficult to ascertain why the streambed sediment at RRKm 7.8 has such an anomalously low δ^{202}Hg value, and whether this value is representative of in-situ fractionation processes such as microbial reduction or sequential leaching of a sorbed Hg phase (Kritee et al., 2007; Jiskra et al., 2012), a different Hg source, or a combination of both mechanisms.

Overall, the streambed sediments and bank soils reflect the dominance of Hg from the industrial contamination throughout the downstream reaches of the South River. Downstream

reaches (RRKm 3.9 – 26.4) appear to have significantly less variation in the Hg isotopic composition of these large Hg reservoirs than the reach adjacent to the former DuPont facility (RRKm -1.1 – 3.9) suggesting that natural contamination attenuation processes such as sediment dilution may be affecting this reach of the South River. However, the more limited spatial coverage of samples in downstream reaches limits our ability to draw firm conclusions about the absolute Hg isotope variation within the South River.

3.3.2 Hg in Surface Waters

The THg values and Hg isotopic composition of filtered surface water and suspended particulates, collected at sites between RRKm -1.1 to 2.2, are presented in Table 3.1 and Figures 3.1, 3.2, 3.3, and 3.11. The THg values for both filtered surface water samples (0.35 to 1.51 ng/L) and suspended particulates (0.32 to 4.60 ng/L) were relatively low compared to samples collected in the same reach in 2014. The relatively lower THg values observed in 2016 may reflect a dilution effect in the river channel related to elevated flow conditions during sampling, with discharge at the USGS Waynesboro gage ranging between 7.08 and 3.26 m^3s^{-1} during the sampling period. For comparison, discharge during 2014 sampling ranged between 1.64 to 1.84 m^3s^{-1} (USGS, 2017). Flanders et al., 2010 observed a similiar dilution of inorganic Hg on particulates during elevated flows (e.g. storm events). Reflecting this dilution, the field measurement based partition coefficients for 2016 surface water samples ($\log(K_d)$ = 5.40 to 6.04) were lower than those observed in 2014 (6.04 to 6.47). Filtered surface water samples from 2016 have a range of Hg isotope values (δ^{202}Hg = -0.95 to -0.57‰ and Δ^{199}Hg = -0.20 to 0.09‰) that are similar to that of suspended particulate samples (δ^{202}Hg = -1.29 to -0.67‰ and Δ^{199}Hg = -0.35 to 0.08‰), and neither sample type exhibit any significant isotopic trends with relative distance downstream.

In contrast to 2014 sampling, there was no statistically significant δ^{202}Hg offset observed between filtered surface water and suspended particulate samples throughout the South River study reach in 2016 [paired t-Test, n=8, T=1.25, p=0.25]. Rather, in 2016 filtered surface water and suspended particulate samples appear to have tightly coupled δ^{202}Hg values with differences between associated samples never exceeding 0.12‰ (Figure 3.11). These small offsets were both positive and negative for filtered surface water samples relative to suspended particulates. The δ^{202}Hg values of filtered surface water and suspended particulate samples are intermediate between the δ^{202}Hg values of streambed sediments and bank soils measured at the same sampling locations with the exception of RRKm 0.7 and RRKm -4.0. At RRKm 0.7 the suspended particulates and bank soil are within analytical uncertainty of each other (δ^{202}Hg = -0.88 ± 0.05‰ and -0.93 ± 0.05‰, respectively) and at RRKm -4.0 the suspended particulates are significantly more negative than either the bank soils or streambed sediments (δ^{202}Hg = -1.29 ± 0.05‰, -0.99 ± 0.05‰, and -0.93 ± 0.05‰, respectively).

The δ^{202}Hg values of filtered surface water and suspended particulate samples do not correlate with any of the ancillary chemical parameters (e.g. dissolved oxygen, pH, etc.) measured during sampling [Table 3.3]. Overall, the isotopic composition observed in filtered surface waters and suspended particulates provides additional evidence in support of the erosion of Hg-laden bank soils and resuspension of contaminated streambed sediments as the main source of Hg to the channel at elevated flows (Flanders et al., 2010; URS, 2012).

The lack of δ^{202}Hg offset between filtered surface waters and suspended particulates during this sampling does not discount the fractionation mechanism proposed in Washburn et al. (2017), but rather suggests that the factors necessary for the observation of this fractionation are not present during elevated river discharge conditions. At elevated flow the majority of Hg

entering the South River channel is likely already bound to particulates sourced from bank erosion and sediment re-suspension. Thus, the potential sources of dissolved Hg(II) to the system (such as groundwater influxes or diffusion of Hg from storage in interstitial sediment) that might undergo rapid sorption are likely to be minimal contributors to the total Hg load present in the channel. Dissolved Hg(II) sources would be available to undergo the rapid sorption to high affinity thiol-like moieties on organic colloids and associated fractions proposed by Washburn et al. (2017). The diminished presence of dissolved Hg(II) sources during elevated flow, whether related to dilution of the Hg load or changes in the physiochemical properties of the South River channel during elevated flows, would limit the observation of the δ^{202}Hg offset between filtered surface water and suspended particulates.

The majority of filtered surface water and suspended particulate samples have Δ^{199}Hg values that are within analytical uncertainty (± 0.10‰) of 0.00‰, reflecting the Hg isotopic composition of Hg sourced from industrial contamination. However, the suspended particulates from RRKm -4.0, -1.1/-0.75 composite, -0.6, and 0.25, as well as the filtered surface water samples from RRKm -0.25 and 0.7 have Δ^{199}Hg values that are significantly negative (Δ^{199}Hg = -0.10 to -0.35‰). The most likely explanation for these negative Δ^{199}Hg values is the influence of Hg associated with allocthonous organic matter sourced from riparian zone vegetation and soils. Previous work has demonstrated that Hg associated with organic matter in the forest floor has negative Δ^{199}Hg values (Demers et al., 2013; Zheng et al., 2016). Recent work has also demonstrated that soil runoff from a boreal forest in Sweden had Hg associated with natural organic matter in surface waters with a Hg isotopic composition similar to that of the forest soil, and concluded that the majority of the Hg in the runoff originated from vegetative uptake of atmospheric Hg^0 (Jiskra et al., 2017). Similarly, a recent study demonstrated that Hg exported via

streamflow from a boreal upland-peatland catchment in northern Minnesota, was predominantly sourced from dry deposition of Hg(0) which had become associated with dissolved organic matter (Woerndle et al., 2018). The storm event prior to our sampling of the South River may have carried a significant amount of organic matter detritus into the South River channel, and Hg bound to this organic matter detritus could represent a large portion of the Hg in the surface water during high discharge. The negative Δ^{199}Hg value of the suspended particulates at RRKm -4.0 (-0.26‰), coupled with the negative Δ^{199}Hg values found in both bank soils and streambed sediments at this site (-0.16‰ and -0.13‰, respectively), suggests that within uncontaminated reaches of the South River, influx of Hg-associated with organic matter from the riparian zones is the dominant Hg source to the channel environment and likely would be throughout a range of discharge conditions.

3.3.3 Hg in Channel Margin Hyporheic Zone Porewaters

THg values for filtered porewater and porewater suspended particulates are presented in Table 3.1 and Figure 3.1. Porewater suspended particulates have elevated THg (average = 1.22 ± 2.00 μg/L, n=15, ±1SD, up to 7.94 μg/L at RRKm 0.0 right bank) compared to suspended particulates collected from surface waters. Despite the elevated THg in some of the porewater suspended particulates, the filtered porewater samples have comparatively low values (never greater than 8.80 ng/L at RRKm -0.25 left bank). This disparity points to the predominance of Hg bound to particulate phases in the hyporheic zones of the channel margins in the South River. There does not appear to be any trend in THg with RRKm, nor does there seem to be any distinction in THg values between porewater samples collected near the left bank or the right bank.

Similar to the lack of THg concentration trends, there does not appear to be any trend in the Hg isotopic composition of porewaters collected from either bank or between left and right bank samples at the same sampling site (see Figure 3.9). However, filtered porewaters exhibit a significant linear relationship between δ^{202}Hg values and 1/THg [n=7, linear regression slope = 0.65, R^2=0.65, p-value = 0.03]. Filtered porewaters and porewater suspended particulates have a significantly different δ^{202}Hg isotopic composition than filtered surface water and surface water suspended particulates [Unpaired t-Test, n_1=17, n_2=22, T=3.00, p=0.004]. Two porewater suspended particulate samples (RRKm -0.75 right bank and RRKm -0.6 left bank) have the highest δ^{202}Hg values observed for any samples in the South River (δ^{202}Hg = 0.23 ± 0.05‰ and 0.87 ± 0.05‰, respectively) and neither has an anomalous THg value (1.36 and 0.18 ug/L, respectively). Removing these two outliers from the porewater samples does not change the statistical difference between porewater and surface water populations [Unpaired t-Test, n_1=17, n_2=20, T=3.10, p=0.004]. Filtered porewaters and porewater suspended particulates have more positive δ^{202}Hg values than the filtered surface water and suspended particulates from the same locations with the exception of filtered porewater from RRKm -0.25 left bank and porewater suspended particulates from RRKm 1.3 right bank. The dissolved Hg fraction in hyporheic zone porewaters collected in a recent study of East Fork Poplar Creek, TN, had δ^{202}Hg values that were similar to or more positive than the associated overlying surface water, which is in accordance with observations of hyporheic porewaters in the South River (Demers et al., 2018). In the South River, porewater suspended particulates follow similar Δ^{199}Hg trends to bank soils and streambed sediments in the sampled reach, with negative values at the upstream reference site, RRKm -4.0 (Δ^{199}Hg = -0.39± 0.05‰), increasing downstream to Δ^{199}Hg values near 0.00‰ at RRKm 0.0 (Δ^{199}Hg = 0.02± 0.05‰). Filtered porewaters follow a similar increasing Δ^{199}Hg

trend at the reach scale, with the exception of 3 samples with significantly elevated positive Δ^{199}Hg values that are discussed in detail below.

There are a number of possible explanations for the relatively more positive δ^{202}Hg values observed in filtered porewaters and porewater suspended particulates. The first possible explanation is that the Hg isotopic composition of porewater samples is reflective of mixing between end-members. This interpretation is supported by the observation of a significant correlation between δ^{202}Hg values and 1/THg for filtered porewaters, but with no significant correlation for porewater suspended particulates. Additionally, no Hg source to the South River has been identified with a positive or near-zero δ^{202}Hg value, so a mixing model would be speculative. The second possible explanation is that the Hg present in the porewaters has undergone fractionation. Any fractionation mechanism postulated to explain the observed pattern in δ^{202}Hg cannot impart an odd MIF signature, as all but three of the porewater samples have Δ^{199}Hg values that are near 0.00‰.

One such possible fractionation mechanism to explain the isotopic composition observed in filtered porewaters and porewater suspended particulates is microbially mediated reduction of Hg, because this process results in a Hg(II) pool that has a more positive δ^{202}Hg value than the starting Hg reservoir (Kritee et al., 2007). Microbial reduction is likely to occur in the anoxic settings of the hyporheic zone, however significant amounts of Hg would have to be reduced and lost by evasion to produce the magnitude of positive δ^{202}Hg shifts detected for some filtered porewater and suspended particulate samples (up to 70% Hg loss by evasion if surface water is considered as the isotopic source of Hg to the hyporheic zones).

Another possible fractionation mechanism is dark, abiotic reduction of Hg(II) by dissolved organic matter (Zheng and Hintelmann, 2010). This mechanism seems unlikely as

neither the filtered porewater nor the porewater suspended particulates have a $\Delta^{199}Hg/\Delta^{201}Hg$ slope that is consistent with the experimentally derived value of 1.6 (Zheng and Hintelmann, 2010; Ghosh et al., 2013), instead exhibiting a $\Delta^{199}Hg/\Delta^{201}Hg$ linear regression slope of 0.96±0.27 [±1SE] [Figure S3].

A third potential explanation is that fractionation related to sorption processes is creating a $Hg(II)_{diss}$ pool with more positive $\delta^{202}Hg$ values relative to the starting reservoir, with streambed sediments as a potential initial Hg reservoir (Jiskra et al., 2012; Wiederhold et al., 2010). The fractionated pool of $Hg(II)_{diss}$ might then infiltrate into the hyporheic zone at channel margins, through diffusive fluxes or movement along flow gradients. The fraction of $Hg(II)_{diss}$ being exported from the streambed sediments is presumably small compared to the large quantity of Hg stored within this reservoir; hence we have been unable to delineate the Hg isotopic composition of the released $Hg(II)_{diss}$ due to Hg mass balance considerations.

Alternatively, a recent study documented release of $Hg^0_{(aq)}$ from nanoparticulate β-HgS within a contaminated riparian soil during simulated flooding, which created a strongly reducing environment (Poulin et al., 2016). Because β-HgS is thought to be the predominant species of Hg within the South River banks (URS, 2012), a similar release of $Hg^0_{(aq)}$ could be occurring within the banks or streambed of the South River. Exposure of the mobilized $Hg^0_{(aq)}$ to changing redox conditions within the hyporheic zone might result in oxidation of the $Hg^0_{(aq)}$, and subsequently undergo speciation to a range of $R\text{-}Hg(II)_{diss}$ species. This new pool of $R\text{-}Hg(II)_{diss}$ would be subject to sorption reactions, providing a source of Hg for the process described above.

Our inability to distinguish among the processes outlined above as controls on Hg isotopic composition within porewaters is partly due to the lack of information about the hydrologic conditions and flow patterns in the hyporheic zone. Without these data, we cannot

differentiate between sites that receive largely unidirectional flow (e.g. groundwater discharge) versus sites with dynamic flow regimes (surface water exchange). There is evidence that flow regime can play a dominant role in Hg dynamics within fluvial hyporheic zones. The studies conducted to date suggest that there is a gradient in filtered THg [FTHg] along flow paths within hyporheic zones, displaying initially elevated THg relative to surface water, with decreasing THg down gradient (Hinkle et al., 2014). Other studies have observed distinct THg peaks along vertical profiles within the hyporheic zone (Creswell et al., 2008), and seasonal variations in THg related to groundwater discharge (Stoor et al., 2006). A strong positive correlation between FTHg and dissolved organic carbon [DOC] has been in observed in hyporheic porewaters of an Oregon stream (Hinkle et al., 2014). All of these factors (flow regime, sampling location along hydrologic gradient, DOC) could be impacting our measured Hg isotope ratios in porewater samples. Although we lack enough additional information to suggest which of these explanations is most likely, it is possible that several or all of the hypothesized mechanisms are occurring within the hyporheic zones simultaneously and to varying degrees. The similar patterns in isotopic composition observed for Hg within the hyporheic zones of East Fork Poplar Creek and the South River, two distinctly different contaminated fluvial systems, may point towards a more fundamental process controlling the isotopic partitioning of Hg into hyporheic zones (Demers et al., 2018).

As mentioned above, three of the filtered porewater samples, RRKm -4.0 to -0.6 composite, RRKm 0.25 left bank, and RRKm 1.3 right bank, have significantly elevated Δ^{199}Hg values relative to other samples analyzed for this study (Δ^{199}Hg = 0.27 to 0.39, 0.33± 0.06‰ [mean± 1SD]), as well as large magnitude even MIF anomalies (Δ^{200}Hg = 0.17 to 0.22, 0.19± 0.03‰; Δ^{204}Hg = -0.29 to -0.41, -0.36± 0.06‰ [mean± 1SD]) [see Table 3.1, Figures 3.3, 3.9].

These samples have MIF signatures that are most similar to Hg measured in North American precipitation, and to date significant even MIF anomalies have only been observed in samples with atmospheric origins (Gratz et al., 2010; Chen et al., 2012; Demers et al., 2013; Cai and Chen, 2015). The ratio of $\Delta^{200}Hg$ /$\Delta^{204}Hg$ in these three porewater samples (-0.46, -0.51, -0.62) is similar to the -0.5 slope observed in samples with atmospheric origins (precipitation and TGM) (Blum and Johnson, 2017). Due to the observation of positive odd MIF and large magnitude even MIF signatures in these filtered porewater samples, we hypothesize that Hg originating from precipitation has infiltrated the channel margin hyporheic zone at these locations, perhaps as part of the hydrologic flow regime during elevated flow events. These three filtered porewater samples have low THg (0.87 to 2.83 ng/L), so a relatively small amount of dissolved Hg from precipitation could significantly shift the Hg isotopic composition of the porewaters. These three porewater samples also have the least negative $\delta^{202}Hg$ values observed ($\delta^{202}Hg$ = -0.35 to -0.03‰), again consistent with mixing of the industrial Hg source with a precipitation source that has a less negative or positive $\delta^{202}Hg$ value. The average Hg isotope composition of North American precipitation ($\delta^{202}Hg$= -0.48 ± 1.04, $\Delta^{199}Hg$ = 0.36±0.57‰, 2SD, n=64) suggests that binary mixing between precipitation and the identified industrial Hg endmember within the South River could explain the anomalous MIF values observed in these three porewater samples (Zheng et al., 2016 and references therein). Hg originating from precipitation could be subjected to a number of fractionation mechanisms that result in MDF shifts only (e.g. sorption, microbial reduction) and still retain the MIF signatures of atmospheric cycling.

3.3.4 Temporal Variations in Hg Isotope Composition as Observed in a Floodplain Sediment Profile

Hg was released into the South River over thirty one years from 1929 to 1950. Thus, a potential source of isotopic variability in Hg measured in the channel at the present could be past release of Hg with varying isotopic composition due to either a changing Hg ore source for the mercuric sulfate catalyst used in the acetate fiber production process, or changes in the regime of Hg release to the channel (e.g. direct loss of elemental mercury to soils, changing contaminated groundwater flow, loss from Hg-containing waste, etc.). No archives of the Hg used at the plant are known to exist, but one proxy for Hg release is floodplain overbank sediments, where accumulation of contaminated streambed sediment from the river channel provides a record of Hg entering the South River ecosystem over time. We analyzed the Hg isotopic composition of sediments from a floodplain profile from RRKm 4.75, located on the outside left bank of a meandering bend that had been previously dated using fallout radionuclides (^{210}Pb and ^{137}Cs; Pizzuto et al., 2016). The THg profile of these floodplain sediments (Figure 3.4, Table 3.4) is in good agreement with other floodplain profiles analyzed from the South River (Pizzuto et al., 2016) as well as fine-grained channel margin sediment cores (Skalak and Pizzuto, 2010), with peak THg values (1958, 147 μg/g) coming directly after the period of Hg use at the former DuPont plant ended in 1950. Interestingly, THg values in sediments that have been dated to times prior to known Hg use at the former DuPont facility (prior to 1929) are also significantly elevated (1.56 to 13.7 μg/g) compared to regional background bank soils THg (~30 ng/g). This may be the result of the uncertainty associated with the age model (at a depth of 70-75cm, the age estimates range from 1869.5 to 1903.0) or due to downward infiltration of Hg into the sediment profile.

The average isotopic composition of RRKm 4.75 floodplain sediment samples is δ^{202}Hg = -0.48 ± 0.14‰, and Δ^{199}Hg = 0.04 ± 0.03‰ (n=17, ±1SD). There are three significant δ^{202}Hg outliers observed in the floodplain profile (1994.5, δ^{202}Hg = -0.11‰; 1987.5, δ^{202}Hg = -0.71‰; 1940.6, δ^{202}Hg = -0.27‰), but each sediment sample has a Δ^{199}Hg value within 1SD of the mean Δ^{199}Hg value for the floodplain profile. Removing these three outliers from the mean calculation does not significantly alter the mean δ^{202}Hg value of RRKm 4.75 floodplain sediments (δ^{202}Hg = -0.51 ± 0.07‰, n=14, ±1SD). The average isotopic composition of the floodplain sediments is similar to the industrial end-member identified from 2014 streambed sediments (δ^{202}Hg = -0.59± 0.11‰).

The three sediment samples that have δ^{202}Hg values that can be considered outliers may be representative of temporary shifts in Hg isotopic composition of past Hg released, rather than being the result of in situ fractionation processes. For in situ fractionation processes to cause the variation in δ^{202}Hg values observed, processes that would cause both positive and negative MDF would have to be occurring within the sediment profile. Additionally, significant amounts of Hg would have to be removed from the system to cause shifts in the isotopic composition of total Hg. For example, for microbial reduction of Hg(II) to produce the +0.40‰ shift observed from the average δ^{202}Hg value in the floodplain sediments to the 9-14cm depth sediment, between ~18-27% of the Hg(II) present in the sediments would have to be lost as Hg^0 according to the experimentally derived fractionation factors presented in Kritee et al. (2007); such a loss is not reflected in the THg values of the floodplain sediments as a deviation from the expected trends. The positively shifted sediment samples (median ages 1994.5 and 1940.6) have δ^{202}Hg values (-0.11 ± 0.05‰ and -0.27 ± 0.05‰, respectively) that most closely resemble bank soils from RRKm 2.2 (-0.28 ± 0.05‰; 2016) and RRKm 13.9 (-0.18 ± 0.04‰; 2014). The positively shifted

floodplain sediments also have similar δ^{202}Hg values as the suspended particulates measured in Outfall 001 (-0.34 ± 0.04‰; 2015), a discharge outfall connected to the storm water sewer system at the former DuPont facility that enters the South River channel at RRKm -0.75 that characterizes the limited amounts of Hg being released at present. The observation of a similar isotopic composition of Hg being released from the plant at present, combined with a similarity to the isotopic composition in spatially distributed surficial bank soils, suggests a source of Hg at the former DuPont facility that has been released sporadically with a less negative δ^{202}Hg value. A series of recent studies have demonstrated that the calcine waste products of Hg ore retorting can exhibit a very wide range in δ^{202}Hg values (-1.91 to 2.10‰) for bulk material. Hg mobilized in leachates from these calcine wastes can have positively shifted δ^{202}Hg values (shifts of +0.84 to 1.25‰). Variability of the isotopic composition of calcines can be averaged in impacted creek sediments by mixing (-0.58 to 0.84‰) (Wiederhold et al., 2013; Smith et al., 2015). Thus the process of retorting Hg-containing waste sludge at the DuPont facility could have produced Hg reservoirs with varying isotopic compositions, and preferential release of Hg from these reservoirs could have contributed to the variability observed in the floodplain profile reported here (Washburn et al., 2017).

3.3.5 3 End-Member Isotopic Mixing Model

A number of previous studies have demonstrated the utility of end-member mixing models in source tracing of Hg contamination in aqueous settings (Donovan et al., 2014; Liu et al., 2011; Wiederhold et al., 2015), although this can become complicated in settings with Hg sources that have high isotopic variability (Smith et al., 2105). Washburn et al. (2017) concluded that a three end-member mixing model was necessary to account for the full range of isotopic composition observed within the South River system. However, limited sampling prevented the

identification of the source of an "unknown" end member (relatively elevated THg conc., δ^{202}Hg value ~-1.10‰) that was influencing the isotopic composition of Hg in the surface waters near the former DuPont plant. In Figure 3.5 we present an updated version of the 3 end-member mixing model proposed by Washburn et al. (2017), incorporating the additional data gathered during the 2016 sampling effort and reported in this study. Streambed sediments from 2016 in the river reach adjacent to the former DuPont facility (δ^{202}Hg average = -1.11 ± 0.17‰, n=10, ±1SD) have the same Hg concentration and isotopic composition as the unknown end-member previously proposed (Washburn et al., 2017). The majority of the sediments sampled in 2016 were upstream of the sites at which the unknown Hg isotopic end-member was observed in 2014. Thus the streambed sediments sampled in 2016 may represent the source of the unknown end-member as the previous mixing model utilized measurements of suspended particulates, whose isotopic composition could be influenced by re-suspension of sediment located upstream of the surface water sampling site.

One potential explanation for the lower δ^{202}Hg values observed in the 2016 streambed sediments is that they reflect the influence of Hg derived from coal, either as direct inputs of coal fines or fly ash into the river, or long-term deposition of Hg from coal combustion. A recent study has shown that Hg in fly ash from the TVA Kingston coal fired power plant located in Tennessee, USA had an average δ^{202}Hg = -1.78 ± 0.35‰ and an average THg conc. of 123 ± 23 ng/g, while all bulk coal mined in the USA has an average δ^{202}Hg of about -1.44‰ (Bartov et al., 2013; Sun et al., 2016). Three small coal fired utility boilers were in operation at the former DuPont facility until 2014, and feed coal was stored onsite. Mixing of Hg from coal fines or fly ash with the source of industrial contamination from the former DuPont plant could therefore explain both the lower THg conc. and relatively lower δ^{202}Hg values in the 2016 streambed

sediments. Washburn et al. (2017) suggested that the source of the low δ^{202}Hg end-member could be related to release of Hg that had undergone fractionation as part of either the acetate fiber production or the onsite Hg retorting processes.

In between the 2014 and 2016 sampling efforts, various actions were undertaken as part of planned remediation on the contaminated storm water sewer system at the former DuPont Facility. The storm water sewer system drained areas of the former DuPont facility where elemental Hg had been found, including the site of the former building that housed the retorting furnace (URS, 2015). These remediation efforts could have released Hg with a differing isotopic composition into the South River channel. Elevated Hg concentrations in groundwater have been observed at the plant site (URS, 2015), and transport and release of Hg in groundwater could be an additional source of Hg with a varying isotopic composition to the South River channel. However, we currently lack enough supporting information to unequivocally identify the source of this additional Hg end-member.

In 2016 sufficient volumes of stream water were collected to obtain Hg isotope data for the suspended particulates at the upstream reference site, RRKm -4.0. We have updated the mixing model so that it now uses the composition of the suspended particulates from this reference site to represent the regional background end-member, because it more accurately reflects the composition of Hg being delivered to contaminated reaches of the South River that have relatively low THg values. The δ^{202}Hg value of the suspended particulates from RRKm -4.0 in 2016 was within analytical uncertainty of the Middle River reference site suspended particulates from 2014 (δ^{202}Hg = -1.29± 0.05‰ and -1.22± 0.04‰, respectively), which was previously used to delineate the regional background end-member, however the RRKm -4.0 suspended particulates had a much lower THg value (THg values of 0.32 ng/L and 2.03 ng/L,

respectively). Suspended particulates from the contamination impacted reach collected in 2016 show a similar range of δ^{202}Hg values to those collected in 2014 (2016: -1.05 to -0.67 ± 0.05‰; 2014: -1.06 to -0.57 ± 0.04‰). However, there is a much greater variability in THg conc. in the 2016 suspended particulates compared to the 2014 samples, likely due to the dilution effects discussed in Section 3.3.2.

The isotopic end-members identified in the δ^{202}Hg mixing model should also be able to explain the observed variation in surface water suspended particulate Δ^{199}Hg values (Figure 3.12). The two industrial-contamination end-members (2014 and 2016 streambed sediments) have very similar average Δ^{199}Hg values (0.02 ± 0.03‰ and 0.05 ± 0.09‰ respectively, [mean ± 1SD]), effectively functioning as a single end-member. The regional background end-member has a negative Δ^{199}Hg value (-0.26 ± 0.05‰), likely reflecting the influence of riparian zone foliage and soils on the isotopic composition of Hg within the channel at unimpacted locations (Demers et al., 2013; Zheng et al., 2016; Jiskra et al., 2017). Isotopic mixing of these two end-members is able to explain the variability of the surface water suspended particulate MIF values, except for the suspended particulates collected at RRKm -0.6 and 0.25. At these two sites, the suspended particulates have Δ^{199}Hg values that are shifted towards more negative values (-0.35± 0.05‰ and -0.22± 0.05‰, respectively) than would be predicted from the mixing model. This suggests that the RRKm -4.0 suspended particulate sample does not account for the full heterogeneity in the isotopic composition of the unimpacted riparian zone Hg inputs to the channel.

Overall, a three end-member isotopic mixing model is able to account for both the mass dependent and mass independent Hg isotope variation of samples collected from the South River channel environment in both 2014 and 2016. It is important to note that although we have chosen

to use the average composition of streambed sediments to represent the industrial end-member, the average composition of bank soils is interchangeable as a representation of the industrial end-member as the bank soils have on average a very similar isotopic composition and THg value as the 2014 streambed sediments. Thus, the end-member mixing model supports the conceptual model of Hg within the South River channel proposed by others previously (Flanders et al., 2010; URS, 2012), but the conceptual model needs modification to account for the multiple Hg isotopic end-members within the Hg reservoirs that are the dominant inputs to the channel system, namely bank soils and streambed sediments. However, the three end-member isotopic mixing model is unable to account for the hydrologically connected channel margin hyporheic zones. This adds further evidence to the arguments laid out in Section 3.3.3 that the hyporheic zones of the South River are being influenced by a set of Hg sources and/or fractionation mechanisms that are distinct from those that have been delineated for the South River channel.

3.4 Conclusions and Future Work

The present study has significantly expanded on the dataset presented in Washburn et al. (2017) by exploring the spatial, temporal, and hydrologic controls on the Hg isotope composition of different sample types within the South River. Increased spatial resolution sampling in the reach adjacent to the former DuPont industrial facility allowed for the identification of the physical source, upstream streambed sediments, of the third endmember needed to explain the full range of Hg isotope variation observed within the South River channel. Hydrologic conditions were demonstrated to alter the isotopic partitioning of Hg between dissolved and particulate phases in surface waters. Channel margin hyporheic zone porewaters were found to have a significantly differing isotopic composition from surface waters, suggesting that varying Hg sources and processes influence Hg dynamics within these zones. Temporal excursions in

δ^{202}Hg values were observed in sediments from a floodplain profile, indicating that past releases of Hg to the South River did not have a completely homogenous isotopic composition. This study has demonstrated the need for future studies utilizing Hg stable isotopes in complex environmental settings to account for the full range of biogeochemical conditions and potential source variations.

One area identified in this study that requires substantial future investigation is the dynamics of Hg within hyporheic zones. The complex and changing redox conditions and hydrologic gradients are likely to have a significant impact on the isotopic composition of Hg within hyporheic zones. The impact these hydrologically connected zones may have on Hg isotope dynamics within river channels has not been sufficiently explored. The use of Hg stable isotopes to identify and trace Hg sources in environmental systems has become widespread, particularly through the application of endmember mixing models. The present study has underscored the necessity for future studies to take a full accounting of the spatial and temporal variations that can affect Hg endmembers.

Acknowledgements

We thank Marcus Johnson for his patient assistance and guidance in operating the CV-MC-ICP-MS. We would also like to thank the members of the South River Science Team for their beneficial discussions and assistance, particularly Scott Gregory and Erin Mack. The authors acknowledge partial funding from E.I. du Pont de Nemours and Company, although this entity exercised no editorial control over the content of this manuscript.

Figure 3.1 THg Longitudinal Profile

Longitudinal profile along the South River near the former DuPont plant of THg concentration values of samples collected in 2016 presented on a logarithmic scale. Filtered surface water (FSW), suspended particulates associated with filtered surface waters (FSW Susp. Part.), filtered channel margin pore water (PW), and suspended particulates associated with pore waters (PW Susp. Part.) are reported in THg conc. units of ng of Hg/L of water, while streambed sediments (Sed) and bank soils (BS) are reported in THg conc. units of ng of Hg/g of material, dry weight.

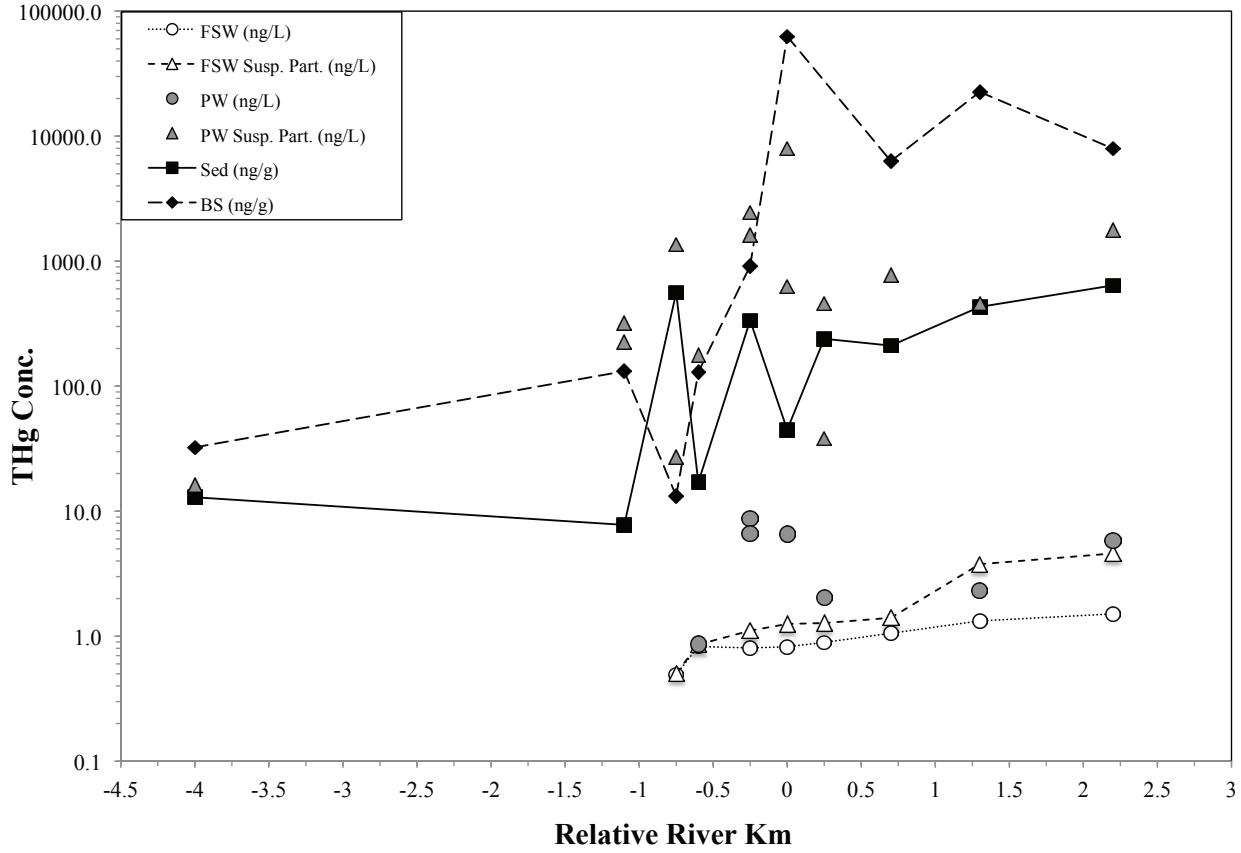

Figure 3.2 δ^{202}Hg Longitudinal Profile

Longitudinal profile along the South River near the former DuPont plant of δ^{202}Hg values (‰) of samples collected in 2016. Sampling locations are presented in relative river kilometers. The analytical uncertainty of Hg isotopic measurements (2σ) is presented based on the sample preparation method used, with bank soils, sediments, and suspended particulates represented as combusted samples, and filtered surface waters and filtered porewaters associated with the uncertainty of filtered water samples.

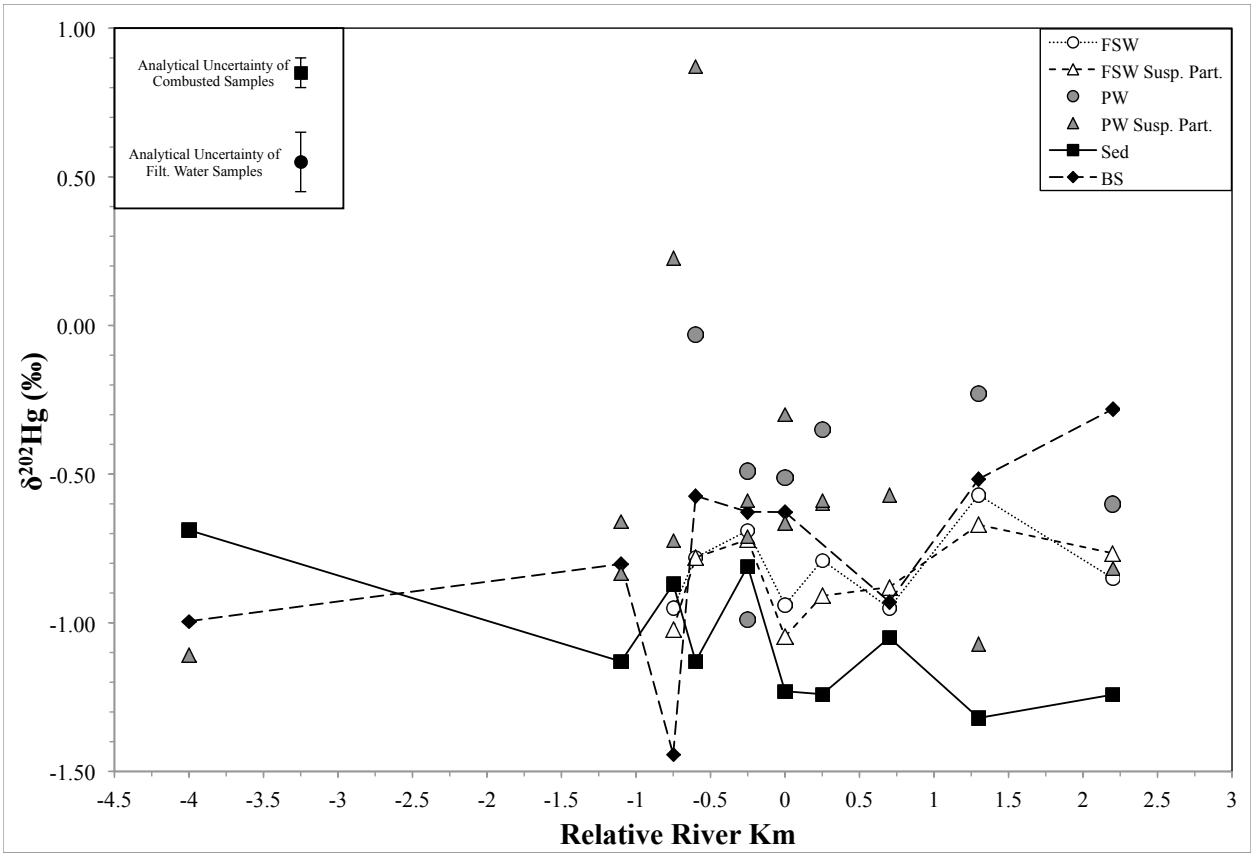

Figure 3.3 Δ^{199}Hg Longitudinal Profile

Longitudinal profile along the South River near the former DuPont plant of Δ^{199}Hg values (‰) of samples collected in 2016. Sampling locations are presented in relative river kilometers. The analytical uncertainty of Hg isotopic measurements (2σ) is presented based on the sample preparation method used, with bank soils, sediments, and suspended particulates represented as combusted samples, and filtered surface waters and filtered porewaters associated with the uncertainty of filtered water samples.

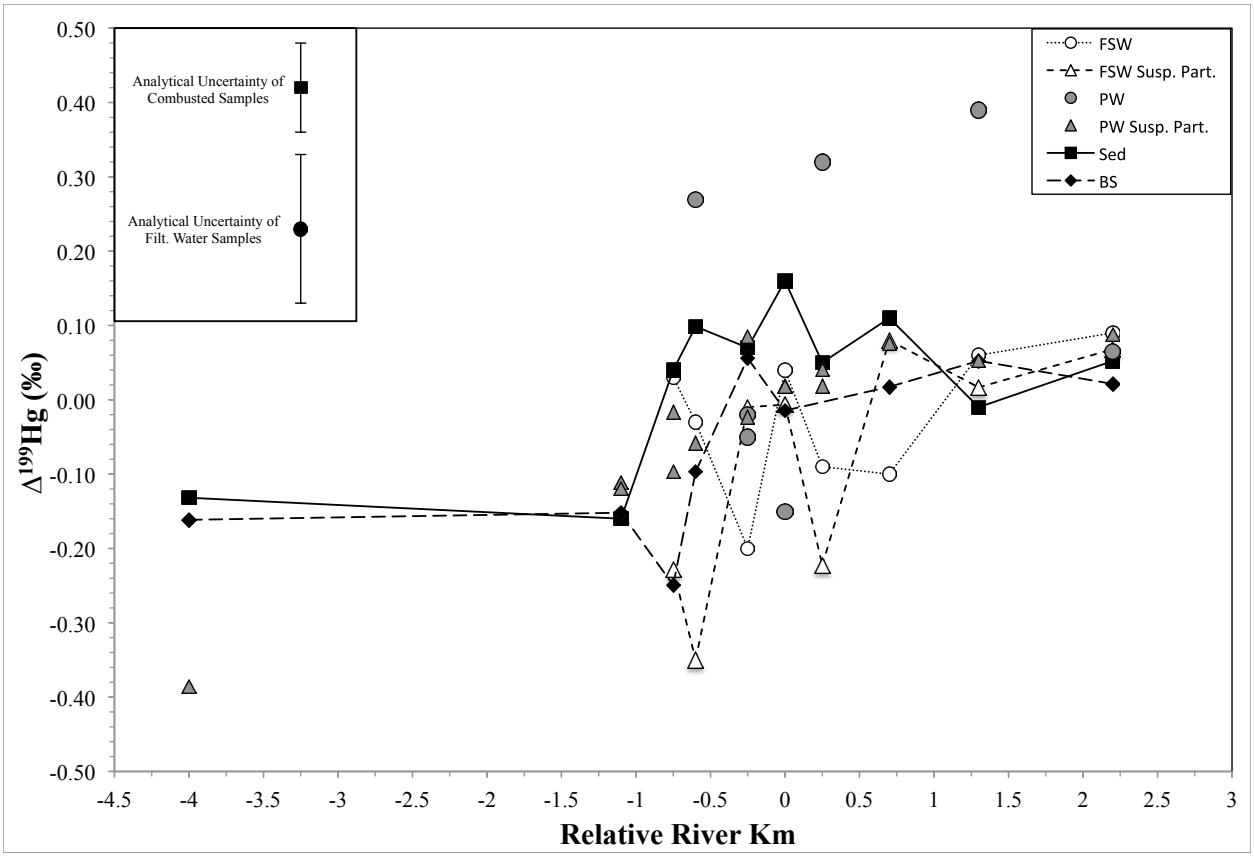

Figure 3.4 Hg Depth Profile for RRKm 4.75 Floodplain Profile

Profile of THg (black squares) and Hg isotopic composition (δ^{202}Hg values with blue squares and Δ^{199}Hg values with red squares) of RRKm 4.75 floodplain sediments. Samples are shown at the estimated median age for the sampling depth, calculated from the median sedimentation rate reported in Ref. (Pizzuto et al., 2016). Error bars on the THg values represent the uncertainty associated with the age model, as determined from the range of sedimentation rates. The period of Hg use at the former DuPont facility (1929-1950) is shown with the light red background.

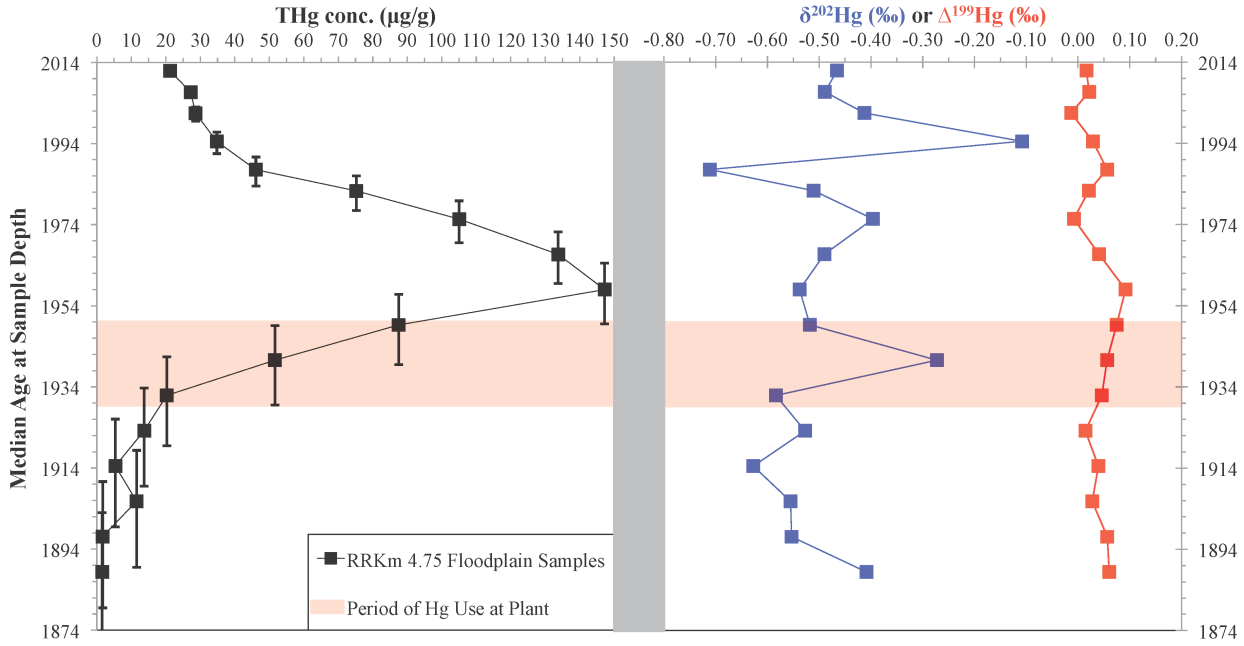

Figure 3.5 End-Member Isotopic Mixing Model for Hg in the South River

Three end-member isotopic mixing model for suspended particulates, presented as 1/THg conc. (kg material/ng of Hg) vs. δ^{202}Hg values (‰). Analytical uncertainty of Hg isotopic measurements (2σ) is displayed for suspended particulates. The mean (±1σ) of δ^{202}Hg values for 2014 (black square) and 2016 (blue square) streambed sediments are shown for reference. Grey areas represent suggested end-member ranges, and black lines (solid and dashed) are lines of isotopic mixing. 2014 data taken from Ref. (Washburn et al., 2017).

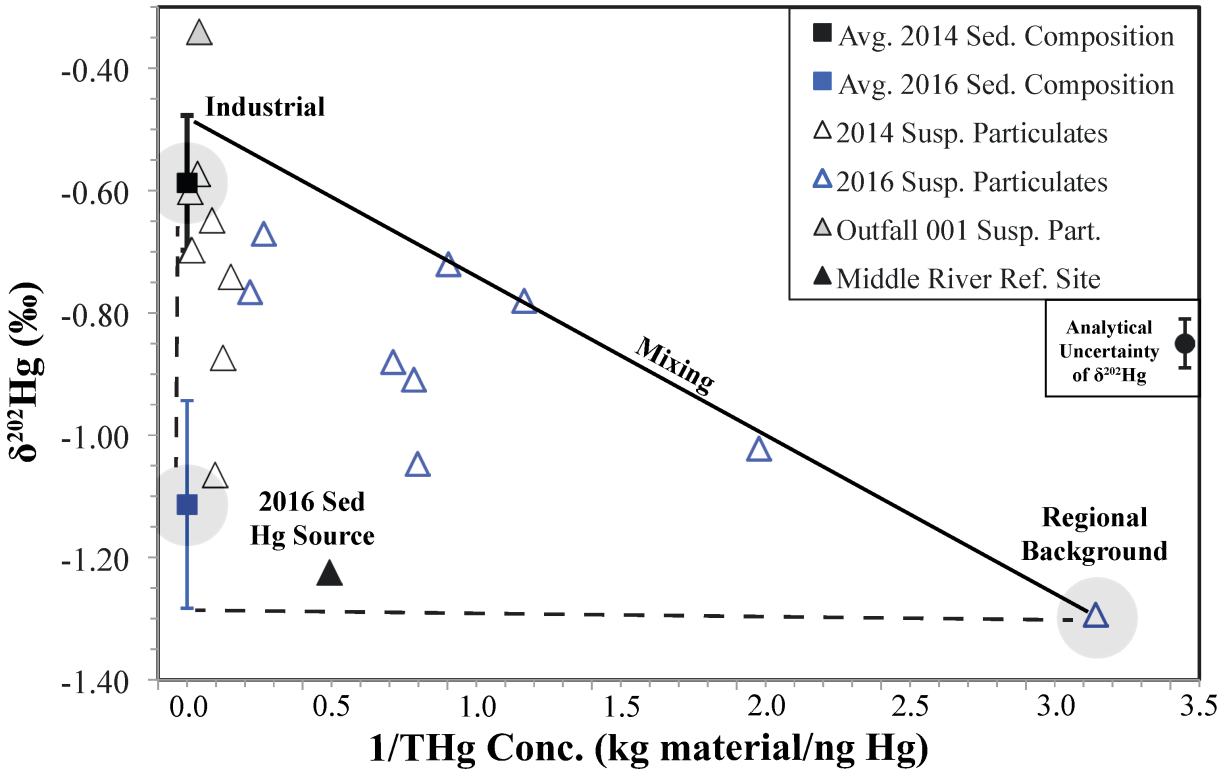

References

(1) Baptista-Salazar, C.; Hintelmann, H.; Biester, H. Distribution of Mercury Species and Mercury Isotope Ratios in Soils and River Suspended Matter of a Mercury Mining Area. Environ. Sci. Process. Impacts 2018, 0, 1–11 DOI: 10.1039/C7EM00443E.

(2) Bartov, G.; Deonarine, A.; Johnson, T. M.; Ruhl, L.; Vengosh, A.; Hsu-Kim, H. Environmental Impacts of the Tennessee Valley Authority Kingston Coal Ash Spill. 1. Source Apportionment Using Mercury Stable Isotopes. *Environ. Sci. Technol.* **2013**, *47* (4), 2092–2099 DOI: 10.1021/es303111p.

(3) Bergeron, C. M.; Bodinof, C. M.; Unrine, J. M.; Hopkins, W. A. Mercury Accumulation along a Contamination Gradient and Nondestructive Indices of Bioaccumulation in Amphibians. *Environ. Toxicol. Chem.* **2010**, *29* (4), 980–988 DOI: 10.1002/etc.121.

(4) Biswas, A.; Blum, J. D.; Bergquist, B. A.; Keeler, G. J.; Xie, Z. Natural Mercury Isotope Variation in Coal Deposits and Organic Soils. *Environ. Sci. Technol.* **2008**, *42* (22), 8303–8309 DOI: 10.1021/es801444b.

(5) Blum, J. D.; Bergquist, B. A. Reporting of Variations in the Natural Isotopic Composition of Mercury. *Anal. Bioanal. Chem.* **2007**, *388* (2), 353–359 DOI: 10.1007/s00216-007-1236-9.

(6) Blum, J. D.; Johnson, M. W. Recent Developments in Mercury Stable Isotope Analysis. *Rev. Mineral. Geochemistry* **2017**, *82* (1), 733–757 DOI: https://doi.org/10.2138/rmg.2017.82.17.

(7) Blum, J. D.; Sherman, L. S.; Johnson, M. W. Mercury Isotopes in Earth and Environmental Sciences. *Annu. Rev. Earth Planet. Sci.* **2014**, *42* (1), 249–269 DOI: 10.1146/annurev-earth-050212-124107.

(8) Brent, R. N.; Berberich, D. A. Use of Artificial Stream Mesocosms to Investigate Mercury Uptake in the South River, Virginia, USA. *Arch. Environ. Contam. Toxicol.* **2014**, *66* (2), 201–212 DOI: 10.1007/s00244-013-9964-7.

(9) Brent, R. N.; Kain, D. G. Development of an Empirical Nonlinear Model for Mercury Bioaccumulation in the South and South Fork Shenandoah Rivers of Virginia. *Arch. Environ. Contam. Toxicol.* **2011**, *61* (4), 614–623 DOI: 10.1007/s00244-011-9664-0.

(10) Cai, H.; Chen, J. Mass-Independent Fractionation of Even Mercury Isotopes. *Sci. Bull.* **2015**, *61* (January), 116–124 DOI: 10.1007/s11434-015-0968-8.

(11) Carter, L. J. Chemical Plants Leave Unexpected Legacy for Two Virginia Rivers. *Science (80-.).* **1977**, *198* (4321), 1015–1020 DOI: 10.1126/science.198.4321.1015.

(12) Chen, J. Bin; Hintelmann, H.; Feng, X. Bin; Dimock, B. Unusual Fractionation of Both Odd and Even Mercury Isotopes in Precipitation from Peterborough, ON, Canada. *Geochim. Cosmochim. Acta* **2012**, *90*, 33–46 DOI: 10.1016/j.gca.2012.05.005.

(13) Chen, J.; Hintelmann, H.; Zheng, W.; Feng, X.; Cai, H.; Wang, Z.; Yuan, S.; Wang, Z. Isotopic Evidence for Distinct Sources of Mercury in Lake Waters and Sediments. *Chem. Geol.* **2016**, *426*, 33–44 DOI: 10.1016/j.chemgeo.2016.01.030.

(14) Creswell, J. E.; Kerr, S. C.; Meyer, M. H.; Babiarz, C. L.; Shafer, M. M.; Armstrong, D. E.; Roden, E. E. Factors Controlling Temporal and Spatial Distribution of Total Mercury and Methylmercury in Hyporheic Sediments of the Allequash Creek Wetland, Northern Wisconsin. *J. Geophys. Res. Biogeosciences* **2008**, *113* (G2), n/a-n/a DOI: 10.1029/2008JG000742.

(15) Cristol, D. A; Brasso, R. L.; Condon, A. M.; Fovargue, R. E.; Friedman, S. L.; Hallinger, K. K.; Monroe, A. P.; White, A. E. The Movement of Aquatic Mercury through Terrestrial Food Webs. *Science (80-.).* **2008**,

320 (5874), 335 DOI: 10.1126/science.1154082.

(16) Demers, J. D.; Blum, J. D.; Zak, D. R. Mercury Isotopes in a Forested Ecosystem: Implications for Air-Surface Exchange Dynamics and the Global Mercury Cycle. *Global Biogeochem. Cycles* **2013**, *27*, n/a-n/a DOI: 10.1002/gbc.20021.

(17) Demers, J. D.; Blum, J. D.; Brooks, S.; Donovan, P. M.; Riscassi, A.; Miller, C. L.; Zheng, W.; Gu, B. Hg Isotopes Reveal in-Stream Processing and Legacy Inputs in East Fork Poplar Creek, Oak Ridge, Tennessee, USA. Environ. Sci. Process. Impacts 2018 DOI: 10.1039/C7EM00538E.

(18) Donovan, P. M.; Blum, J. D.; Demers, J. D.; Gu, B.; Brooks, S. C.; Peryam, J. Identification of Multiple Mercury Sources to Stream Sediments near Oak Ridge, TN, USA. *Environ. Sci. Technol.* **2014**, *48* (7), 3666–3674.

(19) Donovan, P. M.; Blum, J. D.; Singer, M. B.; Marvin-DiPasquale, M.; Tsui, M. T. K. Isotopic Composition of Inorganic Mercury and Methylmercury Downstream of a Historical Gold Mining Region. *Environ. Sci. Technol.* **2016**, acs.est.5b04413 DOI: 10.1021/acs.est.5b04413.

(20) Donovan, P. M.; Blum, J. D.; Singer, M. B.; Marvin-DiPasquale, M.; Tsui, M. T. K. Methylmercury Degradation and Exposure Pathways in Streams and Wetlands Impacted by Historical Mining. *Sci. Total Environ.* **2016** DOI: 10.1016/j.scitotenv.2016.04.139.

(21) Driscoll, C. T.; Mason, R. P.; Chan, H. M.; Jacob, D. J.; Pirrone, N. Mercury as a Global Pollutant: Sources, Pathways, and Effects. *Environ. Sci. Technol.* **2013**, *47* (10), 4967–4983 DOI: 10.1021/es305071v.

(22) Enrico, M.; Roux, G. Le; Marusczak, N.; Heimbürger, L.-E.; Claustres, A.; Fu, X.; Sun, R.; Sonke, J. E. Atmospheric Mercury Transfer to Peat Bogs Dominated by Gaseous Elemental Mercury Dry Deposition. *Environ. Sci. Technol.* **2016**, acs.est.5b06058 DOI: 10.1021/acs.est.5b06058.

(23) Estrade, N.; Carignan, J.; Donard, O. F. X. Tracing and Quantifying Anthropogenic Mercury Sources in Soils of Northern France Using Isotopic Signatures. *Environ. Sci. Technol.* **2011**, *45* (4), 1235–1242 DOI: 10.1021/es1026823.

(24) Flanders, J. R.; Turner, R. R.; Morrison, T.; Jensen, R.; Pizzuto, J.; Skalak, K.; Stahl, R. Distribution, Behavior, and Transport of Inorganic and Methylmercury in a High Gradient Stream. *Appl. Geochemistry* **2010**, *25* (11), 1756–1769 DOI: 10.1016/j.apgeochem.2010.09.004.

(25) Foran, C. M.; Baker, K. M.; Grosso, N. R.; Linkov, I. An Enhanced Adaptive Management Approach for Remediation of Legacy Mercury in the South River. *PLoS One* **2015**, *10* (2), 1–15 DOI: 10.1371/journal.pone.0117140.

(26) Foucher, D.; Hintelmann, H.; Al, T. a.; MacQuarrie, K. T. Mercury Isotope Fractionation in Waters and Sediments of the Murray Brook Mine Watershed (New Brunswick, Canada): Tracing Mercury Contamination and Transformation. *Chem. Geol.* **2013**, *336*, 87–95 DOI: 10.1016/j.chemgeo.2012.04.014.

(27) Ghosh, S.; Schauble, E. a.; Lacrampe Couloume, G.; Blum, J. D.; Bergquist, B. A. Estimation of Nuclear Volume Dependent Fractionation of Mercury Isotopes in Equilibrium Liquid–vapor Evaporation Experiments. *Chem. Geol.* **2013**, *336*, 5–12 DOI: 10.1016/j.chemgeo.2012.01.008.

(28) Gray, J. E.; Van Metre, P. C.; Pribil, M. J.; Horowitz, A. J. Tracing Historical Trends of Hg in the Mississippi River Using Hg Concentrations and Hg Isotopic Compositions in a Lake Sediment Core, Lake Whittington, Mississippi, USA. *Chem. Geol.* **2015**, *395*, 80–87 DOI: 10.1016/j.chemgeo.2014.12.005.

(29) Guedron, S.; Amouroux, D.; Sabatier, P.; Desplanque, C.; Develle, A. L.; Barre, J.; Feng, C.; Guiter, F.;

Arnaud, F.; Reyss, J. L.; Charlet, L. A Hundred Year Record of Industrial and Urban Development in French Alps Combining Hg Accumulation Rates and Isotope Composition in Sediment Archives from Lake Luitel. *Chem. Geol.* **2016**, *431*, 10–19 DOI: 10.1016/j.chemgeo.2016.03.016.

(30) Hinkle, S. R.; Bencala, K. E.; Wentz, D. A.; Krabbenhoft, D. P. Mercury and Methylmercury Dynamics in the Hyporheic Zone of an Oregon Stream. *Water. Air. Soil Pollut.* **2014**, *225* (1) DOI: 10.1007/s11270-013-1694-y.

(31) Hurley, J. P.; Cowell, S. E.; Shafer, M. M.; Hughes, P. E. Partitioning and Transport of Total and Methyl Mercury in the Lower Fox River, Wisconsin http://pubs.acs.org/doi/pdf/10.1021/es970685b (accessed Dec 9, 2016).

(32) Jackson, A. K.; Evers, D. C.; Folsom, S. B.; Condon, A. M.; Diener, J.; Goodrick, L. F.; McGann, A. J.; Schmerfeld, J.; Cristol, D. A. Mercury Exposure in Terrestrial Birds Far Downstream of an Historical Point Source. *Environ. Pollut.* **2011**, *159* (12), 3302–3308 DOI: 10.1016/j.envpol.2011.08.046.

(33) Jiskra, M.; Wiederhold, J. G.; Bourdon, B.; Kretzschmar, R. Solution Speciation Controls Mercury Isotope Fractionation of Hg(II) Sorption to Goethite. *Environ. Sci. Technol.* **2012**, *46* (12), 6654–6662 DOI: 10.1021/es3008112.

(34) Jiskra, M.; Wiederhold, J. G.; Skyllberg, U.; Kronberg, R. M.; Hajdas, I.; Kretzschmar, R. Mercury Deposition and Re-Emission Pathways in Boreal Forest Soils Investigated with Hg Isotope Signatures. *Environ. Sci. Technol.* **2015**, *49* (12), 7188–7196 DOI: 10.1021/acs.est.5b00742.

(35) Jiskra, M.; Wiederhold, J.; Skyllberg, U.; Kronberg, R.-M.; Kretzschmar, R. Source Tracing of Natural Organic Matter Bound Mercury in Boreal Forest Runoff with Mercury Stable Isotopes. *Environ. Sci. Process. Impacts* **2017**, *0*, 1–14 DOI: 10.1039/C7EM00245A.

(36) Kocman, D.; Horvat, M.; Pirrone, N.; Cinnirella, S. Contribution of Contaminated Sites to the Global Mercury Budget. *Environ. Res.* **2013**, *125*, 160–170 DOI: 10.1016/j.envres.2012.12.011.

(37) Kocman, D.; Wilson, S. J.; Amos, H. M.; Telmer, K. H.; Steenhuisen, F.; Sunderland, E. M.; Mason, R. P.; Outridge, P.; Horvat, M. Toward an Assessment of the Global Inventory of Present-Day Mercury Releases to Freshwater Environments. *Int. J. Environ. Res. Public Health* **2017**, *14* (2) DOI: 10.3390/ijerph14020138.

(38) Kritee, K.; Barkay, T.; Blum, J. D. Mass Dependent Stable Isotope Fractionation of Mercury during Mer Mediated Microbial Degradation of Monomethylmercury. *Geochim. Cosmochim. Acta* **2009**, *73* (5), 1285–1296 DOI: 10.1016/j.gca.2008.11.038.

(39) Kritee, K.; Blum, J. D.; Johnson, M. W.; Bergquist, B. A.; Barkay, T. Mercury Stable Isotope Fractionation during Microbial Reduction of Hg(II) to Hg(0). *Environ. Sci. Technol.* **2007**, *41* (6), 1889–1895.

(40) Lauretta, D. S.; Klaue, B.; Blum, J. D.; Buseck, P. R. Mercury Abundances and Isotopic Compositions in the Murchison (CM) and Allende (CV) Carbonaceous Chondrites. *Geochim. Cosmochim. Acta* **2001**, *65* (16), 2807–2818 DOI: 10.1016/S0016-7037(01)00630-5.

(41) Lepak, R. F.; Yin, R.; Krabbenhoft, D. P.; Ogorek, J. M.; DeWild, J. F.; Holsen, T. M.; Hurley, J. P. Use of Stable Isotope Signatures to Determine Mercury Sources in the Great Lakes. *Environ. Sci. Technol. Lett.* **2015**, *2* (12), 335–341 DOI: 10.1021/acs.estlett.5b00277.

(42) Liu, J.; Feng, X.; Yin, R.; Zhu, W.; Li, Z. Mercury Distributions and Mercury Isotope Signatures in Sediments of Dongjiang, the Pearl River Delta, China. *Chem. Geol.* **2011**, *287* (1–2), 81–89 DOI: 10.1016/j.chemgeo.2011.06.001.

(43) Ma, J.; Hintelmann, H.; Kirk, J. L.; Muir, D. C. G. Mercury Concentrations and Mercury Isotope Composition in Lake Sediment Cores from the Vicinity of a Metal Smelting Facility in Flin Flon, Manitoba. *Chem. Geol.* **2013**, *336*, 96–102 DOI: 10.1016/j.chemgeo.2012.10.037.

(44) Marshall, B. G.; Veiga, M. M.; Kaplan, R. J.; Adler Miserendino, R.; Schudul, G.; Bergquist, B. A.; Guimarães, J. R. D.; Sobral, L. G. S.; Gonzalez-Mueller, C. Evidence of Transboundary Mercury and Other Pollutants in the Puyango-Tumbes River Basin, Ecuador-Peru. Environ. Sci. Process. Impacts 2018 DOI: 10.1039/C7EM00504K.

(45) Murphy, G. W.; Newcomb, T. J.; Orth, D. J. Sexual and Seasonal Variations of Mercury in Smailmouth Bass. *J. Freshw. Ecol.* **2007**, *22* (1), 135–144 DOI: 10.1080/02705060.2007.9664153.

(46) Neufeld, D. S. G. Mercury Accumulation in Caged Corbicula: Rate of Uptake and Seasonal Variation. *Environ. Monit. Assess.* **2010**, *168* (1–4), 385–396 DOI: 10.1007/s10661-009-1121-4.

(47) Perrot, V.; Epov, V. N.; Pastukhov, M. V; Grebenshchikova, V. I.; Zouiten, C.; Sonke, J. E.; Husted, S.; Donard, O. F. X.; Amouroux, D. Tracing Sources and Bioaccumulation of Mercury in Fish of Lake Baikal--Angara River Using Hg Isotopic Composition. *Environ. Sci. Technol.* **2010**, *44* (21), 8030–8037 DOI: 10.1021/es101898e.

(48) Pizzuto, J.; O'Neal, M. Increased Mid-Twentieth Century Riverbank Erosion Rates Related to the Demise of Mill Dams, South River, Virginia. *Geology* **2009**, *37* (1), 19–22 DOI: 10.1130/G25207A.1.

(49) Pizzuto, J.; Skalak, K.; Pearson, A.; Benthem, A. Active Overbank Deposition during the Last Century, South River, Virginia. *Geomorphology* **2016**, *257*, 164–178 DOI: 10.1016/j.geomorph.2016.01.006.

(50) Poulin, B. A.; Aiken, G. R.; Nagy, K. L.; Manceau, A.; Krabbenhoft, D. P.; Ryan, J. N. Mercury Transformation and Release Differs with Depth and Time in a Contaminated Riparian Soil during Simulated Flooding. *Geochim. Cosmochim. Acta* **2016**, *176*, 118–138 DOI: 10.1016/j.gca.2015.12.024.

(51) Rhoades, E. L.; O'Neal, M. a.; Pizzuto, J. E. Quantifying Bank Erosion on the South River from 1937 to 2005, and Its Importance in Assessing Hg Contamination. *Appl. Geogr.* **2009**, *29* (1), 125–134 DOI: 10.1016/j.apgeog.2008.08.005.

(52) Shanley, J. B.; Kamman, N. C.; Clair, T. A.; Chalmers, A. Physical Controls on Total and Methylmercury Concentrations in Streams and Lakes of the Northeastern USA. *Ecotoxicology* **2005**, *14* (1–2), 125–134 DOI: 10.1007/s10646-004-6264-z.

(53) Sherman, L. S.; Blum, J. D. Mercury Stable Isotopes in Sediments and Largemouth Bass from Florida Lakes, USA. *Sci. Total Environ.* **2013**, *448*, 163–175 DOI: 10.1016/j.scitotenv.2012.09.038.

(54) Skalak, K.; Pizzuto, J. The Distribution and Residence Time of Suspended Sediment Stored within the Channel Margins of a Gravel-Bed Bedrock River. *Earth Surf. Process. Landforms* **2010**, 35, 435–446 DOI: 10.1002/esp.1926.

(55) Smith, R. S.; Wiederhold, J. G.; Jew, A. D.; Brown, G. E.; Bourdon, B.; Kretzschmar, R. Stable Hg Isotope Signatures in Creek Sediments Impacted by a Former Hg Mine. *Environ. Sci. Technol.* **2015**, *49* (2), 767–776 DOI: 10.1021/es503442p.

(56) Sonke, J. E.; Schäfer, J.; Chmeleff, J.; Audry, S.; Blanc, G.; Dupré, B. Sedimentary Mercury Stable Isotope Records of Atmospheric and Riverine Pollution from Two Major European Heavy Metal Refineries. *Chem. Geol.* **2010**, *279* (3–4), 90–100 DOI: 10.1016/j.chemgeo.2010.09.017.

(57) Stoor, R. W.; Hurley, J. P.; Babiarz, C. L.; Armstrong, D. E. Subsurface Sources of Methyl Mercury to Lake Superior from a Wetland-Forested Watershed. *Sci. Total Environ.* **2006**, *368* (1), 99–110 DOI:

10.1016/j.scitotenv.2005.10.019.

(58) Sun, R.; Sonke, J. E.; Liu, G. Biogeochemical Controls on Mercury Stable Isotope Compositions of World Coal Deposits : A Review. *Earth Sci. Rev.* **2016**, *152*, 1–13 DOI: 10.1016/j.earscirev.2015.11.005.

(59) Tsui, M. T. K.; Blum, J. D.; Finlay, J. C.; Balogh, S. J.; Kwon, S. Y. Photodegradation of Methylmercury in Stream Ecosystems. *Limnol. Oceanogr.* **2013**, *58* (1), 13–22 DOI: 10.4319/lo.2013.58.1.0013.

(60) Tsui, M. T. K.; Blum, J. D.; Kwon, S. Y.; Finlay, J. C.; Balogh, S. J.; Nollet, Y. H. Sources and Transfers of Methylmercury in Adjacent River and Forest Food Webs. *Environ. Sci. Technol.* **2012**, *46* (20), 10957–10964 DOI: 10.1021/es3019836.

(61) Tsui, M. T. K.; Blum, J. D.; Finlay, J. C.; Balogh, S. J.; Nollet, Y. H.; Palen, W. J.; Power, M. E. Variation in Terrestrial and Aquatic Sources of Methylmercury in Stream Predators as Revealed by Stable Mercury Isotopes. *Environ. Sci. Technol.* **2014**, *48* (17), 10128–10135 DOI: 10.1021/es500517s.

(62) Turner, R. R.; Southworth, G. R. Mercury-Contaminated Industrial and Mining Sites in North America: An Overview with Selected Case Studies. In *Mercury Contaminated Sites: Characterization, Risk Assessment and Remediation*; Ebinghaus, R., Turner, R. R., de Lacerda, L. D., Vasiliev, O., Salomons, W., Eds.; Springer Berlin Heidelberg: Berlin, Heidelberg, 1999; pp 89–112.

(63) USEPA. 1999. Method 160.2: Total Suspended Solids (TSS). U.S. Environmental Protection Agency, Office of Water, Engineering and Analysis Division (4303), Washington, D.C. USA.

(64) USEPA. 2002. Method 1631, Revision E: Mercury in Water by Oxidation, Purge and Trap, and Cold Vapor Atomic Fluorescence U.S. Environmental Protection Agency, Office of Water, Engineering and Analysis Division (4303), Washington, D.C. USA.

(65) USEPA. 1996. Method 1669: Sampling Ambient Water for Trace metals at EPA Water Quality Criteria Levels. U.S. Environmental Protection Agency, Office of Water, Engineering and Analysis Division (4303), Washington, D.C. USA.

(66) URS Corporation. *Final Report: Ecological Study of the South River and a Segment of the South Fork Shenandoah River, Virginia*. Revised 2012. southriverscienceteam.org/news

(67) URS Corporation. *Comprehensive RFI Report. Former DuPont Waynesboro Plant, Waynesboro, Virginia*. Revised 2015. southriverscienceteam.org/news

(68) Washburn, S. J.; Blum, J. D.; Demers, J. D.; Kurz, A. Y.; Landis, R. C. Isotopic Characterization of Mercury Downstream of Historic Industrial Contamination in the South River, Virginia. *Environ. Sci. Technol.* **2017**, *51* (19), 10965–10973 DOI: 10.1021/acs.est.7b02577.

(69) Washburn, S. J.; Blum, J. D.; Johnson, M. W.; Tomes, J. M.; Carnell, P. J. Isotopic Characterization of Mercury in Natural Gas via Analysis of Mercury Removal Unit Catalysts. ACS Earth Sp. Chem. **2018**, DOI: 10.1021/acsearthspacechem.7b00118.

(70) Wiederhold, J. G.; Skyllberg, U.; Drott, A.; Jiskra, M.; Jonsson, S.; Björn, E.; Bourdon, B.; Kretzschmar, R. Mercury Isotope Signatures in Contaminated Sediments as a Tracer for Local Industrial Pollution Sources. *Environ. Sci. Technol.* **2015**, *49* (1), 177–185.

(71) Wiederhold, J. G.; Cramer, C. J.; Daniel, K.; Infante, I.; Bourdon, B.; Kretzschmar, R. Equilibrium Mercury Isotope Fractionation between Dissolved Hg (II) Species and Thiol-Bound Hg. *Environ. Sci. Technol.* **2010**, *44* (11), 4191–4197.

(72) Wiederhold, J. G.; Smith, R. S.; Siebner, H.; Jew, A. D.; Brown, G. E.; Bourdon, B.; Kretzschmar, R. Mercury

Isotope Signatures as Tracers for Hg Cycling at the New Idria Hg Mine. *Environ. Sci. Technol.* **2013**, *47* (12), 6137–6145 DOI: 10.1021/es305245z.

(73) Woerndle, G.; Tsui, M. T.-K.; Sebestyen, S.; Blum, J. D.; Nie, X.; Kolka, R. K. New Insights on Ecosystem Mercury Cycling Revealed by Stable Isotopes of Mercury in Water Flowing from a Headwater Peatland Catchment. *Environ. Sci. Technol.* **2018**, acs.est.7b04449 DOI: 10.1021/ACS.EST.7B04449.

(74) Xu, X.; Zhang, Q.; Wang, W. X. Linking Mercury, Carbon, and Nitrogen Stable Isotopes in Tibetan Biota: Implications for Using Mercury Stable Isotopes as Source Tracers. *Sci. Rep.* **2016**, *6* (September 2015), 1–10 DOI: 10.1038/srep25394.

(75) Yin, R.; Feng, X.; Hurley, J. P.; Krabbenhoft, D. P.; Lepak, R. F. Mercury Isotopes as Proxies to Identify Sources and Environmental Impacts of Mercury in Sphalerites. *Sci. Rep.* **2016**, No. November 2015, 1–8 DOI: 10.1038/srep18686.

(76) Yin, R.; Feng, X.; Hurley, J. P.; Krabbenhoft, D. P.; Lepak, R. F.; Kang, S.; Yang, H.; Li, X. Historical Records of Mercury Stable Isotopes in Sediments of Tibetan Lakes. *Sci. Rep.* **2016**, *6*, 1–10 DOI: 10.1038/srep23332.

(77) Yin, R.; Feng, X.; Wang, J.; Li, P.; Liu, J.; Zhang, Y.; Chen, J.; Zheng, L.; Hu, T. Mercury Speciation and Mercury Isotope Fractionation during Ore Roasting Process and Their Implication to Source Identification of Downstream Sediment in the Wanshan Mercury Mining Area, SW China. *Chem. Geol.* **2013**, *336*, 72–79 DOI: 10.1016/j.chemgeo.2012.04.030.

(78) Yin, R.; Lepak, R. F.; Krabbenhoft, D. P.; Hurley, J. P. Sedimentary Records of Mercury Stable Isotopes in Lake Michigan. *Elem. Sci. Anthr.* **2016**, *4*, 86 DOI: 10.12952/journal.elementa.000086.

(79) Yu, R. Q.; Flanders, J. R.; MacK, E. E.; Turner, R.; Mirza, M. B.; Barkay, T. Contribution of Coexisting Sulfate and Iron Reducing Bacteria to Methylmercury Production in Freshwater River Sediments. *Environ. Sci. Technol.* **2012**, *46* (5), 2684–2691 DOI: 10.1021/es2033718.

(80) Zheng, W.; Hintelmann, H. Nuclear Field Shift Effect in Isotope Fractionation of Mercury during Abiotic Reduction in the Absence of Light. *J. Phys. Chem. A* **2010**, No. 1, 4238–4245.

(81) Zheng, W.; Obrist, D.; Weis, D.; Bergquist, B. A. Mercury Isotope Compositions across North American Forests. *Global Biogeochem. Cycles* **2016**, *30*, 1475–1492 DOI: 10.1002/2015GB005323

3.5 Supporting Information

Figure 3.6 Detailed Longitudinal Profile of δ^{202}Hg values (‰) of collected porewater samples

Detailed longitudinal profile along the South River near the former DuPont plant of δ^{202}Hg values (‰) of collected porewater samples**.** Sampling locations are presented in relative river kilometers, with samples collected from the right bank (downstream orientation) [RBPW] represented with open symbols, and those porewaters collected from the left bank [LBPW] represented with closed black symbols. Composite porewater samples that had to be aggregated from multiple sampling locations are represented with gray symbols, and placed at the most downstream sampling location. The analytical uncertainty of Hg isotopic measurements (2σ) is presented based on the sample preparation method used, with porewater suspended particulates represented as combusted samples, and dissolved phase Hg associated with the uncertainty of filtered porewater samples.

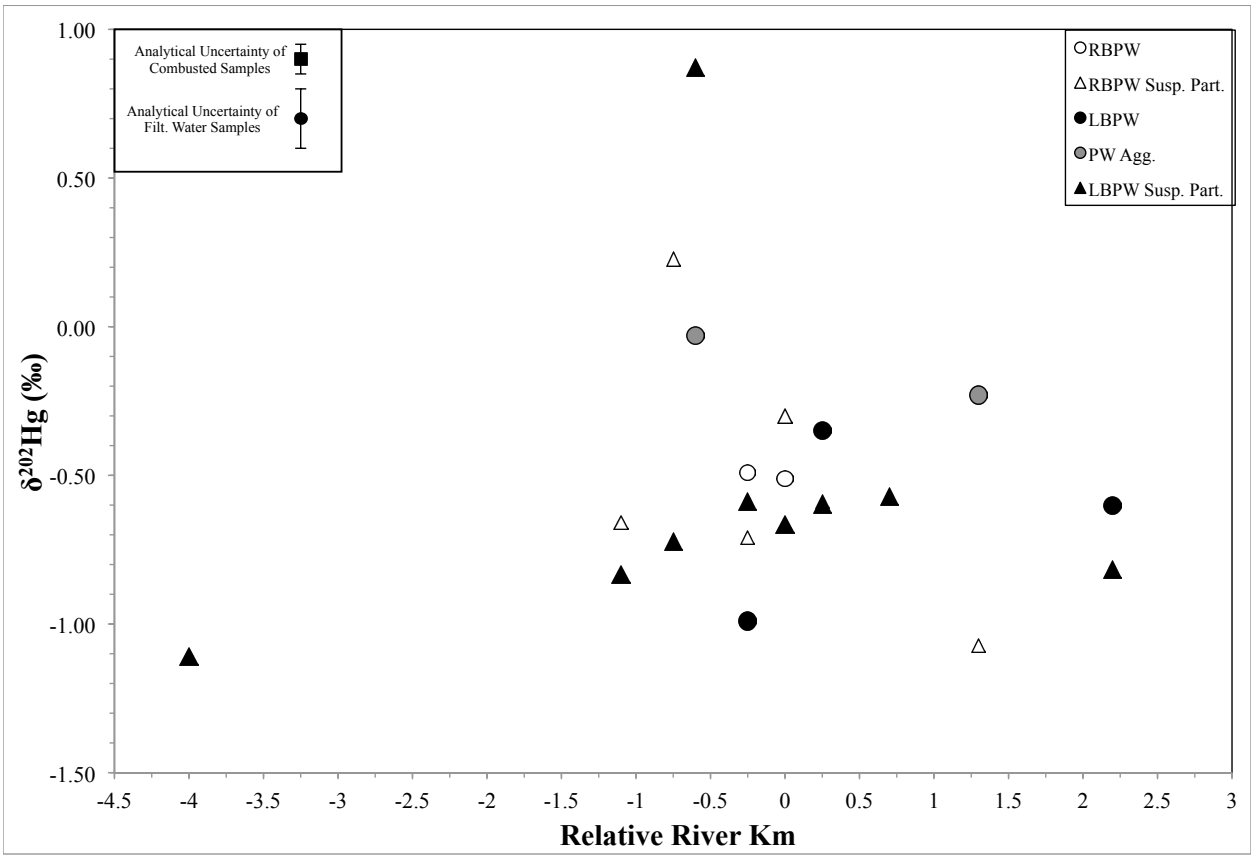

Figure 3.7 Plot of δ^{202}Hg values vs. Δ^{199}Hg values

Plot of δ202Hg values (‰) vs. Δ199Hg values (‰). The analytical uncertainty of Hg isotopic measurements (2σ) is presented based on the sample preparation method used, with bank soils, sediments, and suspended particulates represented as combusted samples, and filtered surface waters and filtered porewaters associated with the uncertainty of filtered water samples.

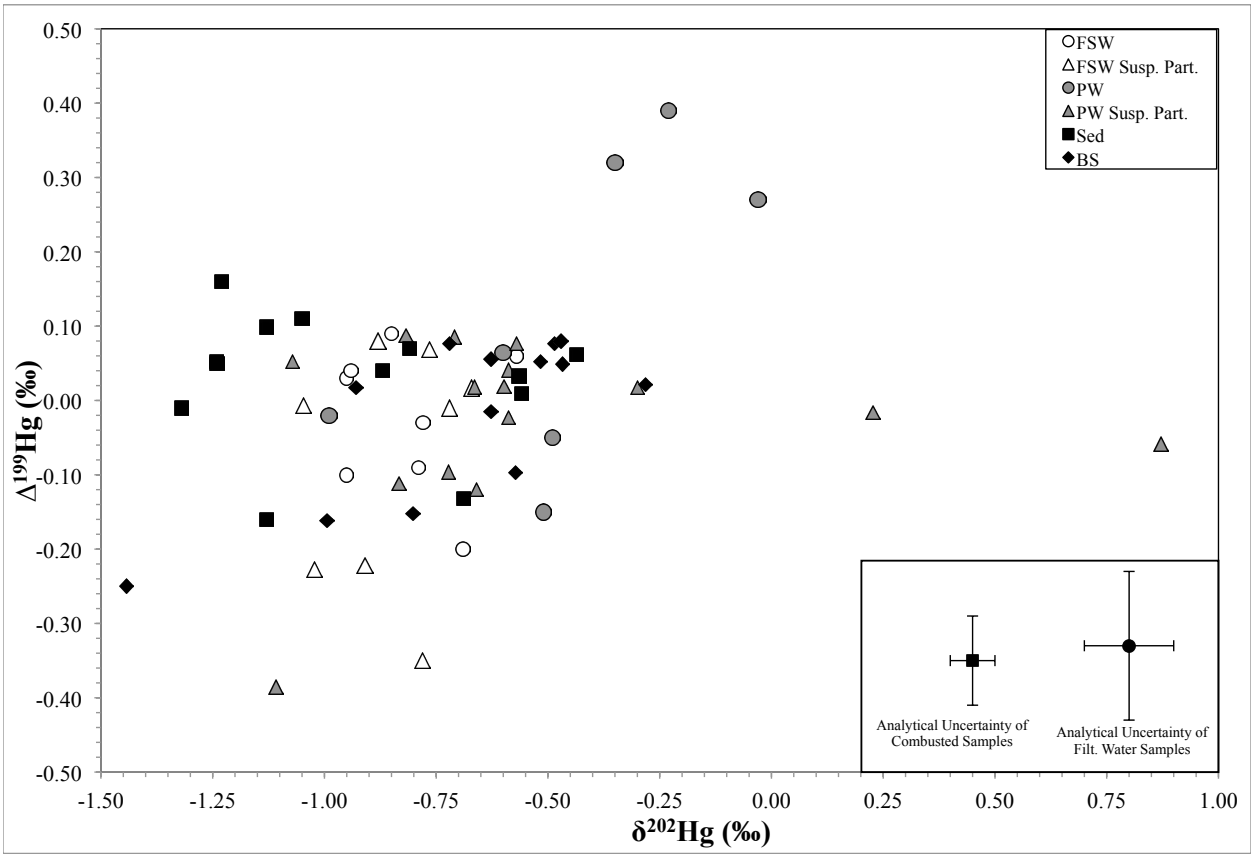

Figure 3.8 Plot of Δ^{201}Hg values vs. Δ^{199}Hg values

Plot of Δ^{201}Hg values (‰) vs. Δ^{199}Hg values (‰). The analytical uncertainty of Hg isotopic measurements (2σ) is presented based on the sample preparation method used, with bank soils, sediments, and suspended particulates represented as combusted samples, and filtered surface waters and filtered porewaters associated with the uncertainty of filtered water samples. Experimentally derived slopes for Hg(II) photoreduction (1.0; Berqguist and Blum 2007) & nuclear volume effects (1.6; Ghosh et al., 2013) as dotted and dashed black lines, respectively. A linear regression of all of the samples is shown as a solid black line.

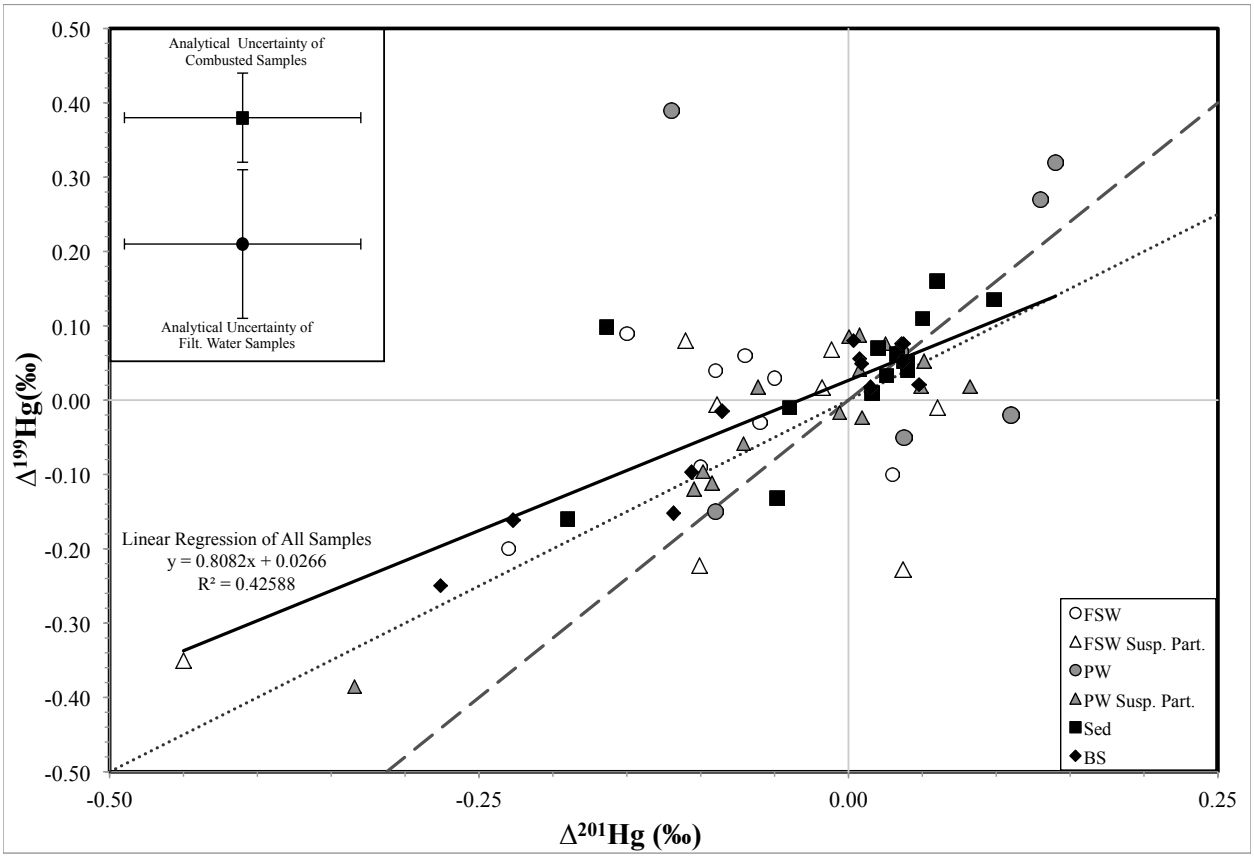

Figure 3.9 Plot of Δ^{204}Hg values vs. Δ^{200}Hg values

Plot of Δ^{204}Hg values (‰) vs. Δ^{200}Hg values (‰). The analytical uncertainty of Hg isotopic measurements (2σ) is presented based on the sample preparation method used, with bank soils, sediments, and suspended particulates represented as combusted samples, and filtered surface waters and filtered porewaters associated with the uncertainty of filtered water samples.

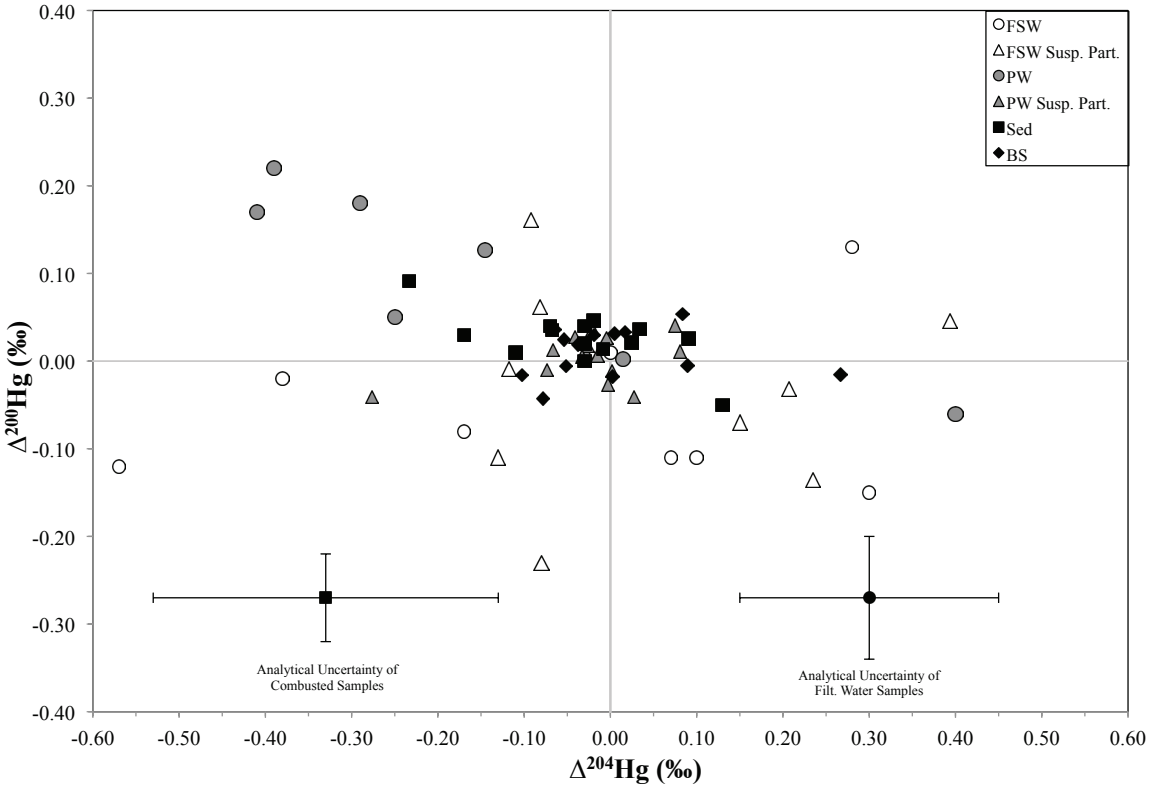

Figure 3.10 Detailed Longitudinal Profile of δ^{202}Hg values of Bank Soils and Streambed Sediments

Longitudinal profile along the South River near the former DuPont plant of δ^{202}Hg values (‰) of bank soils (diamonds) and streambed sediments (squares) collected in 2016 (blue symbols) and 2014 (black symbols). Sampling locations are presented in relative river kilometers. 2014 data taken from Ref. (Washburn et al., 2017)

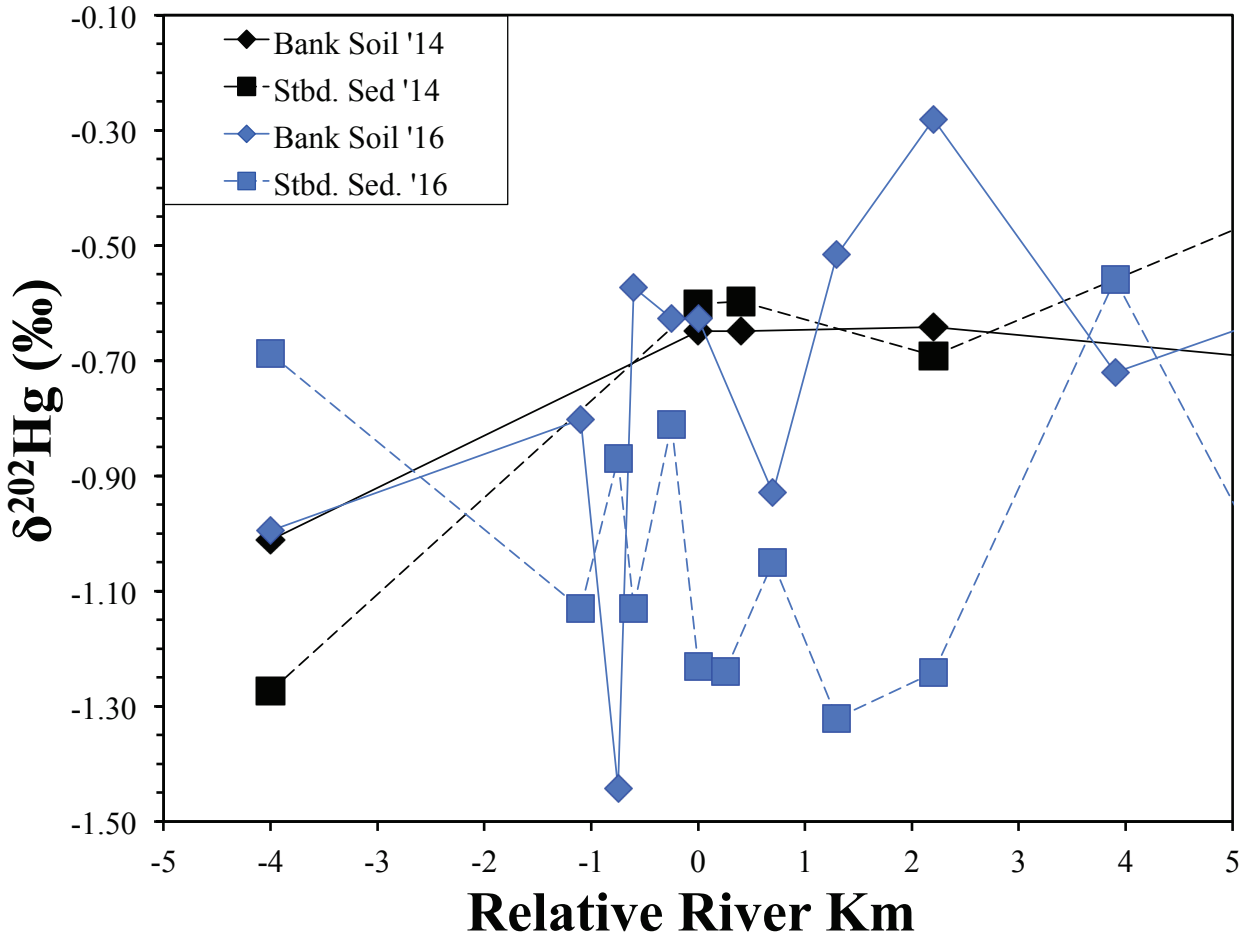

Figure 3.11 Detailed Longitudinal Profile of δ^{202}Hg values of Filtered Surface Waters and Suspended Particulates

Longitudinal profile along the South River near the former DuPont plant of δ^{202}Hg values (‰) of filtered surface waters (open circles) and suspended particulates (open triangles) collected in 2016 (blue symbols) and 2014 (black symbols). Sampling locations are presented in relative river kilometers. 2014 data taken from Ref. (Washburn et al., 2017).

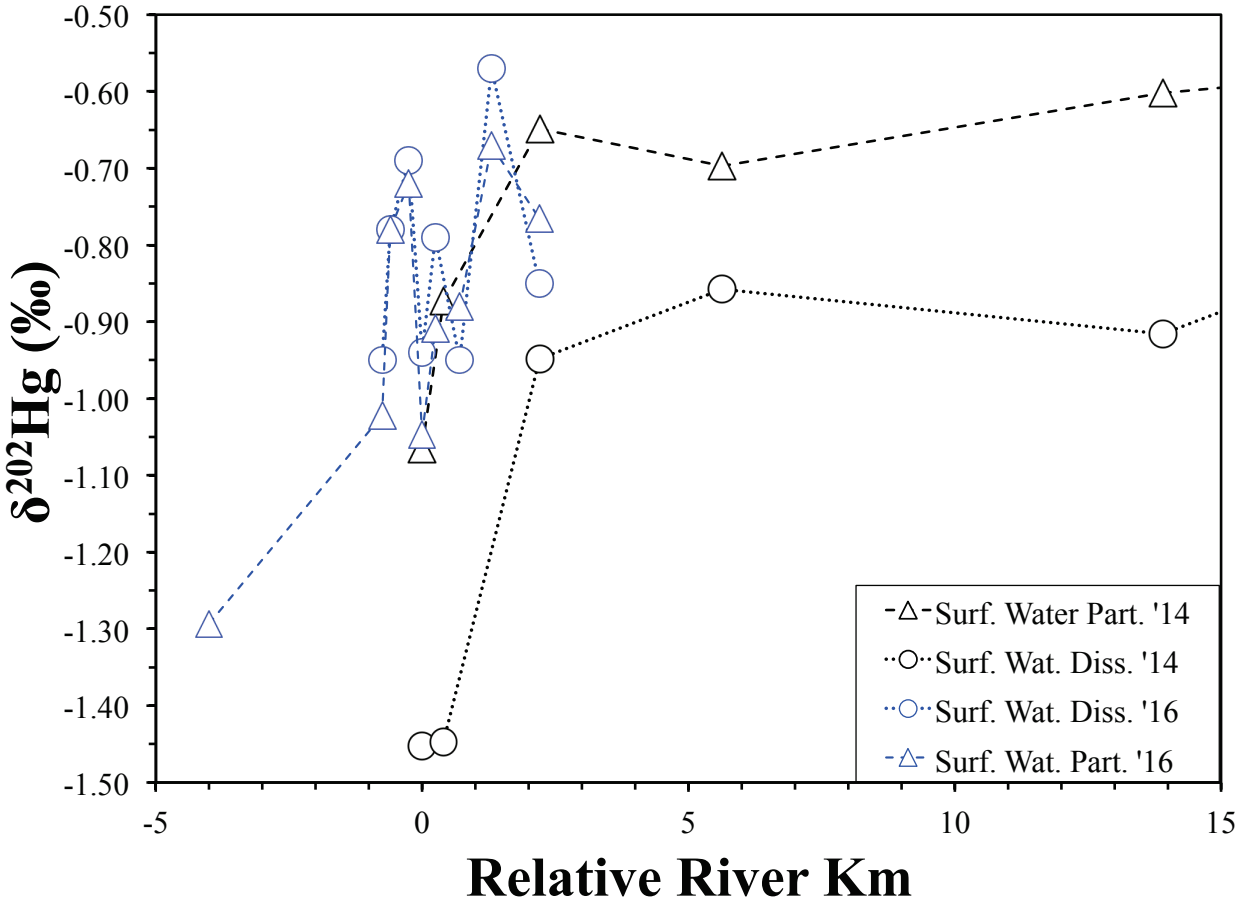

Figure 3.12 Three End-member Isotopic Mixing Model for Suspended Particulates

Three end-member isotopic mixing model for suspended particulates, presented as 1/THg conc. (kg material/ng of Hg) vs. Δ^{199}Hg values (‰). Analytical uncertainty of Hg isotopic measurements (2σ) is displayed for suspended particulates. The mean (±1σ) of Δ^{199}Hg values for 2014 (black square) and 2016 (blue square) streambed sediments are shown for reference. Solid black lines are lines of isotopic mixing. 2014 data taken from Ref. (Washburn et al., 2017).

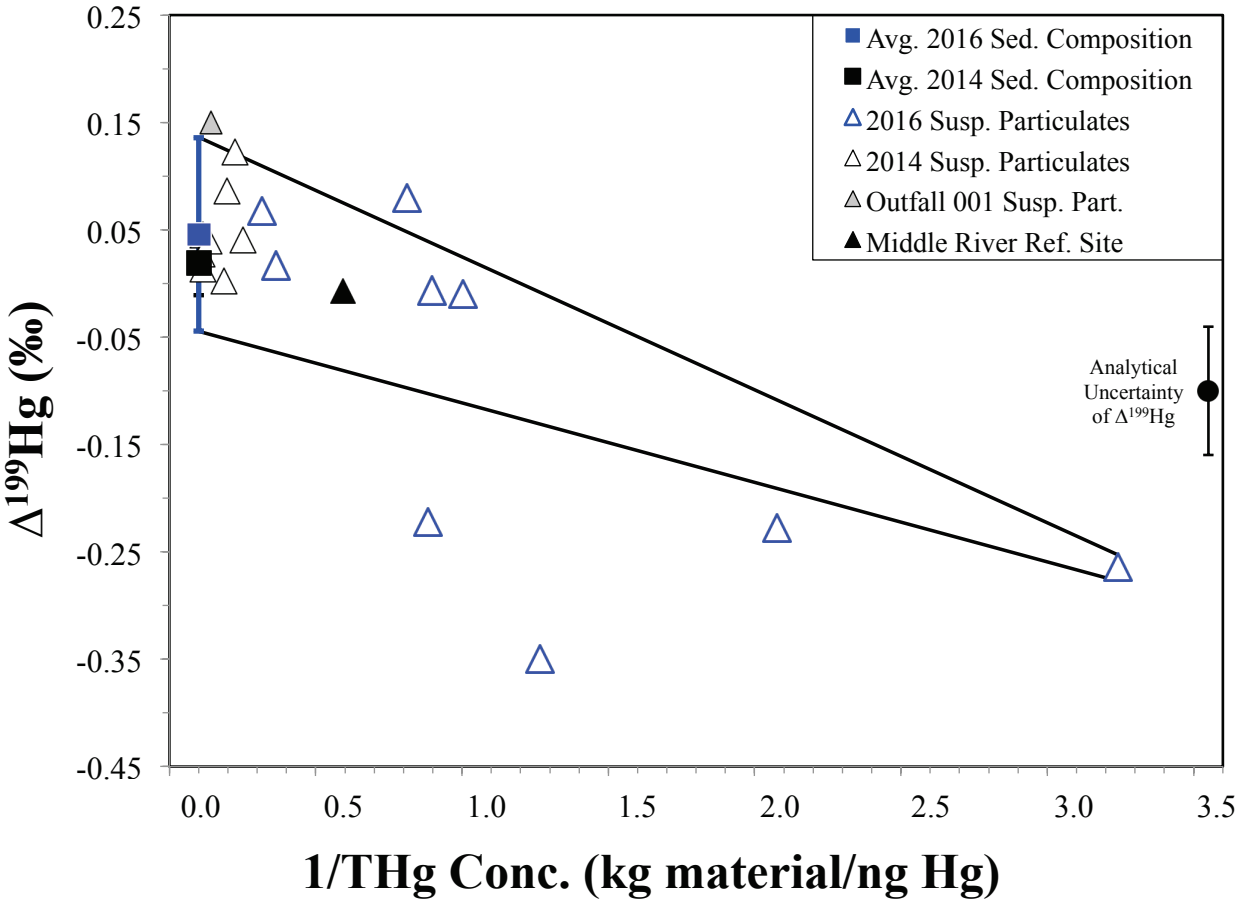

Table 3.1 Summary of THg Concentration and Hg Stable Isotope Data of South River Samples

Summary of THg concentration and Hg stable isotope data of collected samples from the South River channel. Where filtered surface water or filtered porewater samples have been aggregated together to obtain a composite Hg isotope measurement, this has been noted with a superscript following the sample type ([a,b,*,**,§]). The Hg isotope values obtained for composite samples are presented at the most downstream location for the sample type.

Location	Sample Type	THg	THg	log(K_d)	δ^{204}Hg	δ^{202}Hg	δ^{201}Hg	δ^{200}Hg	δ^{199}Hg	Δ^{204}Hg	Δ^{201}Hg	Δ^{200}Hg	Δ^{199}Hg
		ng/L	ng/g (d.w.)		‰	‰	‰	‰	‰	‰	‰	‰	‰
Upstream Reference Site RRKm - 4.0	Filtered Surface Water								NA				
	Suspended Material	0.32			-1.54	-1.29	-1.19	-0.60	-0.59	0.39	-0.22	0.05	-0.26
	Streambed Sediment		12.93		-0.99	-0.69	-0.57	-0.31	-0.31	0.03	-0.05	0.04	-0.13
	Bulk Bank Soil		32.41		-1.54	-0.99	-0.98	-0.48	-0.41	-0.05	-0.23	0.02	-0.16
	Left Bank PW Susp.	16.26			-1.93	-1.11	-1.17	-0.60	-0.66	-0.28	-0.33	-0.04	-0.39
	Left Bank Filt. PW*	0.40							*				
RRKm - 1.1	Filtered Surface Water[a]	0.35		5.49					a				
	Suspended Material[b]	0.42							b				
	Streambed Sediment		7.77		-1.86	-1.13	-1.05	-0.54	-0.45	-0.17	-0.19	0.03	-0.16
	Bulk Bank Soil		131.76		-1.23	-0.80	-0.72	-0.38	-0.35	-0.04	-0.12	0.02	-0.15
	Center Channel PW Susp.	224.67			-1.22	-0.83	-0.72	-0.46	-0.32	0.03	-0.09	-0.04	-0.11
	Center Channel Filt. PW*	0.95							*				
	Right Bank PW Susp.	318.52			-0.99	-0.66	-0.60	-0.36	-0.29	0.00	-0.10	-0.03	-0.12
	Right Bank Filt. PW*	1.35							*				
RRKm - 0.75	Filtered Surface Water[a]	0.64		5.31	-1.42	-0.95	-0.77	-0.47	-0.21	0.00	-0.05	0.01	0.03
	Suspended Material[b]	0.59			-1.61	-1.02	-0.73	-0.45	-0.49	-0.08	0.04	0.06	-0.23
	Streambed Sediment		560.20		-1.41	-0.87	-0.62	-0.43	-0.17	-0.11	0.04	0.01	0.04
	Bulk Bank Soil		13.26		-1.89	-1.44	-1.36	-0.74	-0.61	0.27	-0.28	-0.02	-0.25
	Left Bank PW Susp.	27.19			-1.11	-0.72	-0.64	-0.35	-0.28	-0.03	-0.10	0.01	-0.10
	Left Bank Filt. PW*	0.37							*				
	Right Bank PW Susp.	1357.60			0.27	0.23	0.16	0.13	0.04	-0.07	-0.01	0.01	-0.02
	Right Bank Filt. PW*	1.89							*				
RRKm - 0.6	Filtered Surface Water	0.83		5.48	-0.89	-0.78	-0.65	-0.27	-0.23	0.28	-0.06	0.13	-0.03
	Suspended Material	0.86			-1.24	-0.78	-1.04	-0.62	-0.55	-0.08	-0.45	-0.23	-0.35
	Streambed Sediment		17.04		-1.92	-1.13	-1.01	-0.48	-0.19	-0.23	-0.16	0.09	0.10
	Bulk Bank Soil		129.47		-0.96	-0.57	-0.54	-0.30	-0.24	-0.10	-0.11	-0.02	-0.10
	Left Bank PW Susp.	176.95			1.27	0.87	0.58	0.45	0.16	-0.03	-0.07	0.02	-0.06

	Left Bank Filt. PW*	0.25			-0.34	-0.03	0.11	0.16	0.26	-0.29	0.13	0.18	0.27
RRKm - 0.25	Filtered Surface Water	0.81		5.7	-1.60	-0.69	-0.75	-0.47	-0.37	-0.57	-0.23	-0.12	-0.20
	Suspended Material	1.11			-0.92	-0.72	-0.48	-0.43	-0.19	0.15	0.06	-0.07	-0.01
	Streambed Sediment		336.09		-1.23	-0.81	-0.59	-0.39	-0.14	-0.03	0.02	0.02	0.07
	Bulk Bank Soil		917.58		-0.85	-0.63	-0.46	-0.26	-0.10	0.08	0.01	0.05	0.06
	Left Bank PW Susp.	1624.93			-0.90	-0.59	-0.43	-0.26	-0.17	-0.02	0.01	0.04	-0.02
	Left Bank Filt. PW	8.80			-1.08	-0.99	-0.64	-0.56	-0.27	0.40	0.11	-0.06	-0.02
	Right Bank PW Susp.	2443.89			-1.06	-0.71	-0.53	-0.33	-0.09	0.00	0.00	0.03	0.09
	Right Bank Filt. PW	6.63			-0.72	-0.49	-0.33	-0.24	-0.17	0.01	0.04	0.00	-0.05
RRKm 0.0	Filtered Surface Water	0.82		5.65	-1.11	-0.94	-0.80	-0.63	-0.20	0.30	-0.09	-0.15	0.04
	Suspended Material	1.25			-1.33	-1.05	-0.88	-0.66	-0.27	0.23	-0.09	-0.14	-0.01
	Streambed Sediment		44.84		-1.90	-1.23	-0.87	-0.58	-0.15	-0.07	0.06	0.04	0.16
	Bulk Bank Soil		62872.13		-0.93	-0.63	-0.56	-0.33	-0.17	0.00	-0.09	-0.02	-0.01
	Left Bank PW Susp.	627.82			-0.99	-0.66	-0.45	-0.34	-0.15	0.00	0.05	-0.01	0.02
	Left Bank Filt. PW§	2.37							§				
	Right Bank PW Susp.	7940.40			-0.37	-0.30	-0.29	-0.14	-0.06	0.08	-0.06	0.01	0.02
	Right Bank Filt. PW	6.57			-1.01	-0.51	-0.47	-0.21	-0.27	-0.25	-0.09	0.05	-0.15
RRKm 0.25	Filtered Surface Water	0.89		5.64	-1.10	-0.79	-0.70	-0.51	-0.28	0.07	-0.10	-0.11	-0.09
	Suspended Material	1.28			-1.15	-0.91	-0.78	-0.49	-0.45	0.21	-0.10	-0.03	-0.22
	Streambed Sediment		239.19		-1.87	-1.24	-0.89	-0.62	-0.26	-0.03	0.04	0.00	0.05
	Bulk Bank Soil		NA						NA				
	Left Bank PW Susp.	38.23			-0.97	-0.60	-0.37	-0.31	-0.13	-0.07	0.08	-0.01	0.02
	Left Bank Filt. PW§	1.72			-0.93	-0.35	-0.13	-0.01	0.23	-0.41	0.14	0.17	0.32
	Right Bank PW Susp.	457.55			-0.92	-0.59	-0.44	-0.27	-0.11	-0.04	0.01	0.03	0.04
RRKm 0.7	Filtered Surface Water	1.06		5.64	-1.32	-0.95	-0.68	-0.58	-0.33	0.10	0.03	-0.11	-0.10
	Suspended Material	1.40			-1.44	-0.88	-0.78	-0.55	-0.14	-0.13	-0.11	-0.11	0.08
	Streambed Sediment		211.24		-1.61	-1.05	-0.74	-0.49	-0.15	-0.03	0.05	0.04	0.11
	Bulk Bank Soil		6304.25		-1.46	-0.93	-0.68	-0.51	-0.22	-0.08	0.01	-0.04	0.02
	Left Bank PW Susp.	773.19			-0.78	-0.57	-0.40	-0.25	-0.07	0.08	0.03	0.04	0.08
	Left Bank Filt. PW**	1.79							**				
RRKm 1.3	Filtered Surface Water	1.32		6.04	-1.23	-0.57	-0.50	-0.31	-0.09	-0.38	-0.07	-0.02	0.06
	Suspended Material	3.77			-1.09	-0.67	-0.52	-0.18	-0.15	-0.09	-0.02	0.16	0.02
	Streambed Sediment		430.45		-1.83	-1.32	-1.03	-0.71	-0.34	0.13	-0.04	-0.05	-0.01
	Bulk Bank Soil		22587.04		-0.68	-0.52	-0.35	-0.26	-0.08	0.09	0.04	-0.01	0.05
	Right Bank PW Susp.	458.00			-1.61	-1.07	-0.75	-0.53	-0.22	-0.01	0.05	0.01	0.05
	Right Bank Filt. PW**	2.83			-0.72	-0.23	-0.29	0.11	0.33	-0.39	-0.12	0.22	0.39
RRKm	Filtered Surface	1.51		6.03	-1.44	-0.85	-0.79	-0.50	-0.12	-0.17	-0.15	-0.08	0.09

2.2	Water												
	Suspended Material	4.60			-1.26	-0.77	-0.59	-0.39	-0.12	-0.12	-0.01	-0.01	0.07
	Streambed Sediment		639.96		-1.86	-1.24	-0.90	-0.61	-0.26	-0.01	0.04	0.01	0.05
	Bulk Bank Soil		7937.56		-0.47	-0.28	-0.16	-0.15	-0.05	-0.05	0.05	-0.01	0.02
	Left Bank PW Susp.	1771.60			-1.25	-0.82	-0.61	-0.41	-0.12	-0.03	0.01	0.01	0.09
	Left Bank Filt. PW	5.85			-1.04	-0.60	-0.42	-0.18	-0.09	-0.15	0.03	0.13	0.06
RRKm 3.9	Streambed Sediment		3792.25	NA	-0.81	-0.56	-0.40	-0.26	-0.13	0.02	0.02	0.02	0.01
	Bulk Bank Soil		6327.90		-1.09	-0.72	-0.51	-0.33	-0.11	-0.02	0.04	0.03	0.08
RRKm 7.8	Streambed Sediment		1541.44	NA	-2.89	-1.93	-1.35	-0.92	-0.35	-0.02	0.10	0.05	0.14
	Bulk Bank Soil		45183.79		-0.76	-0.47	-0.34	-0.20	-0.07	-0.07	0.01	0.04	0.05
RRKm 15.9	Streambed Sediment		3675.76	NA	-0.91	-0.57	-0.40	-0.25	-0.11	-0.07	0.03	0.04	0.03
	Bulk Bank Soil		40336.29		-0.72	-0.49	-0.33	-0.21	-0.05	0.00	0.04	0.03	0.08
RRKm 26.4	Streambed Sediment		17748.46	NA	-0.56	-0.44	-0.29	-0.19	-0.05	0.09	0.03	0.03	0.06
	Bulk Bank Soil		16942.11		-0.69	-0.47	-0.35	-0.20	-0.04	0.02	0.00	0.03	0.08

Table 3.2 Summary of THg Concentration and Hg Stable Isotope Data of Standard Reference Materials

Summary of THg concentration and Hg stable isotope data of Standards and Reference Materials. For SRMS's, N1 denotes the total number of process replicates and N2 denotes the total number of isotope measurements during all analytical sessions. Theta denotes the standard error of the mean values for process replicates. For UM-Almaden (In-Run), N1 denotes the number of analytical sessions that UM-Almaden was measured, N2 denotes the number of isotope measurements, and theta represents the SD of Hg isotope values for individual UM-Almaden replicates.

Reference Material	N1	N2	THg	2σ	$\delta^{204}Hg$	2σ	$\delta^{202}Hg$	2σ	$\delta^{201}Hg$	2σ	$\delta^{200}Hg$	2σ	$\delta^{199}Hg$	2σ	$\Delta^{204}Hg$	2σ	$\Delta^{201}Hg$	2σ	$\Delta^{200}Hg$	2σ	$\Delta^{199}Hg$	2σ
			μg/g	μg/g	‰	‰	‰	‰	‰	‰	‰	‰	‰	‰	‰	‰	‰	‰	‰	‰	‰	‰
NIST 2711 Proc. Ref.	12	25	6.43	0.38	-0.32	0.05	-0.20	0.02	-0.35	0.03	-0.11	0.02	-0.26	0.02	-0.01	0.02	-0.20	0.03	-0.01	0.01	-0.21	0.02
UM-Almaden Proc. Ref.	7	7			-1.01	0.22	-0.72	0.10	-0.60	0.11	-0.41	0.10	-0.23	0.12	0.07	0.15	-0.05	0.08	-0.05	0.07	-0.05	0.10
UM-Almaden (In-Run)	8	41			-0.87	0.22	-0.57	0.05	-0.47	0.10	-0.30	0.06	-0.16	0.05	-0.02	0.16	-0.05	0.07	-0.01	0.05	-0.01	0.05

Table 3.3 Summary of Ancillary Water Chemistry Data

Summary of sampling locations and ancillary water chemistry data collected during sampling.

Site Name	RRK m	Date	Time	N Lat	W Long	Water Temp. (C)	Diss. Oxygen (mg/L)	Specific Conductance (µS/cm)	pH
SR-01	-4	5/25/16	14:00	38 03' 34.9"	78 54' 38.7"	16.8	10.34	111.5	8.01
Lyndhurst St. Bridge	-1.1	5/26/16	9:00	38 03' 38.6"	78 53' 38.9"	16.4	10.21	136.8	8.08
Outfall 001	-0.75	5/26/16	15:30	38 03' 33.2"	78 53' 26.2"	18.6	10.1	140.7	8.41
Mid Plant 1	-0.6	5/27/16	9:45	38 03' 36.5"	78 53' 18.9"	16.6	9.74	150.4	8
Mid Plant 2	-0.25	5/28/16	11:00	38 03' 42.3"	78 53' 09.1"	18.1	9.88	159.8	8.19
Outfall 011	0	5/29/16	9:00	38 03' 50.6"	78 53' 05.6"	17.8	9.19	167.7	8.02
Constitution Park	0.25	5/29/16	12:30	38 03' 58.4"	78 53' 04.1"	18.3	10.03	169.5	8.36
Broad St. Bridge	0.7	5/31/16	10:30	38 04' 10.9"	78 53' 06.9"	18.4	9.71	183.5	8.21
North Park Path	1.3	5/30/16	10:45	38 04' 29.9"	78 53' 00.8"	17.4	10.05	177.8	8.29
2nd St. Bridge	2.2	5/30/16	16:00	38 04' 45.9"	78 52' 29.4"	20	10.29	177.2	8.66
Hopeman Pkwy Bridge	3.9	5/25/16	10:30	38 05' 25.8"	78 52' 37.4"	14.9	10.18	146.1	7.84
Above Dooms Mill Dam	7.8	5/24/16	15:00	38 06' 22.5"	78 51' 52.6"	16.5	10.57	149.1	8.12
Crimora Park	15.9	5/24/16	11:15	38 09' 22.3"	78 51' 12.5"	14.8	9.97	135.8	7.78
Patterson Mill Rd Bridge	26.4	5/24/16	8:45	38 13' 06.4"	78 50' 12.3"	14.5	9.64	133.5	7.7

Table 3.4 Summary of RRKm 4.75 Floodplain Profile THg concentration and Hg Stable Isotope Data

Summary of THg concentration and Hg stable isotope data of collected samples from the RRKm 4.75 floodplain profile.

Depth Range	Age at Middle Depth	THg	$\delta^{204}Hg$	$\delta^{202}Hg$	$\delta^{201}Hg$	$\delta^{200}Hg$	$\delta^{199}Hg$	$\Delta^{204}Hg$	$\Delta^{201}Hg$	$\Delta^{200}Hg$	$\Delta^{199}Hg$
		µg/g (d.w.)	‰	‰	‰	‰	‰	‰	‰	‰	‰
0 - 3 cm	2011.9	21.2	-0.68	-0.47	-0.32	-0.25	-0.10	0.02	0.03	-0.02	0.02
3 - 6 cm	2006.7	27.2	-0.69	-0.49	-0.36	-0.26	-0.10	0.04	0.01	-0.01	0.02
6 - 9 cm	2001.5	28.6	-0.54	-0.41	-0.29	-0.22	-0.12	0.07	0.02	-0.01	-0.01
9 - 14 cm	1994.5	34.8	-0.19	-0.11	-0.11	-0.05	0.00	-0.03	-0.02	0.01	0.03
14 - 17 cm	1987.5	46.1	-1.00	-0.71	-0.55	-0.38	-0.12	0.06	-0.01	-0.02	0.06
17 - 20 cm	1982.3	75.2	-0.78	-0.51	-0.37	-0.24	-0.11	-0.01	0.01	0.02	0.02
20 - 25 cm	1975.4	105	-0.58	-0.40	-0.28	-0.21	-0.11	0.02	0.02	-0.01	-0.01
25 - 30 cm	1966.7	134	-0.77	-0.49	-0.35	-0.22	-0.08	-0.04	0.02	0.03	0.04
30 - 35 cm	1958.0	147	-0.79	-0.54	-0.37	-0.23	-0.04	0.02	0.04	0.04	0.09
35 - 40 cm	1949.3	87.5	-0.80	-0.52	-0.35	-0.21	-0.06	-0.03	0.04	0.05	0.07
40 - 45 cm	1940.6	51.6	-0.43	-0.27	-0.13	-0.13	-0.01	-0.02	0.08	0.01	0.06
45 - 50 cm	1931.9	20.3	-0.89	-0.58	-0.46	-0.27	-0.10	-0.02	-0.02	0.02	0.05
50 - 55 cm	1923.2	13.7	-0.85	-0.53	-0.39	-0.28	-0.12	-0.07	0.01	-0.01	0.01
55 - 60 cm	1914.5	5.35	-0.99	-0.63	-0.50	-0.34	-0.12	-0.05	-0.03	-0.02	0.04
60 - 65 cm	1905.8	11.5	-0.92	-0.56	-0.41	-0.27	-0.11	-0.09	0.00	0.00	0.03
65 - 70 cm	1897.1	1.71	-0.83	-0.55	-0.43	-0.25	-0.08	0.00	-0.01	0.03	0.06
70 - 75 cm	1888.4	1.56	-0.64	-0.41	-0.29	-0.17	-0.04	-0.03	0.01	0.04	0.06
75 - 80 cm	1879.7	2.17									

References

(1) Bergquist, B. A; Blum, J. D. Mass-Dependent and -Independent Fractionation of Hg Isotopes by Photoreduction in Aquatic Systems. Science 2007, 318 (5849), 417–420 DOI: 10.1126/science.1148050.

(2) Ghosh, S.; Schauble, E. a.; Lacrampe Couloume, G.; Blum, J. D.; Bergquist, B. A. Estimation of Nuclear Volume Dependent Fractionation of Mercury Isotopes in Equilibrium Liquid–vapor Evaporation Experiments. *Chem. Geol.* **2013**, *336*, 5–12 DOI: 10.1016/j.chemgeo.2012.01.008.

(3) Washburn, S. J.; Blum, J. D.; Demers, J. D.; Kurz, A. Y.; Landis, R. C. Isotopic Characterization of Mercury Downstream of Historic Industrial Contamination in the South River, Virginia. *Environ. Sci. Technol.* **2017**, *51* (19), 10965–10973 DOI: 10.1021/acs.est.7b02577.

Chapter 4 Isotopic Characterization of Mercury in Natural Gas via Analysis of Mercury Removal Unit Catalysts

Authors: Spencer J. Washburn, Joel D. Blum, Marcus W. Johnson, Jodie M. Tomes, and Peter J. Carnell

Citation: Washburn, S. J.; Blum, J. D.; Johnson, M. W.; Tomes, J. M.; Carnell, P. J. Isotopic Characterization of Mercury in Natural Gas via Analysis of Mercury Removal Unit Catalysts. *ACS Earth Sp. Chem*. **2018**. DOI: 10.1021/acsearthspacechem.7b00118.

Abstract: Natural gas (NG) represents an important and rapidly growing global energy source, and some commercially relevant reserves of NG are reported to contain mercury (Hg) at concentrations between 0.01 and 5,000 μg/m3. The overall amount of Hg released to the atmosphere from gas production and combustion is largely unknown, but gaseous elemental Hg release is likely an increasing contribution to the global atmospheric Hg pool. However, no Hg isotopic compositions have been published for Hg entering the atmosphere from NG. In an effort to characterize the isotopic composition of Hg released from NG, we analyzed the stable isotopic compositions of mercury removal unit (MRU) catalysts that were loaded with Hg from NG production and supplied by Johnson Matthey Inc. We suggest that the bulk of Hg adsorbed to catalysts near the inlet of each MRU reactor is representative of the Hg isotopic composition of the NG source. In different gas fields values of δ^{202}Hg and Δ^{199}Hg range from -3.75‰ to -0.68‰ and -0.02‰ to 0.65‰, respectively. Analysis of four samples from different positions within a single MRU reactor demonstrates significant isotopic fractionation of a small fraction of Hg that

is not removed at the entrance to the MRU. We suggest that this fractionation is due to sorption of Hg to the catalyst surface from the gas phase, and that this process follows a Rayleigh fractionation model with $\varepsilon \approx -0.40‰$. In total, these results suggest that Hg isotopic analysis may be a feasible monitoring tool for Hg emissions from NG production in some gas fields. With further analyses of NG from around the world, a global average isotopic composition of NG hosted Hg could be estimated to characterize this input to atmospheric Hg isotope models.

4.1 Introduction

Mercury (Hg) is a toxic trace metal whose global distribution and geochemical cycling have important environmental and human health implications. Anthropogenic activity has altered how Hg species cycle through the environment and many questions remain regarding critical aspects of these cycles.[1] Natural gas represents an important, and growing, global energy source, especially in the United States where domestic reserves are abundant.[2] Although largely undocumented, it is known that commercially relevant hydrocarbon sources contain trace levels of Hg, and Hg is commonly observed in natural gas at concentrations between 0.01 and 5,000 $\mu g/m^3$.[3] Hg concentrations in natural gas have been shown to vary by more than 3 orders of magnitude at both the basin level and within a single gas field.[4] However, the geologic origin of Hg in natural gas is not well known, with both thermal maturation of source rocks and hydrothermal origins proposed.[4,5] Release of gaseous mercury (Hg^0) to the atmosphere from gas production is a largely unknown input to the global Hg cycle, and further research into the fate of Hg from natural gas is needed to better constrain and mitigate the potential human health and environmental impacts of this expanding energy sector. Hg^0 found in the production gas stream threatens natural gas processing and distribution systems by amalgamating with, and weakening, aluminum components.[6] Over time, this amalgamation can cause corrosion and failure of critical

components and this presents a threat to both human health and infrastructure. The natural gas industry has in some instances identified the need to remove Hg from gas prior to its entry into gas processing facilities to assure safe plant operation. As a result of these factors, suppliers at gas fields with particularly high Hg have developed mercury removal units (MRU's) using pelletized catalysts. These are generally composed of inorganic metal sulfides suspended in a large fixed-bed reactor chamber through which the gas stream is passed.[7,8] Although MRU's remove the majority of Hg species from the gas within the first few meters of the fixed-bed reactor (typical MRU performance results in total Hg (THg) of <10 ng Hg/m^3 in gas streams and <1.0 ng Hg/g in liquid streams), environmentally appreciable amounts of Hg can still be emitted due to the vast quantities of gas processed at some facilities. In addition, many gas fields do not utilize Hg removal technologies. Although seldom measured and not regulated, release of Hg from NG to the atmosphere could also have important environmental impacts, particularly at the local scale. Most studies of Hg emissions have concluded that emissions of Hg from NG are a negligible contributor to the global atmospheric Hg cycle.[9] However, previous studies conducted near NG processing facilities have demonstrated local increases in ambient air Hg concentrations related to processing activities,[10] and these elevated local events have been shown to correlate with Hg content of co-located bioindicators such as epiphytic lichens.[11] Release of Hg from NG consumption by residential consumers could also pose a human health risk – if NG THg exceeds ~1000 μg/m^3, residential indoor air could exceed the WHO guideline of 1 μg/m^3 based on average gas consumption (~5.0m^3/day) and US home sizes in 2010 (~201.5 m^2).[12-14]

Recent advances in analytical techniques now allow the accurate measurement of stable isotope ratios of Hg in a wide variety of media and environmental samples. Previous work has shown that mass-dependent fractionation (MDF) and mass-independent fractionation (MIF) of

Hg isotopes can be used to determine sources, sinks, and biogeochemical reaction pathways as Hg moves through the environment.[15,16] Hg isotopes provide a useful new tool to enhance understanding of complex systems involving Hg because specific chemical mechanisms result in MDF and MIF. A number of recent studies have shown that stable Hg isotope ratios can be used to identify the sources, transformations, and fate of hydrocarbon fuel sources other than natural gas. Recently, it has been demonstrated that coal from varying geographic sources may contain diagnostic Hg isotopic "fingerprints".[17,18] Research has shown that Hg isotopic signatures of precipitation downwind from coal-fired utility boilers in Florida were distinct from background Hg isotopic compositions.[19] The isotopic composition of anthropogenic Hg emissions has also been detected in bioindicators such as epiphytic lichens and deciduous tree leaves which are subject to atmospheric deposition of the emitted Hg species.[20-22] Previous studies have also shown that Hg emissions from natural gas treatment facilities can be detectable in the Hg concentrations in nearby biota,[11] and unconventional natural gas extraction ("fracking") in Northwestern Pennsylvania led to increased THg in stream water affected by extraction operations.[23] The environmental impact of the Hg emissions from natural gas production and associated processing facilities may be similarly traceable with Hg isotopic analysis of a wide variety of media (e.g. precipitation, surface waters, and vegetation) if Hg sourced from natural gas deposits has a unique isotopic signature or if the transport and refinement processes modify the isotopic signature of NG associated Hg in a characteristic manner.

In an effort to better understand Hg dynamics within NG production, we have analyzed content and stable isotope compositions of THg captured by MRU catalysts. These catalysts, sold commercially under the trade name PURASPEC and provided by Johnson Matthey Inc., were used in a number of production facilities that processed NG sourced from globally

distributed gas fields, including Malaysia, the North Sea, Brazil, Australia, Northern Europe, and Southeast Asia. This wide geographic distribution allows assessment of the variation in Hg isotopic composition of NG and projections about the potential impacts of NG production on the global Hg cycle. Analysis of samples obtained from reservoirs containing NG originating from geologically and geographically distinct sources may lead to the development of a NG Hg isotopic "fingerprint," similar to that developed for world coal deposits.[18]

4.2 Materials and Methods

4.2.1 Sample Collection and Processing

Catalyst samples were collected from MRU's operated at gas processing facilities in each of the following locations: Australia, Northern Europe, the North Sea, Brazil, Malaysia, and Southeast Asia. Due to the proprietary nature of these catalyst samples and the natural gas production industry, we were unable to obtain information regarding the exact locations of the natural gas deposits that were the source of the natural gas processed by the facilities that housed these MRU's. We also do not know if the MRU's analyzed in this study processed gas from the same wellheads throughout their period of operation. Hg concentrations have been demonstrated to vary significantly for different gas reservoirs even within the same geologic basin,[4] so the Hg isotopic analyses presented here must be interpreted at a broad scale. Despite this lack of detailed information about the potential geologic sources of the natural gas, there is significant information to be gained from this sample set given the lack of information available in the literature about Hg in natural gas.

Catalyst samples were collected from MRU reactors that had been discharged. The discharge process involved using a vacuum nozzle to carefully remove layers of catalysts from the reactor beds. Bulk sample grabs were collected from the drums into which the spent catalysts

were sequentially distributed from a discharged MRU reactor. The relative bed location (given as "% through reactor bed" throughout the manuscript) within the MRU reactor for each catalyst sample was estimated from known bed volumes based on the volume of catalyst discharged. For this study, samples are presented with a standardized nomenclature of "Region_R#reactor_#sample", with the region of NG origin, the number of the sampled reactor for a region, and then a sample number, with lower numbered samples being closer to the inlet of the reactor units. Samples that are described as "inlet" samples are from 0 to 10% of the distance through a reactor bed with no available catalyst samples preceding them, while "downstream" samples are those from positions 10 to 100% through the reactor bed.

4.2.2 Sample Preparation for Isotope Analysis and THg Analysis

Given the high Hg concentrations found in catalyst samples (Table 4.1), it was necessary to "dilute" the samples prior to analysis to reduce weighing errors and avoid contamination of analytical equipment. Approximately 1.0g of each catalyst sample was pulverized with an acid cleaned glass mortar and pestle. Then ~1.0mg of catalyst powder was added to ~5.0g of alumina powder and thoroughly mixed in an acid cleaned 40mL ICHEM glass vial. Alumina was heated to 750 ºC for 6 hours and then cooled before use to reduce the Hg blank to undetectable levels. A subset of catalyst samples were ground and diluted in duplicate or triplicate to evaluate the reproducibility of the dilution method.

Hg in catalyst powder dilutions was separated for THg concentration analysis and Hg stable isotope measurement by offline combustion, as described in detail elsewhere.[17,24] Briefly, 0.01 to 1.00 g of the diluted samples was packed into a ceramic boat and placed into the first stage of a two-furnace combustion system. The first-stage furnace was slowly ramped to 750 ºC over a six hour period while the second-stage furnace was held at 1000 ºC. Hg released from the

sample matrix was carried through the combustion tube in a flow of Hg-free O_2 and into a 1% $KMnO_4$ trapping solution. Sample powder dilution replicates were found to have replicable THg values, with THg variations between samples of less than 0.94% relative standard error (RSE) (average % RSE = 0.22%, n= 10 replicates) (Table 4.3).

Trapping solutions of combustion samples were partially reduced with a 30% solution of $NH_2OH{\cdot}HCl$, using an amount equal to 2% of the total sample by weight (w/w) and a small aliquot was taken and measured for THg by CV-AAS (MA-2000, Nippon Instruments). Hg in combustion traps was then purged into a secondary 1% $KMnO_4$ trapping solution to remove potential matrix components from combustion residues and to match Hg concentrations to standard solutions prior to isotopic analysis.[25,26] Hg recovery during this transfer into secondary 1% $KMnO_4$ trapping solution was evaluated by taking small aliquots of the secondary trapping solutions and analyzing the THg via CV-AAS. Hg recoveries for this process ranged from 73.9% to 107.6% with an average of 95.8±8.1% (1SD, n=43, only 2 samples below 85% recovery).

4.2.3 Hg Isotope Analysis

The Hg isotopic composition of the secondary trapping solution was measured by cold vapor multi-collector inductively couple plasma mass spectrometry (CV-MC-ICP-MS, Nu Plasma, Nu Instruments). Secondary trapping solutions were partially reduced with aliquots of a 30% solution of $NH_2OH{\cdot}HCl$ at 2% of the total sample by weight and diluted with a similarly reduced 1%$KMnO_4$ solution to between 1.6 and 5.0 ng/g. Hg was reduced online to Hg^0 by the addition of 2% (w/w) $SnCl_2$ and separated from solution using a frosted tip gas-liquid separator.[27] Hg^0 was then carried into the MC-ICP-MS inlet by an Ar gas stream. An internal Tl standard (NIST 997) was introduced as a dry aerosol into the Ar gas stream and used to correct for instrumental mass bias. Strict sample-standard bracketing with a solution of NIST 3133 that

was matched for both concentration and solution matrix was further used for mass bias correction.[28] Mercury stable isotope compositions are reported in permil (‰) using delta notation (δ^{xxx}Hg) relative to NIST Standard Reference Material (SRM) 3133 (Eq. 1), with mass dependent fractionation based on the ^{202}Hg/^{198}Hg ratio (δ^{202}Hg).[28] Mass independent fractionation is reported as the deviation from the theoretically predicted δ^{xxx}Hg values based on the kinetic mass fractionation law and is reported with capital delta notation (Δ^{xxx}Hg) according to Eq. 2. In this study MIF is represented as Δ^{199}Hg, Δ^{200}Hg, Δ^{201}Hg, and Δ^{204}Hg, using β = 0.252, β = 0.502, β = 0.752, and β = 1.493, respectively.[28]

Equation 1: $\delta^{xxx}\text{Hg}\ (‰) = ([(^{xxx}\text{Hg}/^{198}\text{Hg})_{\text{Sample}} / (^{xxx}\text{Hg}/^{198}\text{Hg})_{\text{NIST3133}}] - 1) \times 1000$

Equation 2: $\Delta^{xxx}\text{Hg}\ (‰) = \delta^{xxx}\text{Hg} - (\delta^{202}\text{Hg} \times \beta)$

Procedural blanks and SRMs (NIST 2711, Montana Soil) were processed in parallel with samples and THg and Hg isotopic composition were determined. Offline combustion procedural blanks yielded between 57.6 and 508 pg of Hg (n=5, mean = 235±194pg), representing less than 2.8% of Hg in sample combustion trap solutions. The THg of NIST 2711 measured by offline combustion agreed within 5% of certified values (6.04±0.30µg/g, n=5; Table 4.2), and recoveries during secondary trapping were 100.1±1.86% (1SD, n=5, min=97.0 %). The Hg isotopic composition of NIST 2711 was consistent with previously reported values (Table 4.2).[26, 29-32] The long-term analytical uncertainty of Hg isotope measurements was estimated from the standard deviation (2SD) of the analytical session mean Hg isotopic composition of the UM-Almadén secondary standard. External reproducibility of Hg isotope measurements was estimated from measurements of the standard error (2SE) of the mean isotopic composition NIST 2711 replicates. The analytical uncertainty associated with NIST 2711 was lower than the uncertainty associated with the UM-Almadén standard for δ^{202}Hg and Δ^{200}Hg, but higher for Δ^{199}Hg and

Δ^{201}Hg (Table 4.2). We therefore represent the uncertainty of Hg isotope measurements of combusted catalyst samples in this study as whichever uncertainty is greatest: ±0.07‰ for δ^{202}Hg, ±0.07‰ for Δ^{199}Hg, ±0.07‰ for Δ^{201}Hg and ±0.06‰ for Δ^{200}Hg. Sample powder dilution replicates were found to have replicable Hg isotopic compositions, with RSE of Hg isotope values averaging 0.13‰ for δ^{202}Hg, 0.02‰ for Δ^{199}Hg, and 0.01‰ for Δ^{201}Hg.

4.3 Results and Discussion

4.3.1 Mercury Dynamics within Mercury Removal Units

Catalyst inlet samples, as well as catalyst samples as a whole, do not exhibit a significant trend in either δ^{202}Hg or Δ^{199}Hg values versus THg (Figure 4.5; Table 4.1). Ancillary parameters available regarding the operating conditions within the MRU reactor beds including temperature, pressure, and period in duty (Table 4.4) also do not show significant trends versus δ^{202}Hg or Δ^{199}Hg values of the catalyst samples. The lack of trends with these parameters suggests that reactor conditions do not affect the isotopic composition of the catalyst inlet samples, and the measured Hg isotopic variability observed in these catalyst samples is representative of the NG input to the reactor beds.

To investigate the Hg dynamics occurring within a single MRU reactor, a subset of samples were analyzed ("SE Asia_R5_#1 - #4") that came from a number of positions within a single MRU reactor at a NG facility in SE Asia. The THg values of these samples (Figure 4.2; Table 4.1) decreases dramatically from inlet to outlet (28.2 mg/g to 1.50 μg/g, respectively), with SE Asia_R5_#4 and SE Asia_R5_#3 having THg (1.50 μg/g and 1.00 μg/g, respectively) that are not significantly elevated above the THg value of the catalyst blank (0.96 μg/g). Given the significant decrease in THg from inlet to outlet samples observed for all of the analyzed catalyst samples, a significant portion (>95%) of the mass of the Hg stored within a reactor must be

sorbed to the catalyst near the inlet. Considering that such a large portion of the Hg captured by these MRU's is associated with these inlet or near-inlet catalysts, we can make the assumption that the Hg isotopic composition of inlet samples are representative of the Hg isotopic composition of the bulk NG that is processed in a given reactor. For our calculated fractionation factor for the sorption reaction (discussed below), due to mass balance considerations no significant change in isotopic composition (>0.10‰) from the bulk NG Hg value should be observed in catalyst samples at the reactor inlet unless >20% of the Hg is sorbed downstream of the inlet, which is not the case in any of the inlet and downstream catalyst samples from the same reactor (referred to as "paired" samples throughout) analyzed in this study. As MRU reactors are in continuous operation for a significant length of time (a minimum of 7 months for the reactors in this study), the potential to have an altered isotopic composition due to MDF associated with a kinetic sorption reaction is limited. Rather, the catalysts integrate the Hg isotopic composition of the NG over the period of duty, as the sorption capacity of the catalysts is much greater than the Hg load in the NG stream.

Accompanying this shift in THg values along the MRU reactor bed profile are shifts in both the δ^{202}Hg and Δ^{199}Hg values of the catalysts (Figure 4.2; Table 4.1), demonstrating significant fractionation of the small fraction of Hg that is not removed at the entrance to the MRU reactor. SE Asia_R5_#4 and SE Asia_R5_#3, the two catalyst samples closest to the outlet of the reactor bed, have δ^{202}Hg values (-0.27±0.07‰ and 0.21±0.07‰, respectively) that vary only slightly from the δ^{202}Hg value of the catalyst blank (0.01±0.07‰). Given that these samples have only slightly elevated THg compared to the catalyst blank, it seems reasonable that they would not exhibit much variation in their isotopic composition. The two samples located near the inlet of the reactor bed, SE Asia_R5_#2 and SE Asia_R5_#1, exhibit greater variation in their

δ^{202}Hg values (0.76±0.07‰ and -1.60±0.07‰, respectively). Assuming that the Hg isotopic composition of SE Asia_R5_#1 (0% through the reactor bed) is representative of the bulk Hg isotopic composition within the natural gas source for this reactor, this represents a greater than 2.0‰ shift in the isotopic composition within the MRU. Since the vast majority (>99%) of Hg in NG is in the form of Hg^0,[33] it seems unlikely that this isotopic shift could be related to the sequential capture of different Hg species with varied isotopic compositions.

We suggest instead that this isotopic shift is related to a fractionation mechanism associated with the sorption of Hg^0 (or the oxidation of Hg^0 and subsequent sorption of Hg^{2+}) to the catalyst surface from the gas phase. We propose that within the reactor this sorption process follows a Rayleigh distillation style fractionation with a fractionation factor, $\varepsilon_{sorbed\text{-}gas} \approx -0.40‰$ [ε was chosen to fit the data within the SE Asia_R5 reactor, with $\varepsilon_{sorbed\text{-}gas} = \delta^{202}Hg_{sorbed} - \delta^{202}Hg_{gas}$], similar to the $\varepsilon_{sorbed\text{-}dissolved}$ magnitude previously proposed for aqueous Hg^{2+} sorption (Figure 4.3).[34,35] Although no experimental work has been done on the isotopic fractionation that occurs during elemental Hg sorption in the gas phase, it seems logical that lighter isotopes would be preferentially sorbed, similar to aqueous Hg sorption. As Hg^0 is removed from the natural gas stream due to sorption to the high affinity binding surfaces of the catalysts, the remaining pool of Hg^0 within the natural gas stream becomes depleted in the lighter isotopes, resulting in a relatively more positive δ^{202}Hg value. It should be noted that from the current study it is not possible to infer whether this fractionation is related to the chemical sorption process, or a change in Hg speciation prior to the sorption reaction. This pattern of catalyst samples at downstream reactor positions having positive δ^{202}Hg values relative to inlet samples holds for all of the paired catalyst samples we analyzed, with the exception of Malaysia_R1_#1 & #2. The ancillary information about the operation of this particular MRU (see Table 4.4) does not suggest

that unusual operating conditions caused this anomaly. Sample Malaysia_R1_#2's is positioned 40% of the way through the reactor and the THg of this sample is still highly elevated relative to Malaysia_R1_#1 (8.41 and 28.9 mg/g, respectively). This situation may be representative of complete saturation of the catalyst samples near the inlet of this reactor, with the active reaction of catalyst sorption migrating through the reactor vessel bed.

The Δ^{199}Hg values of the SE Asia_R5_#1-#4 catalyst samples decrease from inlet (0.25‰±0.07‰) to outlet (0.08‰±0.07‰), with all of the downstream samples being within analytical uncertainty of the catalyst blank (0.14±0.07‰), which suggests that during the sorption process near MRU inlets the MIF signature of Hg within NG is being retained (Figure 4.2). This pattern is consistent with the trends observed for the δ^{202}Hg values in this particular reactor. However, the Δ^{199}Hg values of reactor paired catalyst samples are variable, with some pairs showing significant positive Δ^{199}Hg shifts from inlet to downstream (Malaysia_R1_#1 & #2, Brazil_R1_#1 & #2), some showing positive but not significant Δ^{199}Hg shifts (North Sea_R1_#1 & #2, Australia_R1_#1 & #2), and others showing negative but not significant Δ^{199}Hg shifts (Malaysia_R2_#1 & #2). Positive Δ^{199}Hg shifts from inlet to downstream would be consistent with the sorption process inducing small amounts of MIF related to nuclear volume effects, as would be predicted based on observations from previous experimental work.[35,36] There is no evidence to suggest that the sorption process would vary between these reactors, so there is no reason to suspect that varying reactions (e.g. varying amounts of NVE-associated MIF) would be occurring within different reactors leading to varying Δ^{199}Hg shifts from inlet to downstream catalyst samples. One potential explanation for the observed variation Δ^{199}Hg shifts within the MRU reactors would be a switch to a NG source with a differing Hg isotopic composition near the end of the period of duty for that reactor. This could create a situation where catalysts at

downstream locations were capturing the differing Δ^{199}Hg value of this new NG source, creating the appearance of a Δ^{199}Hg shift from the bulk Hg captured by the inlet catalysts. Alternatively, different production batches of catalysts could have varying Δ^{199}Hg signatures associated with the Hg in the raw materials, which would alter the "blank" Δ^{199}Hg value that we would expect to find in downstream catalyst samples. At this time we do not have enough information to provide an explanation for the lack of a clear trend in Δ^{199}Hg values within the reactors examined in this study.

4.3.2 Mercury Isotopic Variation of Natural Gas

The catalyst samples analyzed in this study had a wide range of δ^{202}Hg values (-3.75 to 0.76‰) and a narrower but still large range of Δ^{199}Hg values (-0.08 to 0.63‰). Inlet catalyst samples (n=7), assumed to be representative of the NG source isotopic composition, had a somewhat smaller range of δ^{202}Hg values (-3.75 to -0.68‰) and Δ^{199}Hg values (-0.02 to 0.63‰) (Figure 4.1). Even though we have a relatively small sample size and limited geographic distribution of samples, we observe a large amount of isotopic variation. For comparison, a recent review reported that the range of values for all measured coal deposits worldwide (n=216) was of the same magnitude (δ^{202}Hg values of -3.90 to 0.77‰, average = -1.16 ± 0.79‰ [1SD] and Δ^{199}Hg values of -0.63 to 0.34‰, average = -0.11 ± 0.18‰ [1SD]) as observed in this study of NG (Figure 4.1).[18] The range of values for NG samples was larger than that reported for marine sediments and high carbon-content shale rocks (e.g. black shales) (δ^{202}Hg values of -2.97 to -0.38‰, average = -1.51 ± 0.73‰ [1SD] and Δ^{199}Hg values of -0.09 to 0.45‰, average = 0.10 ± 0.11‰ [1SD]), the modern analogues of the source material for the hydrocarbon reservoirs (Figure 3.1).[16,53,54,55] The range of isotopic values reported for hydrothermal precipitates (δ^{202}Hg values of -3.42 to 1.20‰, average = -0.39 ± 0.91‰ [1SD] and Δ^{199}Hg values of -0.30 to 0.27‰,

average = -0.07 ± 0.11‰ [1SD]), is of a similar magnitude as observed for NG samples in this study.[16,56]

In addition to the large range in the isotopic composition of Hg in NG at a global scale, there are also variations in the Hg isotopic composition of NG at a regional scale. The four inlet catalyst samples collected from MRU's in operation in SE Asia have a δ^{202}Hg range of -2.57 to -0.68‰ and Δ^{199}Hg values of -0.02 to 0.11‰. Some of this variability may be related to the depositional environment of the source rocks that drives the heterogeneity in NG reservoir THg that is observed in some locations.[4] Alternatively, this variability in Hg isotopic composition could be the result of mixing at the processing facility of NG sourced from production wells with differing Hg isotopic compositions, integrating the isotopic composition over the period of duty for the MRU. Hg in coal has been documented to have similar levels of variability at the basin level. For example Illinois Basin coals exhibit a δ^{202}Hg range of -2.68 to -0.75 and Δ^{199}Hg values of -0.23 to 0.03‰.[37] The variability observed in Illinois Basin coals was attributed to changes in depositional conditions, and incorporation of epigenetic Hg related to hydrothermal solutions. A similar explanation could explain the isotopic variation observed in NG, but drawing any firm conclusions is beyond the scope of this work.

The large magnitude of variation in the isotopic composition of NG at both the global and regional scale would allow for the discrimination of Hg emissions from those production facilities to the local environment that differ isotopically from the global Hg^0 pool. The global Hg^0 pool, with an average isotopic composition of δ^{202}Hg = 0.22 ± 0.52‰ [1SD], Δ^{199}Hg = -0.15±0.09‰ [1SD] and Δ^{201}Hg = -0.14±0.09‰ (data compiled from [24,38-42] for TGM measurements from remote sites) has, on average, a relatively more positive δ^{202}Hg value and significantly more negative Δ^{199}Hg and Δ^{201}Hg values than the NG catalysts we measured

(Figure 4.4). The contrast between global Hg^0 background and NG isotopic compositions, particularly in regard to odd MIF signatures, would allow for the discrimination of the impacts of these two endmembers near emissions sources, similar to the previously demonstrated ability to discriminate the impact of Hg emissions related to coal combustion near coal fired utility boilers.[14,40,43] This statement carries the caveat that the catalysts measured in this study may not represent the true isotopic composition of the Hg emitted to the atmosphere from NG processing facilities that employ Hg removal technology and NG combustion, due to the potential fractionation that these industrial processes could induce. Fractionation related to natural gas processing is likely to only affect the MDF signatures of emitted Hg,[44,45] which would still allow for source determination based on distinct MIF signatures. However, future work on Hg emissions related to NG would need to carefully account for both the long-term Hg isotope composition related to NG processes and the regional background TGM isotopic composition to determine the feasibility of tracer studies.

4.3.3 Comparison of Mass Independent Fractionation of Hg in Natural Gas to other Hg Reservoirs

The presence of significant MIF signatures in NG samples allows for both an isotopic "fingerprinting" that may aid in tracing emissions sources and the comparison to other natural Hg reservoirs, which may point towards the origin of Hg in NG. The catalyst inlet samples from this study (unaffected by fractionation within the MRU reactor) had positive odd MIF (Δ^{199}Hg range -0.02‰ to 0.65‰, average = 0.15±0.23‰ [1SD], Δ^{201}Hg range -0.13‰ to 0.37‰, average = 0.05±0.17‰ [1SD]) and negligible even MIF, with most values within error of 0.0‰ (Δ^{200}Hg range 0.01‰ to 0.11‰, average = 0.04±0.04‰ [1SD]) (Figure 4.4, Table 4.1). The lack of any significant even-MIF signature (Δ^{200}Hg) provides an additional fingerprint to distinguish NG-

production related emissions from background atmospheric Hg, as atmospheric TGM has a characteristic slight negative Δ^{200}Hg signature (-0.04±0.04‰ [average±1SD]; data compiled from [24,38-42] for TGM measurements from remote sites).

With the exception of coal, there have been a very limited number of reported Hg isotope measurements of fossil fuels or hydrocarbon source materials. Blum et al. (2012) measured the Hg isotopic composition of a small number of oil sand samples from the Athabasca oil sands region of Alberta, Canada. Unlike NG, the oil sands samples have significant negative odd MIF signatures (Δ^{199}Hg = -0.22±0.16‰, Δ^{201}Hg = -0.23±0.13‰ [average±1SD]) (Figure 4).[21] Most of the potential Hg sources to NG reservoirs that have been previously measured, such as organic rich marine sediments and black shales, have odd MIF signatures clustered near 0.0‰ to slightly positive values. The exception is hydrothermal fluids and sinters, which have a slightly positive odd MIF signature (Δ^{199}Hg = 0.12±0.07‰, Δ^{201}Hg = 0.07±0.05‰ [average±1SD]),[46] although hydrothermal precipitates on average have Δ^{199}Hg values clustered near 0.00‰ (average = -0.07 ± 0.11‰ [1SD])[16,56]. Previous work on marine sediments from the geologic record have suggested that differing marine depostional environments can record varying Hg isotope signatures during increased atmospheric Hg loading due to volcanic activity.[47,48] Due to the complexities of determining the Hg isotope compositions associated with the depositional environments from which NG reservoirs may have formed, as well as the potential for isotopic overprinting related to epigenetic Hg (originating from hydrothermal or volcanic activity), it is not possible to draw any conclusions on the origins of Hg in NG from our sample set. Significantly more work is needed to define the range in isotopic composition of Hg in NG, including direct measurements of raw gas. Additional measurements are also needed to characterize the isotopic composition of Hg in modern depositional environments analogous to

those thought to produce hydrocarbon reservoirs, as well as Hg from potential epigenetic Hg sources such as volcanic emissions and hydrothermal systems.

4.4 Conclusions and Implications for Future Work

On a global scale the isotopic composition of Hg in NG has a significant range of values (δ^{202}Hg= -3.75 to -0.68‰ and Δ^{199}Hg = -0.09 to 0.65‰). There is also significant isotopic variation across reservoirs from the same region (SE Asia) (δ^{202}Hg= -2.57 to -0.68‰ and Δ^{199}Hg = -0.02 to 0.25‰). These results suggest that with further sample analysis, particularly direct measurements of Hg within NG, Hg isotopic analysis may be a feasible monitoring tool for Hg emissions from NG production in some gas fields. Previous work has demonstrated the utility of Hg isotope measurements as source tracers of atmospheric Hg in local and regional environments,[19-22, 40] and it has been suggested that with further efforts, Hg isotope measurements might aid in constraining different source contributions to the global atmospheric Hg cycle.[49,50] With further analyses of NG from around the world, a global average Hg isotopic composition of natural gas and associated emissions could be estimated to characterize this input to atmospheric Hg isotope models.

Acknowledgements

We thank Heather Whittenbury and Katie Smart at Johnson Matthey for their assistance and support with the collection of the PURASPEC catalyst samples. The authors would also like to thank Runsheng Yin and two other anonymous reviewers for their insightful suggestions to improve this manuscript. The authors declare no competing financial interests. This work was partially funded from a University of Michigan Department of Earth and Environmental Sciences Scott Turner Award to SJW and the John D MacArthur Professorship to JDB.

Table 4.1 Summary of THg values and Hg stable isotope data of catalyst samples

For duplicated samples, Hg stable isotope values represent an average of duplicate measurements.

Sample Name	Duplicate	Reactor Bed Position	THg	$\delta^{204}Hg$	$\delta^{202}Hg$	$\delta^{201}Hg$	$\delta^{200}Hg$	$\delta^{199}Hg$	$\Delta^{204}Hg$	$\Delta^{201}Hg$	$\Delta^{200}Hg$	$\Delta^{199}Hg$
	n	%	mg/g	‰	‰	‰	‰	‰	‰	‰	‰	‰
Australia_R1_#1	1	5	18.5	-5.61	-3.75	-2.81	-1.86	-0.85	-0.02	0.02	0.03	0.10
Australia_R1_#2	2	60	0.20	-5.02	-3.37	-2.42	-1.65	-0.63	0.00	0.11	0.04	0.22
Brazil_R1_#1	1	0	32.6	-3.53	-2.31	-1.83	-1.15	-0.53	-0.08	-0.09	0.01	0.05
Brazil_R1_#2	1	15	0.42	-1.60	-1.06	-0.61	-0.51	0.10	-0.01	0.19	0.02	0.37
Malaysia_R1_#1	1	0	28.9	-2.34	-1.58	-1.21	-0.76	-0.40	0.02	-0.02	0.03	0.00
Malaysia_R1_#2	1	40	8.41	-4.45	-3.01	-2.13	-1.46	-0.51	0.03	0.13	0.05	0.25
Malaysia_R2_#1	1	0	1.65	-1.04	-0.68	-0.65	-0.33	-0.19	-0.02	-0.13	0.01	-0.02
Malaysia_R2_#2	1	30	3.87	0.61	0.47	0.21	0.26	0.04	-0.09	-0.15	0.02	-0.08
North Sea_R1_#1	1	10	89.8	-2.91	-1.88	-1.35	-0.93	-0.44	-0.10	0.06	0.01	0.04
North Sea_R1_#2	1	30	30.5	-0.98	-0.64	-0.43	-0.27	0.01	-0.02	0.06	0.05	0.17
Northern Europe_R1_#1	2	0	2.65	-4.98	-3.28	-2.10	-1.54	-0.20	-0.08	0.37	0.11	0.63
SE Asia_R1_#1	2	60	12.9	-3.58	-2.39	-1.71	-1.18	-0.42	-0.02	0.09	0.02	0.18
SE Asia_R2_#1	2	60	38.1	-2.39	-1.54	-1.19	-0.79	-0.31	-0.10	-0.04	-0.02	0.08
SE Asia_R3_#1	2	10	5.66	-3.87	-2.57	-1.98	-1.26	-0.57	-0.03	-0.05	0.03	0.08
SE Asia_R4_#1	3	80	0.18	-0.62	-0.33	-0.05	-0.10	0.26	-0.13	0.20	0.07	0.34
SE Asia_R5_#1	3	0	28.2	-2.31	-1.60	-1.09	-0.74	-0.16	0.08	0.11	0.07	0.25
SE Asia_R5_#2	3	26	0.11	1.10	0.76	0.61	0.41	0.33	-0.04	0.03	0.03	0.14
SE Asia_R5_#3	1	78	0.001	0.37	0.21	0.25	0.15	0.21	0.06	0.09	0.05	0.16
SE Asia_R5_#4	3	100	0.001	-0.31	-0.27	-0.17	-0.10	0.02	0.09	0.03	0.03	0.08
Catalyst Blank	2	NA	0.001	0.01	0.01	0.06	0.06	0.15	-0.01	0.05	0.05	0.14

Table 4.2 Summary of THg and Hg stable isotope data of Standards and Reference Materials

For NIST 2711, N1 denotes the total number of process replicates and N2 denotes the total number of isotope measurements during all analytical sessions. Sigma denotes the standard error of the mean values for process replicates. For UM-Almaden, N1 denotes the number of isotope measurements, N2 denotes the number of analytical sessions that UM Almaden was measured and sigma represents the standard deviation of Hg isotope values.

Reference Material	N1	N2	THg	2σ	$\delta^{204}Hg$	2σ	$\delta^{202}Hg$	2σ	$\delta^{201}Hg$	2σ	$\delta^{200}Hg$	2σ	$\delta^{199}Hg$	2σ	$\Delta^{204}Hg$	2σ	$\Delta^{201}Hg$	2σ	$\Delta^{200}Hg$	2σ	$\Delta^{199}Hg$	2σ
			μg/g	μg/g	‰	‰	‰	‰	‰	‰	‰	‰	‰	‰	‰	‰	‰	‰	‰	‰	‰	‰
NIST 2711 Proc. Ref.	5	11	6.04	0.30	-0.26	0.33	-0.19	0.06	-0.33	0.08	-0.09	0.09	-0.27	0.08	0.02	0.24	-0.18	0.07	0.01	0.06	-0.22	0.07
UM-Almaden	20	4	NA	NA	-0.86	0.07	-0.58	0.07	-0.46	0.06	-0.29	0.07	-0.18	0.07	0.00	0.08	-0.03	0.05	0.00	0.04	-0.03	0.06

Figure 4.1 Plot of δ^{202}Hg vs. Δ^{199}Hg values for MRU catalysts

Plot of δ^{202}Hg vs. Δ^{199}Hg values for MRU catalysts, divided into inlet (solid green squares) and downstream (open green squares) samples. The analytical uncertainty (2σ) associated with the samples is shown. For comparison, the average values (circles) and ranges (boxes) observed for coal (grey hashmarked)[18], marine sediments and black shales (blue hashmarked)[16,53,54,55] , and hydrothermal precipitates (red hashmarked) [16,56] are also plotted.

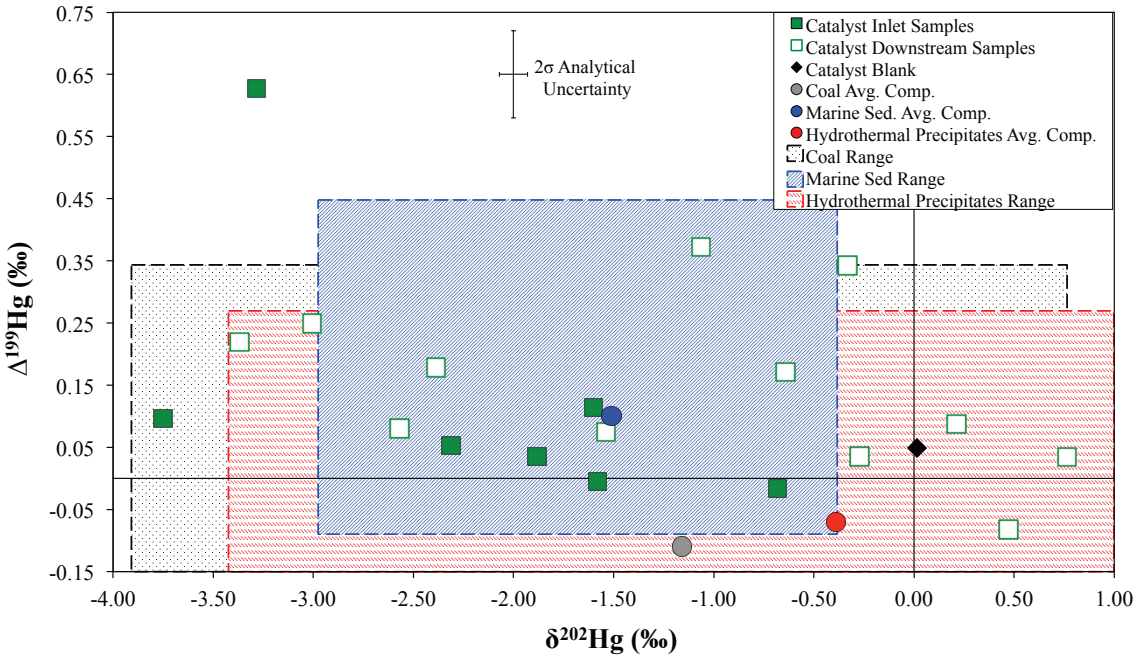

Figure 4.2 Plot of relative reactor position vs. THg and isotope values for SE Asia_R5 reactor

Plot of relative reactor position (% distance through reactor bed) vs. THg (logarithmic scale) (black squares), δ^{202}Hg values (red diamonds), and Δ^{199}Hg values (blue circles) for the SE Asia_R5_#1 - #4 reactor samples, as well as the blank catalyst sample (grey symbols; as determined from unused catalyst material). Analytical uncertainty for δ^{202}Hg values (red diamonds) is smaller than the symbols, and the black error bars represent the analytical uncertainty for Δ^{199}Hg values (±0.07‰).

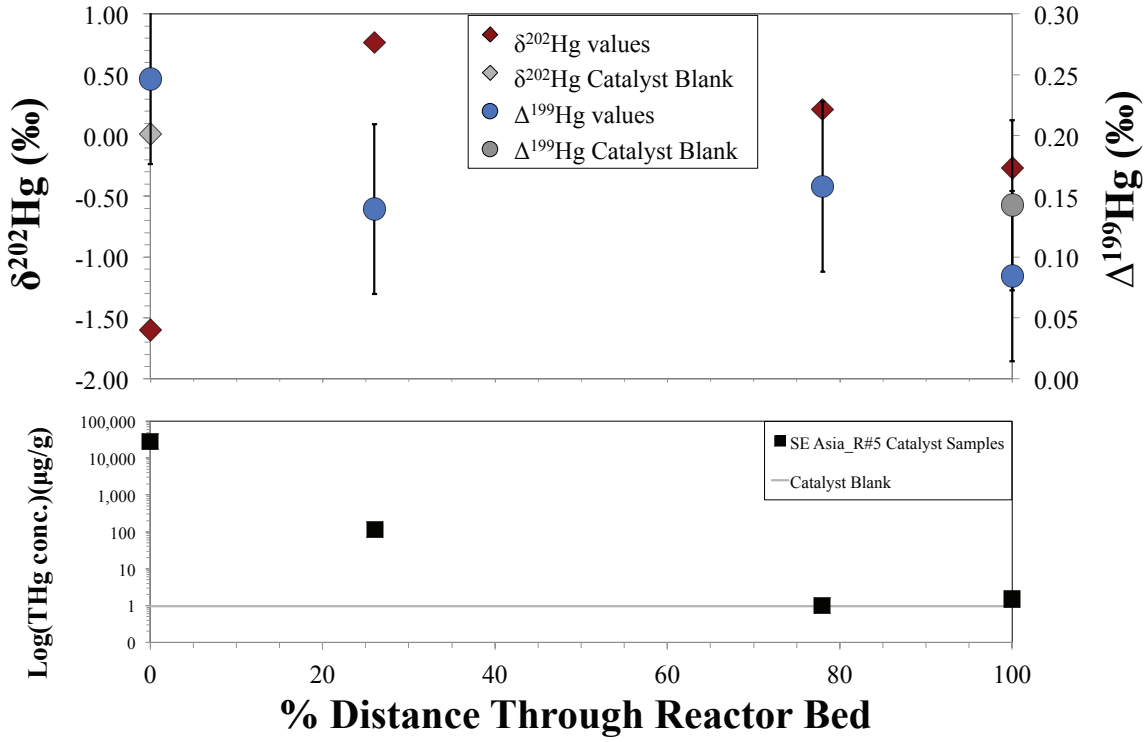

Figure 4.3 Rayleigh fractionation plot for the proposed sorption reaction of Hg to the catalysts

Rayleigh fractionation plot (fraction of the product remaining vs. δ^{202}Hg values) for the proposed sorption reaction of Hg to the catalysts. Hg entrained within the NG stream is assumed to be the reactant, with Hg sorbed to the catalysts the product, with the ε of this sorption reaction set at ε= -0.44‰. The starting reactant isotopic composition was set as the δ^{202}Hg value of SE Asia_R5_#1 (-1.60‰) [dark grey square], with SE Asia_R5_#2 also plotted [light grey square]. The δ^{202}Hg values of the instantaneous reactant [red line] and cumulative product [blue line] are shown. Analytical uncertainty for δ^{202}Hg values of catalyst samples is smaller than the symbols

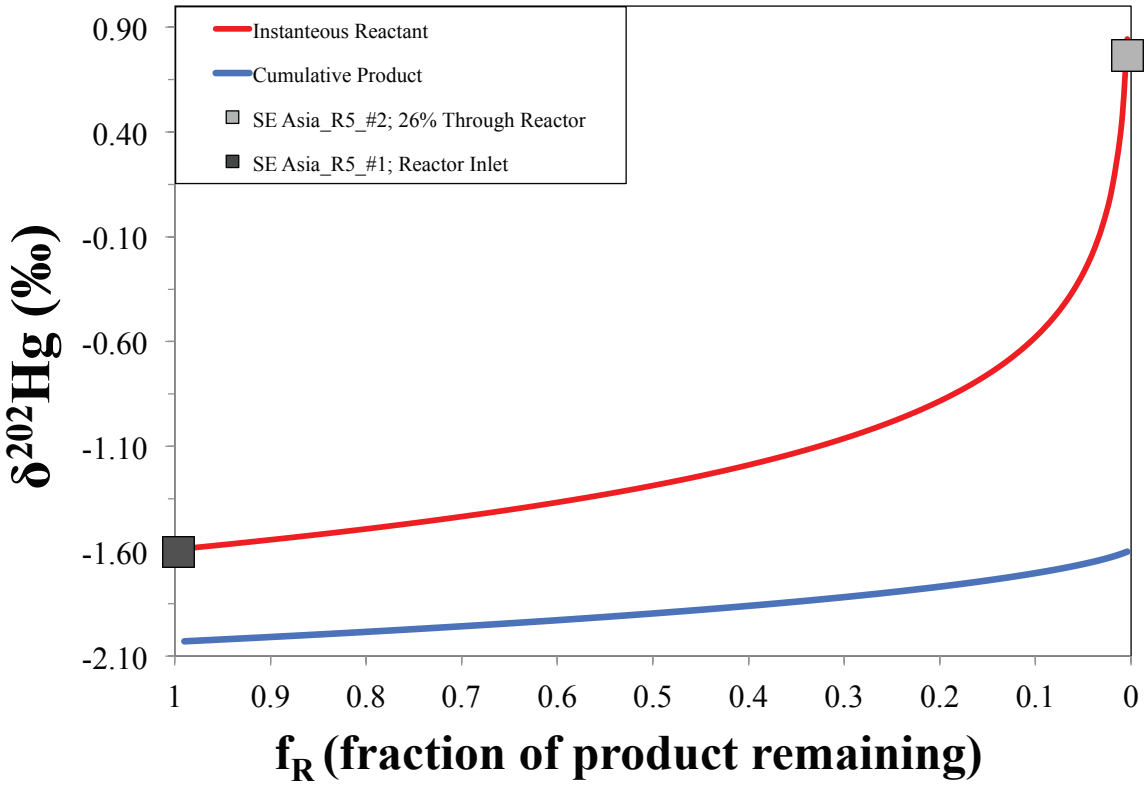

Figure 4.4 Plot of Δ^{201}Hg vs. Δ^{199}Hg values for NG catalyst inlet samples vs potential Hg sources

Plot of Δ^{201}Hg vs. Δ^{199}Hg values for NG catalyst inlet samples (green squares), other hydrocarbon source rocks, and potential Hg sources to NG. Athabasca oil sands (light green triangles) data taken from (Ref. 21). Hydrothermal fluids, sinters, and minerals (lavender diamonds) taken from (Ref. 46, 56). Marine sediments (orange circles) are unimpacted by anthropogenic activity, taken from (Ref. 51, 55). Sapropels and black shales (red circles) taken from (Ref. 52-54). Atmospheric GEM (gray x's) data from sites determined to be unimpacted by anthropogenic emissions, taken from (Ref. 24, 38-42).

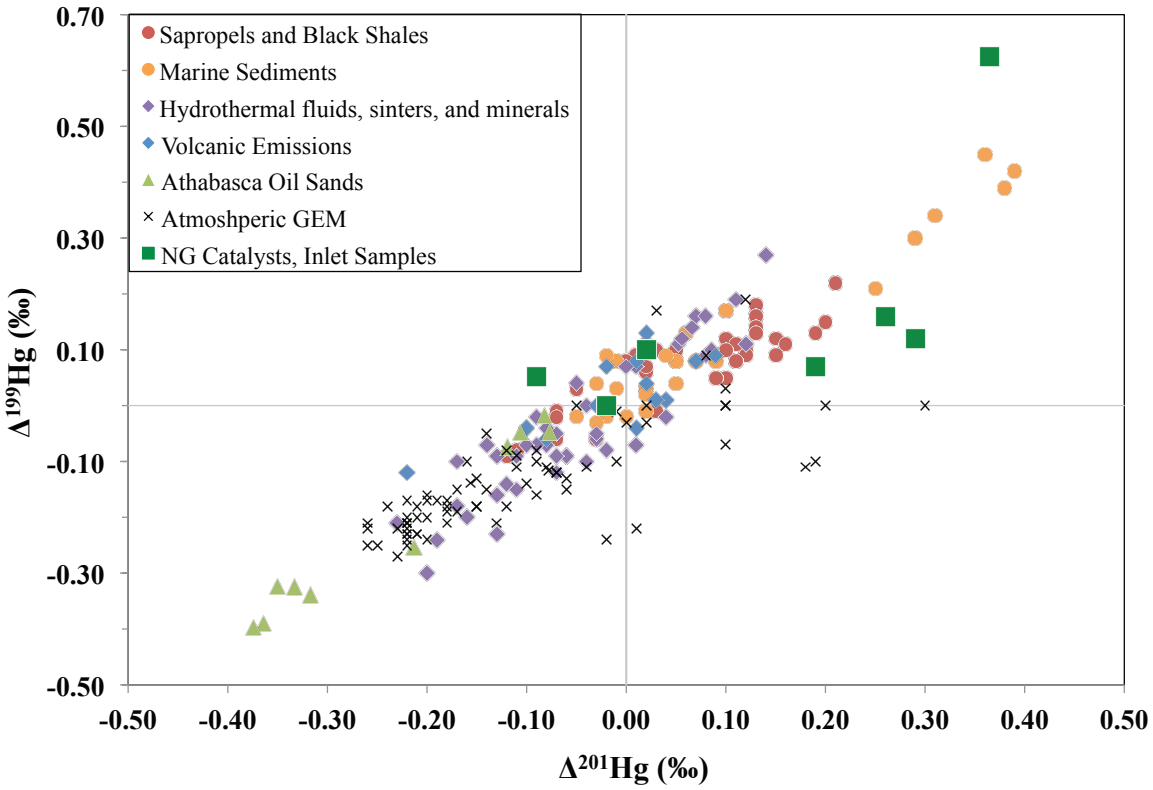

References

(1) Selin, N. E. Global Biogeochemical Cycling of Mercury: A Review. *Annu. Rev. Environ. Resour.* **2009**, *34* (1), 43–63 DOI: 10.1146/annurev.environ.051308.084314.

(2) Wang, Q.; Chen, X.; Jha, A. N.; Rogers, H. Natural Gas from Shale Formation - The Evolution, Evidences and Challenges of Shale Gas Revolution in United States. *Renew. Sustain. Energy Rev.* **2014**, *30*, 1–28 DOI: 10.1016/j.rser.2013.08.065.

(3) Wilhelm, S. M. *Mercury in Petroleum and Natural Gas: Estimation of Emissions from Production, Processing, and Combustion*; **2001**. EPA-600/R-01-066. U.S. Environmental Protection Agency, Office of Research and Development: Washington, DC, 20460.

(4) Liu, Q. Mercury Concentration in Natural Gas and Its Distribution in the Tarim Basin. *Sci. China Earth Sci.* **2013**, *56* (8), 1371–1379 DOI: 10.1007/s11430-013-4609-2.

(5) Miedaner, M. M.; Migdisov, A. A.; Williams-Jones, A. E. Solubility of Metallic Mercury in Octane, Dodecane and Toluene at Temperatures between 100°C and 200°C. *Geochim. Cosmochim. Acta* **2005**, *69* (23), 5511–5516 DOI: 10.1016/j.gca.2005.06.029.

(6) Bell, R., Review of Impact of Mercury on Aluminum Heat Exchangers. Presented at European Ethylene Producers Committees annual HSE Meeting, Prague, Czech Republic, October 6-7, 2005.

(7) Spiric, Z. Innovative Approach to the Mercury Control During Natural Gas Processing. In *Engineering Technology Conference on Energy 2001*; 2001; pp 1–7.

(8) Abai, M.; Atkins, M. P.; Hassan, A.; Holbrey, J. D.; Kuah, Y.; Nockemann, P.; Oliferenko, A. A.; Plechkova, N. V.; Rafeen, S.; Rahman, A. A.; Ramli, R.; Shariff, S. M.; Seddon, K. R.; Srinivasan, G.; Zou, Y. An Ionic Liquid Process for Mercury Removal from Natural Gas. *Dalt. Trans.* **2015**, *44* (18), 8617–8624 DOI: 10.1039/C4DT03273J.

(9) Pirrone, N.; Cinnirella, S.; Feng, X.; Finkelman, R. B.; Friedli, H. R.; Leaner, J.; Mason, R.; Mukherjee, A. B.; Stracher, G. B.; Streets, D. G.; Telmer, K. Global Mercury Emissions to the Atmosphere from Anthropogenic and Natural Sources. *Atmos. Chem. Phys.* **2010**, *10* (13), 5951–5964 DOI: 10.5194/acp-10-5951-2010.

(10) Spirić, Z.; Mashyanov, N. R. Mercury Measurements in Ambient Air near Natural Gas Processing Facilities. *Fresenius. J. Anal. Chem.* **2000**, *366* (5), 429–432 DOI: 10.1007/s002160050087.

(11) Horvat, M.; Jeran, Z.; Špirič, Z.; Jaćimović, R.; Miklavčič, V. Mercury and Other Elements in Lichens near the INA Naftaplin Gas Treatment Plant, Molve, Croatia. *J. Environ. Monit.* **2000**, *2* (2), 139–144 DOI: 10.1039/a906973i.

(12) World Health Organization. *Air Quality Guidelines for Europe, 2nd Ed.*; **2000.** WHO Regional Publications No. 91, ISBN: 92 890 1358 3.

(13) U.S. Census Bureau. *2010 Census.* U.S. Census Bureau. **2010.** Accessed at https://www.census.gov/const/C25Ann/sftotalmedavgsqft.pdf

(14) U.S. Energy Information Administration, Office of Energy Consumption and Efficiency Statistics. *2009 Residential Energy Consumption Survey*. **2013**. DOE-019-5945672389.

(15) Yin, R.; Feng, X.; Shi, W. Application of the Stable-Isotope System to the Study of Sources and Fate of Hg in the Environment: A Review. *Appl. Geochemistry* **2010**, *25* (10), 1467–1477 DOI: 10.1016/j.apgeochem.2010.07.007.

(16) Blum, J. D.; Sherman, L. S.; Johnson, M. W. Mercury Isotopes in Earth and Environmental Sciences. *Annu. Rev. Earth Planet. Sci.* **2014**, *42* (1), 249–269 DOI: 10.1146/annurev-earth-050212-124107.

(17) Biswas, A.; Blum, J. D.; Bergquist, B. A.; Keeler, G. J.; Xie, Z. Natural Mercury Isotope Variation in Coal Deposits and Organic Soils. *Environ. Sci. Technol.* **2008**, *42* (22), 8303–8309 DOI: 10.1021/es801444b.

(18) Sun, R.; Sonke, J. E.; Liu, G. Earth-Science Reviews Biogeochemical Controls on Mercury Stable Isotope Compositions of World Coal Deposits : A Review. *Earth Sci. Rev.* **2016**, *152*, 1–13 DOI: 10.1016/j.earscirev.2015.11.005.

(19) Sherman, L. S.; Blum, J. D.; Keeler, G. J.; Demers, J. D.; Dvonch, J. T. Investigation of Local Mercury Deposition from a Coal-Fired Power Plant Using Mercury Isotopes. *Environ. Sci. Technol.* **2012**, *46* (1), 382–390 DOI: 10.1021/es202793c.

(20) Estrade, N.; Carignan, J.; Donard, O. F. X. Isotope Tracing of Atmospheric Mercury Sources in an Urban Area of Northeastern France. *Environ. Sci. Technol.* **2010**, *44* (16), 6062–6067 DOI: 10.1021/es100674a.

(21) Blum, J. D.; Johnson, M. W.; Gleason, J. D.; Demers, J. D.; Landis, M. S.; Krupa, S. Mercury Concentration and Isotopic Composition of Epiphytic Tree Lichens in the Athabasca Oil Sands Region. *Dev. Environ. Sci.* **2012**, *11*, 373–390 DOI: 10.1016/B978-0-08-097760-7.00016-0.

(22) Wiederhold, J. G.; Smith, R. S.; Siebner, H.; Jew, A. D.; Brown, G. E.; Bourdon, B.; Kretzschmar, R. Mercury Isotope Signatures as Tracers for Hg Cycling at the New Idria Hg Mine. *Environ. Sci. Technol.* **2013**, *47* (12), 6137–6145 DOI: 10.1021/es305245z.

(23) Grant, C. J.; Weimer, A. B.; Marks, N. K.; Perow, E. S.; Oster, J. M.; Brubaker, K. M.; Trexler, R. V.; Solomon, C. M.; Lamendella, R. Marcellus and Mercury: Assessing Potential Impacts of Unconventional Natural Gas Extraction on Aquatic Ecosystems in Northwestern Pennsylvania. *J. Environ. Sci. Heal. - Part A Toxic/Hazardous Subst. Environ. Eng.* **2015**, *50* (5), 482–500 DOI: 10.1080/10934529.2015.992670.

(24) Demers, J. D.; Blum, J. D.; Zak, D. R. Mercury Isotopes in a Forested Ecosystem: Implications for Air-Surface Exchange Dynamics and the Global Mercury Cycle. *Global Biogeochem. Cycles* **2013**, *27*, n/a-n/a DOI: 10.1002/gbc.20021.

(25) Sherman, L. S.; Blum, J. D. Mercury Stable Isotopes in Sediments and Largemouth Bass from Florida Lakes, USA. *Sci. Total Environ.* **2013**, *448*, 163–175 DOI: 10.1016/j.scitotenv.2012.09.038.

(26) Blum, J. D.; Johnson, M. W. Recent Developments in Mercury Stable Isotope Analysis. *Rev. Mineral. Geochemistry* **2017**, *82* (1), 733–757 DOI: https://doi.org/10.2138/rmg.2017.82.17.

(27) Lauretta, D. S.; Klaue, B.; Blum, J. D.; Buseck, P. R. Mercury Abundances and Isotopic Compositions in the Murchison (CM) and Allende (CV) Carbonaceous Chondrites. *Geochim. Cosmochim. Acta* **2001**, *65* (16), 2807–2818 DOI: 10.1016/S0016-7037(01)00630-5.

(28) Blum, J. D.; Bergquist, B. A. Reporting of Variations in the Natural Isotopic Composition of Mercury. *Anal. Bioanal. Chem.* **2007**, *388* (2), 353–359 DOI: 10.1007/s00216-007-1236-9.

(29) Estrade, N.; Carignan, J.; Donard, O. F. X. Tracing and Quantifying Anthropogenic Mercury Sources in Soils of Northern France Using Isotopic Signatures. *Environ. Sci. Technol.* **2011**, *45* (4), 1235–1242 DOI: 10.1021/es1026823.

(30) Jiskra, M.; Wiederhold, J. G.; Skyllberg, U.; Kronberg, R. M.; Hajdas, I.; Kretzschmar, R. Mercury Deposition and Re-Emission Pathways in Boreal Forest Soils Investigated with Hg Isotope Signatures. *Environ. Sci. Technol.* **2015**, *49* (12), 7188–7196 DOI: 10.1021/acs.est.5b00742.

(31) Yin, R.; Feng, X.; Hurley, J. P.; Krabbenhoft, D. P.; Lepak, R. F. Mercury Isotopes as Proxies to Identify Sources and Environmental Impacts of Mercury in Sphalerites. *Sci. Rep.* **2016**, No. November 2015, 1–8 DOI: 10.1038/srep18686.

(32) Washburn, S. J.; Blum, J. D.; Demers, J. D.; Kurz, A. Y.; Landis, R. C. Isotopic Characterization of Mercury Downstream of Historic Industrial Contamination in the South River, Virginia. *Environ. Sci. Technol.* **2017**, acs.est.7b02577 DOI: 10.1021/acs.est.7b02577.

(33) Wilhelm, S. M.; Bloom, N. Mercury in Petroleum. *Fuel Process. Technol.* **2000**, *63* (1), 1–27 DOI: 10.1016/S0378-3820(99)00068-5.

(34) Jiskra, M.; Wiederhold, J. G.; Bourdon, B.; Kretzschmar, R. Solution Speciation Controls Mercury Isotope Fractionation of Hg(II) Sorption to Goethite. *Environ. Sci. Technol.* **2012**, *46* (12), 6654–6662 DOI: 10.1021/es3008112.

(35) Wiederhold, J. G.; Cramer, C. J.; Daniel, K.; Infante, I.; Bourdon, B.; Kretzschmar, R. Equilibrium Mercury Isotope Fractionation between Dissolved Hg (II) Species and Thiol-Bound Hg. *Environ. Sci. Technol.* **2010**, *44* (11), 4191–4197.

(36) Ghosh, S.; Schauble, E. a.; Lacrampe Couloume, G.; Blum, J. D.; Bergquist, B. a. Estimation of Nuclear Volume Dependent Fractionation of Mercury Isotopes in Equilibrium Liquid–vapor Evaporation Experiments. *Chem. Geol.* **2013**, *336*, 5–12 DOI: 10.1016/j.chemgeo.2012.01.008.

(37) Lefticariu, L.; Blum, J. D.; Gleason, J. D. Mercury Isotopic Evidence for Multiple Mercury Sources in Coal from the Illinois Basin. *Environ. Sci. Technol.* **2011**, *45*, 1724–1729 DOI: 10.1021/es102875n.

(38) Gratz, L. E.; Keeler, G. J.; Blum, J. D.; Sherman, L. S. Isotopic Composition and Fractionation of Mercury in Great Lakes Precipitation and Ambient Air. *Environ. Sci. Technol.* **2010**, *44* (20), 7764–7770 DOI: 10.1021/es100383w.

(39) Sherman, L. S.; Blum, J. D.; Johnson, K. P.; Keeler, G. J.; Barres, J. A.; Douglas, T. A. Mass-Independent Fractionation of Mercury Isotopes in Arctic Snow Driven by Sunlight. *Nat. Geosci* **2010**, *3* (3), 173–177.

(40) Demers, J. D.; Sherman, L. S.; Blum, J. D.; Marsik, F. J.; Dvonch, J. T. Coupling Atmospheric Mercury Isotope Ratios and Meteorology to Identify Sources of Mercury Impacting a Coastal Urban-Industrial Region near Pensacola, Florida, USA. *Global Biogeochem. Cycles* **2015**, *29* (10), 1689–1705 DOI: 10.1002/2015GB005146.

(41) Fu, X.; Marusczak, N.; Wang, X.; Gheusi, F.; Sonke, J. E. Isotopic Composition of Gaseous Elemental Mercury in the Free Troposphere of the Pic Du Midi Observatory, France. *Environ. Sci. Technol.* **2016**, *50* (11), 5641–5650 DOI: 10.1021/acs.est.6b00033.

(42) Yu, B.; Fu, X.; Yin, R.; Zhang, H.; Wang, X.; Lin, C.-J.; Wu, C.; Zhang, Y.; He, N.; Fu, P.; Wang, Z.; Shang, L.; Sommar, J.; Sonke, J. E.; Maurice, L.; Guinot, B.; Feng, X. Isotopic Composition of Atmospheric

Mercury in China: New Evidence for Source and Transformation Processes in Air and in Vegetation. *Environ. Sci. Technol.* **2016** DOI: 10.1021/acs.est.6b01782.

(43) Sun, R.; Sonke, J. E.; Heimbürger, L. E.; Belkin, H. E.; Liu, G.; Shome, D.; Cukrowska, E.; Liousse, C.; Pokrovsky, O. S.; Streets, D. G. Mercury Stable Isotope Signatures of World Coal Deposits and Historical Coal Combustion Emissions. *Environ. Sci. Technol.* **2014**, *48* (13), 7660–7668 DOI: 10.1021/es501208a.

(44) Sun, R.; Heimbürger, L.-E.; Sonke, J. E.; Liu, G.; Amouroux, D.; Berail, S. Mercury Stable Isotope Fractionation in Six Utility Boilers of Two Large Coal-Fired Power Plants. *Chem. Geol.* **2012**, *336*, 103–111 DOI: 10.1016/j.chemgeo.2012.10.055.

(45) Tang, S.; Feng, C.; Feng, X.; Zhu, J.; Sun, R.; Fan, H.; Wang, L.; Li, R.; Mao, T.; Zhou, T. Stable Isotope Composition of Mercury Forms in Flue Gases from a Typical Coal-Fired Power Plant, Inner Mongolia, Northern China. *J. Hazard. Mater.* **2017**, *328*, 90–97 DOI: 10.1016/j.jhazmat.2017.01.014.

(46) Sherman, L. S.; Blum, J. D.; Nordstrom, D. K.; McCleskey, R. B.; Barkay, T.; Vetriani, C. Mercury Isotopic Composition of Hydrothermal Systems in the Yellowstone Plateau Volcanic Field and Guaymas Basin Sea-Floor Rift. *Earth Planet. Sci. Lett.* **2009**, *279* (1–2), 86–96 DOI: 10.1016/j.epsl.2008.12.032.

(47) Thibodeau, A. M.; Ritterbush, K.; Yager, J. A.; West, A. J.; Ibarra, Y.; Bottjer, D. J.; Berelson, W. M.; Bergquist, B. A.; Corsetti, F. A. Recovery Following the End-Triassic Mass Extinction. *Nat. Commun.* **2016**, *7*, 1–8 DOI: 10.1038/ncomms11147.

(48) Grasby, S. E.; Shen, W.; Yin, R.; Gleason, J. D.; Blum, J. D.; Lepak, R. F.; Hurley, J. P.; Beauchamp, B. Isotopic Signatures of Mercury Contamination in Latest Permian Oceans. *Geology* **2017**, *45* (1), 55–58 DOI: 10.1130/G38487.1.

(49) Zhang, L.; Lyman, S.; Mao, H.; Lin, C.-J.; Gay, D. A.; Wang, S.; Gustin, M. S.; Feng, X.; Wania, F. A Synthesis of Research Needs for Improving the Understanding of Atmospheric Mercury Cycling. *Atmos. Chem. Phys.* **2017**, *17* (14), 9133–9144 DOI: 10.5194/acp-17-9133-2017.

(50) Sun, R.; Streets, D. G.; Horowitz, H. M.; Amos, H. M.; Liu, G.; Perrot, V.; Toutain, J.-P.; Hintelmann, H.; Sunderland, E. M.; Sonke, J. E. Historical (1850–2010) Mercury Stable Isotope Inventory from Anthropogenic Sources to the Atmosphere. *Elem. Sci. Anthr.* **2016**, *4*, 91 DOI: 10.12952/journal.elementa.000091.

(51) Mil-Homens, M.; Blum, J.; Canário, J.; Caetano, M.; Costa, A. M.; Lebreiro, S. M.; Trancoso, M.; Richter, T.; de Stigter, H.; Johnson, M.; Branco, V.; Cesário, R.; Mouro, F.; Mateus, M.; Boer, W.; Melo, Z. Tracing Anthropogenic Hg and Pb Input Using Stable Hg and Pb Isotope Ratios in Sediments of the Central Portuguese Margin. Chem. Geol. 2013, 336, 62–71 DOI: 10.1016/j.chemgeo.2012.02.018.

(52) Gehrke, G. E.; Blum, J. D.; Meyers, P. A. The Geochemical Behavior and Isotopic Composition of Hg in a Mid-Pleistocene Western Mediterranean Sapropel. Geochim. Cosmochim. Acta 2009, 73 (6), 1651–1665 DOI: 10.1016/j.gca.2008.12.012.

(53) Gleason, J. D.; Blum, J. D.; Moore, T. C.; Polyak, L.; Jakobsson, M.; Meyers, P. A.; Biswas, A. ScienceDirect Sources and Cycling of Mercury in the Paleo Arctic Ocean from Hg Stable Isotope Variations in Eocene and Quaternary Sediments. *Geochim. Cosmochim. Acta* **2017**, *197*, 245–262 DOI: 10.1016/j.gca.2016.10.033.

(54) Yin, R.; Xu, L.; Lehmann, B.; Lepak, R. F.; Hurley, J. P.; Mao, J.; Feng, X.; Hu, R. Anomalous Mercury Enrichment in Early Cambrian Black Shales of South China : Mercury Isotopes Indicate a Seawater Source. *Chem. Geol.* **2017**, *467*, 159–167 DOI: 10.1016/j.chemgeo.2017.08.010.

(55) Yin, R.; Feng, X.; Chen, B.; Zhang, J.; Wang, W.; Li, X. Identifying the Sources and Processes of Mercury in Subtropical Estuarine and Ocean Sediments Using Hg Isotopic Composition. *Environ. Sci. Technol.* **2015**, *49* (3), 1347–1355 DOI: 10.1021/es504070y.

(56) Xu, C.; Yin, R.; Peng, J.; Hurley, J. P.; Lepak, R. F.; Gao, J.; Feng, X.; Hu, R.; Bi, X. Mercury Isotope Constraints on the Source for Sediment-Hosted Lead-Zinc Deposits in the Changdu Area , Southwestern China. *Miner. Depos.* **2017** DOI: 10.1007/s00126-017-0743-7.

4.5 Supporting Information

Table 4.3 Summary of THg and Hg stable isotope data of catalyst duplicate samples.

Sample Name	THg	δ^{204}Hg	δ^{202}Hg	δ^{201}Hg	δ^{200}Hg	δ^{199}Hg	Δ^{204}Hg	Δ^{201}Hg	Δ^{200}Hg	Δ^{199}Hg
	mg/g	‰	‰	‰	‰	‰	‰	‰	‰	‰
Australia_R1_#2	0.20	-4.90	-3.29	-2.36	-1.60	-0.61	0.01	0.11	0.05	0.22
Australia_R1_#2	0.20	-5.14	-3.44	-2.48	-1.70	-0.65	0.00	0.11	0.03	0.22
Northern Europe_R1_#1	1.98	-4.99	-3.29	-2.10	-1.55	-0.23	-0.08	0.37	0.10	0.60
Northern Europe_R1_#1	3.32	-4.97	-3.28	-2.10	-1.53	-0.17	-0.08	0.36	0.12	0.65
SE Asia_R1_#1	15.2	-4.16	-2.78	-2.00	-1.37	-0.53	-0.01	0.09	0.03	0.18
SE Asia_R1_#1	10.7	-3.00	-1.99	-1.41	-0.99	-0.32	-0.02	0.09	0.01	0.18
SE Asia_R2_#1	2.20	-2.44	-1.58	-1.24	-0.86	-0.37	-0.07	-0.05	-0.06	0.03
SE Asia_R2_#1	74.0	-2.35	-1.49	-1.15	-0.73	-0.26	-0.12	-0.03	0.02	0.12
SE Asia_R3_#1	4.58	-3.95	-2.63	-2.03	-1.29	-0.62	-0.03	-0.06	0.02	0.04
SE Asia_R3_#1	6.75	-3.79	-2.51	-1.94	-1.22	-0.52	-0.04	-0.05	0.04	0.12
SE Asia_R4_#1	0.18	-1.05	-0.59	-0.23	-0.25	0.22	-0.18	0.21	0.05	0.37
SE Asia_R4_#1	0.17	-0.36	-0.22	0.03	-0.05	0.28	-0.04	0.19	0.06	0.33
SE Asia_R4_#1	0.19	-0.46	-0.19	0.04	-0.01	0.28	-0.17	0.18	0.09	0.33
SE Asia_R5_#1	27.3	-2.96	-2.05	-1.38	-0.94	-0.25	0.10	0.16	0.09	0.26
SE Asia_R5_#1	17.4	-1.67	-1.14	-0.80	-0.51	-0.10	0.04	0.07	0.07	0.19
SE Asia_R5_#1	39.9	-2.31	-1.61	-1.09	-0.76	-0.12	0.09	0.12	0.05	0.29
SE Asia_R5_#2	0.12	1.08	0.75	0.56	0.40	0.36	-0.05	0.00	0.02	0.17
SE Asia_R5_#2	0.13	1.11	0.73	0.61	0.40	0.31	0.03	0.06	0.04	0.13
SE Asia_R5_#2	0.09	1.12	0.81	0.65	0.44	0.32	-0.09	0.04	0.03	0.12
SE Asia_R5_#4	0.001	0.26	0.12	0.07	0.02	0.04	0.08	-0.02	-0.04	0.01
SE Asia_R5_#4	0.001	-0.15	-0.17	0.04	0.03	0.11	0.11	0.17	0.11	0.15
SE Asia_R5_#4	0.002	-1.06	-0.76	-0.62	-0.36	-0.10	0.08	-0.04	0.03	0.09
Catalyst Blank	0.001	0.12	0.02	0.06	0.06	0.16	0.08	0.04	0.04	0.15
Catalyst Blank	0.001	-0.09	0.00	0.06	0.06	0.13	-0.09	0.06	0.06	0.13

Table 4.4 Summary of available ancillary parameters for the MRU's from which catalyst samples were collected.

Sample Name	THg	Total Bed Volume	Period in Duty	Operating Temperature	Operating Pressure
	mg/g	m^3	months	degrees C	bar
Australia_R1_#1	18.5	NA	NA	40	150
Australia_R1_#2	0.20	NA	NA	40	150
Brazil_R1_#1	32.6	NA	66	40	72
Brazil_R1_#2	0.42	NA	66	40	72
Malaysia_R1_#1	28.9	60	11	41	50
Malaysia_R1_#2	8.41	60	11	41	50
Malaysia_R2_#1	1.65	22	7	43	55
Malaysia_R2_#2	3.87	22	7	43	55
North Sea_R1_#1	89.8	37	13	95	70
North Sea_R1_#2	30.5	37	13	95	70
Northern Europe_R1_#1	2.65	26	34	20	60
SE Asia_R1_#1	12.9	34	17	33	21
SE Asia_R2_#1	38.1	60	7	42	52
SE Asia_R3_#1	5.66	90	28	25	28
SE Asia_R4_#1	0.18	114	16	32	20
SE Asia_R5_#1	28.2	30	8	NA	NA
SE Asia_R5_#2	0.11	30	8	NA	NA
SE Asia_R5_#3	0.001	30	8	NA	NA
SE Asia_R5_#4	0.001	30	8	NA	NA

Figure 4.5 Plot of THg vs. δ^{202}Hg values for MRU catalysts

Plot of THg (on a logarithmic scale) vs. δ^{202}Hg values for MRU catalysts, divided into inlet (solid green squares) and downstream (open green squares) samples. Analytical uncertainty for δ^{202}Hg values is smaller than the symbols.

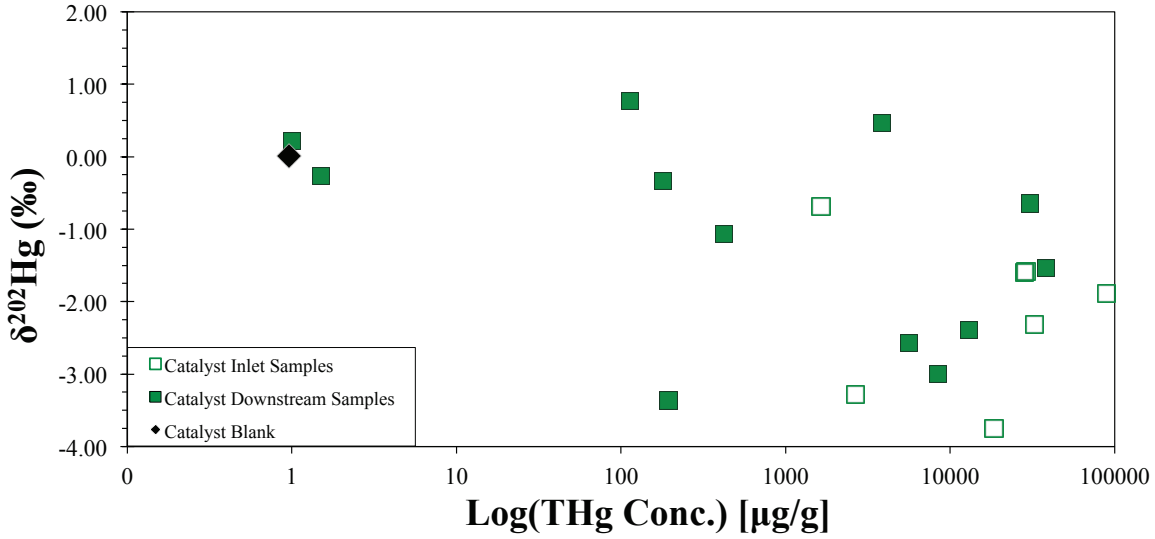

Chapter 5 Conclusion

Mercury (Hg), as a neurotoxic trace metal pollutant with a global distribution, has been the subject of intensive study to better inform efforts to limit both human and wildlife exposure. The persistence of Hg in the environment, particularly at sites impacted by direct anthropogenic Hg releases, necessitates that we continue to expand our understanding of the complex set of environmental processes and biogeochemical conditions that control the mobility and fate of Hg. Identification of multiple Hg sources (e.g. legacy contamination Hg, natural emission source Hg, and modern anthropogenic Hg sources) in the environment can be difficult with conventional Hg concentration measurements – the analysis of Hg stable isotope ratios has added to the toolkit researchers can utilize to study Hg cycling in contaminated ecosystems.

5.1 Review of Key Findings

5.1.1 Source Apportionment within Hg-contaminated Aquatic Ecosystems

In both Chapters 2 and 3, we were once again able to demonstrate the utility of Hg stable isotopic analysis as a tool for source apportionment within Hg-contaminated aquatic ecosystems. A substantial body of work had previously demonstrated the ability of Hg stable isotope ratios to distinguish between Hg sources in the sediments of aquatic ecosystems (Sonke et al., 2010; Perrot et al., 2010; Liu et al., 2011; Foucher et al., 2013; Bartov et al., 2013; Yin et al., 2013; Donovan et al., 2014; Lepak et al., 2015; Smith et al., 2015; Wiederhold et al., 2015; Donovan et al., 2016a; Donovan et al., 2016b), but few studies had extended isotopic end-member mixing models beyond sediments to other Hg reservoirs within aquatic ecosystems (e.g. riparian bank

soils, groundwater, dissolved-phase Hg). In the work conducted at South River, we aimed to take a more holistic approach by examining a number of physical reservoirs of Hg that could be influencing the Hg isotopic composition within the fluvial ecosystem. By analyzing Hg associated with suspended particulates, we were able to suggest that a previously unknown Hg isotopic end-member was influencing the isotopic composition of Hg within the South River channel (Chapter 2, Washburn et al., 2017), as some of the suspended particulates had elevated THg values and relatively low δ^{202}Hg values that could not be a mixture of the regional background and industrial Hg end-members. Subsequently, we were able to identify the source of this end-member in streambed sediments (Chapter 3, Washburn et al., *in review*), and demonstrate that the three end-member mixing model is able to account for the observed variations in Δ^{199}Hg values within the South River channel. As a caveat, the proposed three end-member mixing model is not able to explain the Hg isotopic composition observed within porewaters collected from channel margin hyporheic zones of the South River, which exhibited more positive δ^{202}Hg values than any measured physical reservoir of Hg as well as variable MIF signatures.

5.1.2 Spatial and Temporal Variation of Hg Stable Isotopes within Hg-contaminated Aquatic Ecosystems

In both Chapters 2 and 3 (Washburn et al., 2017; Washburn et al., *in* review), we sought to explore the role both spatial and temporal variability had on the Hg isotopic composition of physical reservoirs of Hg within the contaminated fluvial system. In the South River, hydrologic conditions were demonstrated to have an influence on within-channel Hg isotope fractionation and Hg partitioning, with significant isotopic discrimination (δ^{202}Hg offset ~0.28‰) between suspended particulate Hg and filtered surface water Hg during low or base flow conditions, with

no observation of this phenomenon during elevated flow conditions. We hypothesized that the diminished presence of dissolved Hg(II) sources during elevated flow, whether related to dilution of the Hg load or changes in the physiochemical properties of the South River channel during elevated flows, would limit the proposed fractionation mechanism responsible for the δ^{202}Hg offset between filtered surface water and suspended particulates (Washburn et al., 2017; Washburn et al., *in review*). Our understanding of the role that discharge played in Hg cycling within the South River was only made possible by a sampling campaign that was designed to encompass a large spatial range along a longitudinal transect of the river channel as well as differing hydrologic conditions.

Analysis of a sediment profile collected from a South River floodplain led to the conclusion that that past releases of Hg to the South River did not have a completely homogenous isotopic composition, with brief temporal excursions in δ^{202}Hg values (up to δ^{202}Hg = +0.40‰) from the average composition observed in the modern (δ^{202}Hg = -0.51 ± 0.07‰). The brief, relatively more positive excursions in isotopic composition of the sediments are similar to Hg analyzed in a subset of downstream banks soils, suggesting that past releases of Hg to the South River are influencing observations in the modern. Our work in the South River underscores the need for studies of dynamic contamination-impacted ecosystems to assess the full range of temporal, physiochemical, and spatial variation that are present in these ecosystems, as these parameters can exhibit a strong influence on the observed Hg isotopic composition.

5.1.3 Hg Isotopic Composition of Natural Gas

In Chapter 4 (Washburn et al., 2018), we presented the first measurements of the isotopic composition of Hg in natural gas (NG). We demonstrated that there is a significant variation in the isotopic composition of Hg within NG at a global scale (δ^{202}Hg= -3.75 to -0.68‰ and Δ^{199}Hg

= -0.09 to 0.65‰). In addition, we observed significant isotopic variation for Hg from reservoirs within the same region (SE Asia) (δ^{202}Hg= -2.57 to -0.68‰ and Δ^{199}Hg = -0.02 to 0.25‰). Despite previous work that has suggested that Hg emissions related to NG processing and combustion being a negligible contributor to the global atmospheric Hg cycle (Pirrone et al., 2010), at the local and regional scale NG processing facilities have been demonstrated to increase ambient air Hg concentrations and elevated local events have been shown to correlate with Hg content of co-located bioindicators such as epiphytic lichens (Spiric and Mashyanov, 2000; Horvat et al., 2000). The large range in Hg isotopic composition of NG suggests that Hg stable isotope ratio analysis could be a useful tool for assessing the impacts of Hg emissions related to NG processing on local environments.

5.2 Future Directions

The work presented in this dissertation has added to the growing canon of studies that have used Hg stable isotope analysis to understand environmental Hg cycling, particularly related to the impacts of anthropogenic activity. The results of this dissertation point towards a number of directions that future studies can take to continue the advancement of the understanding of Hg cycling and Hg stable isotope dynamics.

Specifically, the work on the South River presented in this dissertation underscores the need for future studies involving Hg stable isotopic analysis to conduct research that fully accounts for the potential spatial, temporal, and hydrologic variations inherent to complex aquatic environments. Without a full accounting for the influence of these parameters on Hg isotopic composition, inferences about aspects of the biogeochemical cycling of Hg within aquatic systems can be oversimplified. The unexpected observation of an average Hg isotopic composition in hyporheic zone porewaters that differed from that observed in surface waters and

other Hg reservoirs within the South River, as discussed in Chapter 3 (Washburn et al., *in review*), underpinned that Hg dynamics within hyporheic zones are not well constrained and the influence of Hg exchange between channel and hyporheic zones has not been sufficiently explored. The complex, changing redox conditions within hyporheic zones and fluctuating hydrologic gradients are likely to have a significant impact on the isotopic composition of Hg stored within the substrate. Altogether, this suggests that future studies that aim to combine observational field studies with experimental studies about the isotopic partitioning dynamics of Hg in dark, low-oxygen sediments would be highly beneficial to our understanding of fluvial Hg cycling.

The observation of Hg isotopic partitioning between dissolved and suspended particulate fractions in the South River, and the apparent dependence of this partitioning on discharge conditions, was unable to be fully contextualized within a framework of previous experimental work. Experimental studies designed to probe the aqueous isotopic fractionation of Hg to dissolved organic matter, as well as suspended particulates that likely represent aggregates of both organic matter and mineral components, would enhance our understanding of Hg cycling in aquatic ecosystems. Additional field studies that focused on the Hg isotope dynamics of dissolved Hg released into aquatic settings from legacy contamination, particularly at sites with characteristics that differ from the South River (e.g. tidal or estuary settings, lakes, headwater riverine systems) would provide insights that could inform our understanding of the impacts that continued release of legacy Hg sources will have on ecosystems and better guide future remediation efforts.

The significant range in Hg isotopic composition observed in the initial survey of Hg within NG (Chapter 4, Washburn et al., 2018) suggests that there are a number of exciting

directions that future studies could explore to continue to improve our understanding of this growing energy sector. Previous studies that have demonstrated the ability of Hg isotope measurements to identify and trace atmospheric Hg emissions in local and regional environments (Estrade et al., 2010; Sherman et al., 2012; Blum et al., 2012; Demers et al., 2015), and the impacts of Hg emissions from NG processing have not been extensively documented in the literature. Hg isotopic analysis may be a feasible monitoring tool for Hg emissions from NG production in some gas fields if future studies combined targeted sampling of both NG at various stages of processing and environmental receptors. Incorporating Hg isotope measurements into models of global Hg cycling is an area of emerging research (Sonke, 2011; Sun et al., 2016). With further analyses of NG from around the world and investigation of the isotopic fractionation associated with NG processing, global and regional average Hg isotopic composition of natural gas and associated emissions could be estimated to characterize this input to atmospheric Hg isotope models. Although we were not able to discuss the origin of Hg within NG due to constraints related to the proprietary nature of the catalyst samples that comprised our dataset, our study did suggest that additional research into the sub-surface cycling of Hg is needed. In particular, measurements are needed to characterize the isotopic composition of Hg in modern depositional environments analogous to those thought to produce hydrocarbon reservoirs, as well as Hg from potential epigenetic Hg sources such as volcanic emissions and hydrothermal systems.

References

(1) Bartov, G.; Deonarine, A.; Johnson, T. M.; Ruhl, L.; Vengosh, A.; Hsu-Kim, H. Environmental Impacts of the Tennessee Valley Authority Kingston Coal Ash Spill. 1. Source Apportionment Using Mercury Stable Isotopes. *Environ. Sci. Technol.* **2013**, *47* (4), 2092–2099 DOI: 10.1021/es303111p.

(2) Blum, J. D.; Johnson, M. W.; Gleason, J. D.; Demers, J. D.; Landis, M. S.; Krupa, S. Mercury Concentration and Isotopic Composition of Epiphytic Tree Lichens in the Athabasca Oil Sands Region. *Dev. Environ. Sci.* **2012**, *11*, 373–390 DOI: 10.1016/B978-0-08-097760-7.00016-0.

(3) Demers, J. D.; Sherman, L. S.; Blum, J. D.; Marsik, F. J.; Dvonch, J. T. Coupling Atmospheric Mercury Isotope Ratios and Meteorology to Identify Sources of Mercury Impacting a Coastal Urban-Industrial Region near Pensacola, Florida, USA. *Global Biogeochem. Cycles* **2015**, *29* (10), 1689–1705 DOI: 10.1002/2015GB005146.

(4) Donovan, P. M.; Blum, J. D.; Demers, J. D.; Gu, B.; Brooks, S. C.; Peryam, J. Identification of Multiple Mercury Sources to Stream Sediments near Oak Ridge, TN, USA. *Environ. Sci. Technol.* **2014**, *48* (7), 3666–3674.

(5) Donovan, P. M.; Blum, J. D.; Singer, M. B.; Marvin-DiPasquale, M.; Tsui, M. T. K. Methylmercury Degradation and Exposure Pathways in Streams and Wetlands Impacted by Historical Mining. *Sci. Total Environ.* **2016** DOI: 10.1016/j.scitotenv.2016.04.139.

(6) Donovan, P. M.; Blum, J. D.; Singer, M. B.; Marvin-DiPasquale, M.; Tsui, M. T. K. Isotopic Composition of Inorganic Mercury and Methylmercury Downstream of a Historical Gold Mining Region. *Environ. Sci. Technol.* **2016**, acs.est.5b04413 DOI: 10.1021/acs.est.5b04413.

(7) Estrade, N.; Carignan, J.; Donard, O. F. X. Isotope Tracing of Atmospheric Mercury Sources in an Urban Area of Northeastern France. *Environ. Sci. Technol.* **2010**, *44* (16), 6062–6067 DOI: 10.1021/es100674a.

(8) Foucher, D.; Hintelmann, H.; Al, T. a.; MacQuarrie, K. T. Mercury Isotope Fractionation in Waters and Sediments of the Murray Brook Mine Watershed (New Brunswick, Canada): Tracing Mercury Contamination and Transformation. *Chem. Geol.* **2013**, *336*, 87–95 DOI: 10.1016/j.chemgeo.2012.04.014.

(9) Horvat, M.; Jeran, Z.; Špirič, Z.; Jaćimović, R.; Miklavčič, V. Mercury and Other Elements in Lichens near the INA Naftaplin Gas Treatment Plant, Molve, Croatia. *J. Environ. Monit.* **2000**, *2* (2), 139–144 DOI: 10.1039/a906973i.

(10) Lepak, R. F.; Yin, R.; Krabbenhoft, D. P.; Ogorek, J. M.; DeWild, J. F.; Holsen, T. M.; Hurley, J. P. Use of Stable Isotope Signatures to Determine Mercury Sources in the Great Lakes. *Environ. Sci. Technol. Lett.* **2015**, *2* (12), 335–341 DOI: 10.1021/acs.estlett.5b00277.

(11) Liu, J.; Feng, X.; Yin, R.; Zhu, W.; Li, Z. Mercury Distributions and Mercury Isotope Signatures in Sediments of Dongjiang, the Pearl River Delta, China. *Chem. Geol.* **2011**, *287* (1–2), 81–89 DOI: 10.1016/j.chemgeo.2011.06.001.

(12) Perrot, V.; Epov, V. N.; Pastukhov, M. V; Grebenshchikova, V. I.; Zouiten, C.; Sonke, J. E.; Husted, S.; Donard, O. F. X.; Amouroux, D. Tracing Sources and Bioaccumulation of Mercury in Fish of Lake Baikal--Angara River Using Hg Isotopic Composition. *Environ. Sci. Technol.* **2010**, *44* (21), 8030–8037 DOI: 10.1021/es101898e.

(13) Pirrone, N.; Cinnirella, S.; Feng, X.; Finkelman, R. B.; Friedli, H. R.; Leaner, J.; Mason, R.; Mukherjee, A. B.; Stracher, G. B.; Streets, D. G.; Telmer, K. Global Mercury Emissions to the Atmosphere from Anthropogenic and Natural Sources. *Atmos. Chem. Phys.* **2010**, *10* (13), 5951–5964 DOI: 10.5194/acp-10-5951-2010.

(14) Sherman, L. S.; Blum, J. D.; Keeler, G. J.; Demers, J. D.; Dvonch, J. T. Investigation of Local Mercury Deposition from a Coal-Fired Power Plant Using Mercury Isotopes. *Environ. Sci. Technol.* **2012**, *46* (1), 382–390 DOI: 10.1021/es202793c.

(15) Smith, R. S.; Wiederhold, J. G.; Jew, A. D.; Brown, G. E.; Bourdon, B.; Kretzschmar, R. Stable Hg Isotope Signatures in Creek Sediments Impacted by a Former Hg Mine. *Environ. Sci. Technol.* **2015**, *49* (2), 767–776 DOI: 10.1021/es503442p.

(16) Sonke, J. E. A Global Model of Mass Independent Mercury Stable Isotope Fractionation. *Geochim. Cosmochim. Acta* **2011**, *75* (16), 4577–4590 DOI: 10.1016/j.gca.2011.05.027.

(17) Sonke, J. E.; Schäfer, J.; Chmeleff, J.; Audry, S.; Blanc, G.; Dupré, B. Sedimentary Mercury Stable Isotope Records of Atmospheric and Riverine Pollution from Two Major European Heavy Metal Refineries. *Chem. Geol.* **2010**, *279* (3–4), 90–100 DOI: 10.1016/j.chemgeo.2010.09.017.

(18) Spirić, Z.; Mashyanov, N. R. Mercury Measurements in Ambient Air near Natural Gas Processing Facilities. *Fresenius. J. Anal. Chem.* **2000**, *366* (5), 429–432 DOI: 10.1007/s002160050087.

(19) Sun, R.; Streets, D. G.; Horowitz, H. M.; Amos, H. M.; Liu, G.; Perrot, V.; Toutain, J.-P.; Hintelmann, H.; Sunderland, E. M.; Sonke, J. E. Historical (1850–2010) Mercury Stable Isotope Inventory from Anthropogenic Sources to the Atmosphere. *Elem. Sci. Anthr.* **2016**, *4*, 91 DOI: 10.12952/journal.elementa.000091.

(20) Washburn, S. J.; Blum, J. D.; Demers, J. D.; Kurz, A. Y.; Landis, R. C. Isotopic Characterization of Mercury Downstream of Historic Industrial Contamination in the South River, Virginia. *Environ. Sci. Technol.* **2017**, *51* (19), 10965–10973 DOI: 10.1021/acs.est.7b02577.

(21) Washburn, S. J.; Blum, J. D.; Johnson, M. W.; Tomes, J. M.; Carnell, P. J. Isotopic Characterization of Mercury in Natural Gas via Analysis of Mercury Removal Unit Catalysts. *ACS Earth Sp. Chem.* **2018**, DOI: 10.1021/acsearthspacechem.7b00118.

(22) Washburn, S. J.; Blum, J. D.; Kurz, A.Y.; Pizzuto, J.E. Spatial and Temporal Variation in the Isotopic Composition of Mercury in the South River, VA. *Chem. Geol.* **In Review**

(23) Wiederhold, J. G.; Skyllberg, U.; Drott, A.; Jiskra, M.; Jonsson, S.; Björn, E.; Bourdon, B.; Kretzschmar, R. Mercury Isotope Signatures in Contaminated Sediments as a Tracer for Local Industrial Pollution Sources. *Environ. Sci. Technol.* **2015**, *49* (1), 177–185.

(24) Yin, R.; Feng, X.; Wang, J.; Li, P.; Liu, J.; Zhang, Y.; Chen, J.; Zheng, L.; Hu, T. Mercury Speciation and Mercury Isotope Fractionation during Ore Roasting Process and Their Implication to Source Identification of Downstream Sediment in the Wanshan Mercury Mining Area, SW China. *Chem. Geol.* **2013**, *336*, 72–79 DOI: 10.1016/j.chemgeo.2012.04.030